COLLEGE OF ENGINEERING

VIRGINIA POLYTECHNIC INSTITUTE AND STATE UNIVERSITY

BLACKSBURG, VIRGINIA

College of Engineering
Virginia Polytechnic Institute & State University
Blacksburg, Virginia 24061

VPI-E-77-18 June, 1977

Influence of Temper Condition on the Nonlinear Stress-Strain Behavior of Boron-Aluminum

John M. Kennedy [1]
Carl T. Herakovich[2]
Darrel R. Tenney[3]

Department of Engineering Science & Mechanics

Interim Report Number 8
NASA-VPI&SU Cooperative Program in Composite Materials Research and Education

NASA Grant NGR 47-004-129

Prepared for: Materials Application Branch
National Aeronautics & Space Administration
Langley Research Center
Hampton, VA. 23665

[1] Graduate Student

[2] Professor

[3] Materials Engineer - NASA Langley

BIBLIOGRAPHIC DATA SHEET	1. Report No. VPI-E-77-18	2.	3. Recipient's Accession No.
4. Title and Subtitle INFLUENCE OF TEMPER CONDITION ON THE NONLINEAR STRESS-STRAIN BEHAVIOR OF BORON-ALUMINUM			5. Report Date June, 1977 6.
7. Author(s) John M. Kennedy, Carl T. Herakovich & Carl T. Herakovich			8. Performing Organization Rept. No. VPI-E-77-18
9. Performing Organization Name and Address Virginia Polytechnic Institute and State University Engineering Science and Mechanics Blacksburg, Virginia 24061			10. Project/Task/Work Unit No. 11. Contract/Grant No. NASA NGR-47-004-129
12. Sponsoring Organization Name and Address National Aeronautics & Space Administration Langley Research Center Hampton, Virginia 23665			13. Type of Report & Period Covered 14.

15. Supplementary Notes

16. Abstracts

see page ii

17. Key Words and Document Analysis. 17a. Descriptors

Boron-Aluminum, Composites, Tension, Compression, Nonlinear Behavior, Cyclic Loading, Heat Treatment, Cryogenic Exposure

17b. Identifiers/Open-Ended Terms

17c. COSATI Field/Group

18. Availability Statement	19. Security Class (This Report)	21. No. of Pages
Distribution unlimited	UNCLASSIFIED	
	20. Security Class (This Page) UNCLASSIFIED	22. Price

INSTRUCTIONS FOR COMPLETING FORM NTIS-35 (Bibliographic Data Sheet based on COSATI Guidelines to Format Standards for Scientific and Technical Reports Prepared by or for the Federal Government, PB-180 600).

1. **Report Number.** Each individually bound report shall carry a unique alphanumeric designation selected by the performing organization or provided by the sponsoring organization. Use uppercase letters and Arabic numerals only. Examples FASEB-NS-73-87 and FAA-RD-73-09.

2. Leave blank.

3. **Recipient's Accession Number.** Reserved for use by each report recipient.

4. **Title and Subtitle.** Title should indicate clearly and briefly the subject coverage of the report, subordinate subtitle to the main title. When a report is prepared in more than one volume, repeat the primary title, add volume number and include subtitle for the specific volume.

5. **Report Date.** Each report shall carry a date indicating at least month and year. Indicate the basis on which it was selected (e.g., date of issue, date of approval, date of preparation, date published).

6. **Performing Organization Code.** Leave blank.

7. **Author(s).** Give name(s) in conventional order (e.g., John R. Doe, or J.Robert Doe). List author's affiliation if it differs from the performing organization.

8. **Performing Organization Report Number.** Insert if performing organization wishes to assign this number.

9. **Performing Organization Name and Mailing Address.** Give name, street, city, state, and zip code. List no more than two levels of an organizational hierarchy. Display the name of the organization exactly as it should appear in Government indexes such as Government Reports Index (GRI).

10. **Project/Task/Work Unit Number.** Use the project, task and work unit numbers under which the report was prepared.

11. **Contract/Grant Number.** Insert contract or grant number under which report was prepared.

12. **Sponsoring Agency Name and Mailing Address.** Include zip code. Cite main sponsors.

13. **Type of Report and Period Covered.** State interim, final, etc., and, if applicable, inclusive dates.

14. **Sponsoring Agency Code.** Leave blank.

15. **Supplementary Notes.** Enter information not included elsewhere but useful, such as: Prepared in cooperation with . . . Translation of . . . Presented at conference of . . . To be published in . . . Supersedes . . . Supplements . . . Cite availability of related parts, volumes, phases, etc. with report number.

16. **Abstract.** Include a brief (200 words or less) factual summary of the most significant information contained in the report. If the report contains a significant bibliography or literature survey, mention it here.

17. **Key Words and Document Analysis. (a). Descriptors.** Select from the Thesaurus of Engineering and Scientific Terms the proper authorized terms that identify the major concept of the research and are sufficiently specific and precise to be used as index entries for cataloging.
(b). Identifiers and Open-Ended Terms. Use identifiers for project names, code names, equipment designators, etc. Use open-ended terms written in descriptor form for those subjects for which no descriptor exists.
(c). COSATI Field/Group. Field and Group assignments are to be taken from the 1964 COSATI Subject Category List. Since the majority of documents are multidisciplinary in nature, the primary Field/Group assignment(s) will be the specific discipline, area of human endeavor, or type of physical object. The application(s) will be cross-referenced with secondary Field/Group assignments that will follow the primary posting(s).

18. **Distribution Statement.** Denote public releasability, for example "Release unlimited", or limitation for reasons other than security. Cite any availability to the public, other than NTIS, with address, order number and price, if known.

19 & 20. **Security Classification.** Do not submit classified reports to the National Technical Information Service.

21. **Number of Pages.** Insert the total number of pages, including introductory pages, but excluding distribution list, if any.

22. **NTIS Price.** Leave blank.

ACKNOWLEDGEMENTS

This report documents a portion of the work accomplished under NASA Grant NGR 47-004-129 during the period June, 1975 through April, 1977. Mr. Kennedy was in residence at NASA Langley during the period March, 1976 to October, 1976.

The authors are grateful to the technical staff of the Structures Lab, Fatigue Lab, IRD, MP & DS, and MDS of NASA Langley Research Center for assistance with the experimental work. Also thanks are in order to Mrs. Kay Brinkley and Ann Cole of Langley for their contribution in data reduction and to Ms. Frances Carter of VPI&SU for typing the manuscript. Finally, the financial support of USAAMROL at Langley on a portion of the experimental work is appreciated.

INFLUENCE OF TEMPER CONDITION ON THE NONLINEAR STRESS-STRAIN BEHAVIOR OF BORON-ALUMINUM

ABSTRACT

The influence of temper condition on the tensile and compressive stress-strain behavior for six boron-aluminum laminates was investigated. In addition to monotonic tension and compression tests, tension-tension, compression-compression, and tension-compression tests were conducted to study the effects of cyclic loading. The laminates studied were [0], [90], $[\pm 45]_S$, $[0/\pm 45/0]_S$, $[0/\pm 45]_S$, and $[\pm 45/0]_S$, and the temper conditions were "as received" or F, T6 and T6N which was T6 followed by cryogenic exposure.

It is shown that the T6 heat treatment increases the yield stress in both tension and compression. Tensile strength results are a function of the laminate configuration; unidirectional laminates were affected considerably more than other laminates with some strength values increasing and others decreasing. In general, cryogenic exposure of laminates with 0° plies increased the tensile yield stress and reduced the compressive yield stress, but other laminates were not significantly affected.

Results from the cyclic tests show that the linear range of material behavior was increased by cyclic loading to a maximum value for all laminates and temper conditions. Typically, a maximum linear range was established which remained constant except in those cases where material degradation was indicated. Only those laminates with ±45° plies exhibited significant material degradation.

TABLE OF CONTENTS

LIST OF TABLES

LIST OF FIGURES

LIST OF SYMBOLS

Al	aluminum
B	boron
E	elastic modulus
G	elastic shear modulus
H	laminate half thickness
M	inplane resultant moment
N	inplane resultant force
Q_{ij}	ij element of the stiffness matrix
$\overline{Q}_{ij}$	ij element of the transformed stiffness matrix
T	tensor transformation matrix
ΔT	temperature change
V	volume fraction
α	coefficient of thermal expansion
$\overline{\alpha}$	average coefficient of thermal expansion
γ	shear strain
γ°	midplane shear strain
ε	strain
ε°	midplane strain
κ	midplane curvature
ν	Poisson's ratio
σ	stress
$\overline{\sigma}$	resultant stress
τ	shear stress
$\overline{\tau}$	resultant shear

Superscripts

C	curing
k	ply number
L	loading
m	maximum for a cycle
R	residual
T	thermal
u	ultimate
UL	unloading
y	yield

Subscripts

f	fiber
k	ply number
m	matrix
(1,2)	natural coordinate system
(x,y)	arbitrary

1. INTRODUCTION

The rapidly advancing technology of the past decade has made it necessary to develop new materials which will meet demanding standards and perform under extreme operating conditions. These new materials have primarily come about as a result of advances in the aerospace industry and the desire to build more energy efficient structures. One of the more promising advances in materials science has been the development of a new class of materials known as advanced composites.

Advanced composite materials are a unique class of engineering materials in that the designer can tailor fit the material to the particular application. It is possible to design the composite material to meet directional dependent requirements such as stiffness, strength, yield stress, and temperature and moisture properties by choosing suitable fiber, matrix, and laminate stacking sequence. Another important feature of advanced composite materials is that they exhibit very high specific strength and specific stiffness compared to other engineering materials. However, the engineering community is faced with many new problems associated with a new material system. Thus, the researcher must study composite materials to develop a complete understanding of their behavior so they can be a reliable, efficient, and useful engineering material.

Advanced fibrous composite materials can be divided into two classes, those being composites with resin matrix and those with metal matrix. Metal matrix composite materials are the primary concern of this study. There are many characteristics of metal matrix composites

which make them a useful engineering material even though their per pound cost is high compared to resin matrix composites.

Metal matrix composite materials, specifically boron-aluminum, have a larger operating temperature range, higher strength, better transverse properties, and can be braze welded to other parts of a structure. Also the potential problem of moisture absorption into the matrix is not present in the metal matrix system as it is with resin matrix composites.

The applications of metal matrix composite materials have not been as numerous as their counterpart resin matrix composites primarily due to cost considerations. Boron-aluminum has been chosen as the designer's material when a combination of high ultimate strength and operating temperature have been design requirements. Boron-aluminum is presently being considered for use on the YF-12 reconnaisance aircraft [1] where the operating temperature is 450°F. Two other applications have been in jet engines [2] where unidirectional boron-aluminum is used for turbine blades and on the space shuttle [3] where again high temperature environment and weight savings are the driving forces behind its use.

A problem of fundamental importance with boron-aluminum composites is the nonlinear stress-strain behavior of the material. More so than resin matrix composites, the aluminum matrix of boron-aluminum contributes significantly to the overall stress-strain response of the composite laminate. In order to achieve high temperature capabilities with boron-aluminum, it is necessary to use the previously developed alloys of aluminum which have higher operating temperatures. Since these alloys are usually precipitation hardening alloys, exposure to high

temperature environments significantly changes the mechanical properties of the aluminum alloy by annealing or other metallurgical phenomenon. It is beyond the scope of this work to perform a detailed study of the effect of high temperature on the mechanical properties of boron-aluminum; however, it is possible to gain some insight into this problem by choosing one of the precipitation hardening aluminum alloys for the matrix material and studying the mechanical response of the composite with various temper conditions.

The boron-aluminum system chosen for this work was 5.6 mil diameter boron fibers with a 6061 aluminum matrix. This particular aluminum alloy is a precipitation hardening alloy; and therefore, it is possible to heat treat the aluminum to change its mechanical properties and thus the properties of a composite laminate.

Results of tension and compression tests of six different boron-aluminum laminates are reported showing the effect of heat treating. Cyclic tests in both tension and compression and cyclic tension-compression results are also reported for the various laminates and temper conditions. Analytical predictions for some mechanical properties are compared with experimental results and modes of failure are discussed.

Since the heat treating involves high temperature environments, it is necessary to consider the residual stresses in the composite laminate. Analytical predictions of the residual stress in the fiber and matrix of unidirectional boron-aluminum can be made using micromechanics, and laminate analysis can predict the residual stresses in the individual

plies of a composite laminate. The residual stress on the outer ply of a laminate can be determined by an X-ray exposure technique as described by Cheskis and Heckel [4]. Some X-ray residual stress determinations were made on unidirectional boron-aluminum; the results will be presented in a later paper.*

Previous researchers have expended considerable effort into the understanding of the mechanical behavior of boron-aluminum; this study is an extension of that effort to bring about an improved understanding of the nonlinear behavior of metal matrix composite materials.

* X-Ray residual stess determinations were performed by E. Illg with the supervision of B. Lisagor and D. R. Tenney.

2. LITERATURE REVIEW

Over the past 15 years much effort has been put forth to investigate the mechanical behavior of metal matrix composite materials. Experimental investigations have generally shown metal matrix composites to exhibit nonlinear response to mechanical loading. Efforts have been made to understand why they behave nonlinearly and to model the stress-strain behavior mathematically. The explanations of the nonlinear behavior of metal matrix composites which have come about as a result of this research are complex and encompass the fields of material science and engineering mechanics.

One of the earliest endeavors to investigate the nonlinear stress-strain behavior of metal matrix composite materials was by Baker and Cratchley [5] in 1965. A composite system of unidirectional silica fibers in an aluminum matrix was used as the material for the study. Cyclic tension tests were performed on the material and it was found that the stress-strain behavior came about as a direct combination of the matrix and fiber, where the fiber behaved as a linear-elastic material and the matrix behaved in an elastic-plastic fashion. It was also shown that the stiffness of the composite depends upon previous load history. At stress values below the highest previous stress the modulus is greater than at values above the maximum prior stress.

The mechanical properties of unidirectional boron-aluminum or Borsic-aluminum composite materials have been reported by several authors. Krieder and Marciano [6] presented results of tensile and compressive tests of Borsic-aluminum. Long [7] conducted a research

program on unidirectional Borsic-aluminum reporting results of tensile tests for loading parallel and perpendicular to the fiber direction. Three aluminum alloys were used for the matrix material and experimental results were compared. Cyclic tensile tests were also performed on the [0] laminates with results showing the same strain hardening behavior of the aluminum matrix as reported in the Baker and Cratchley work. Failure strengths from the tests performed on the unidirectional material were lower than expected, but examination of the strength of the Borsic fibers showed it also to be much lower than anticipated. Garrett et al [3] conducted an experimental program investigating the static tensile and compressive behavior of boron-aluminum. Coupons and sandwich beams were used for tensile tests and sandwich beams were used for the compression tests. Unidirectional boron-aluminum was tested and both longitudinal and transverse properties were determined.

Herakovich et al [8] presented results of an experimental program with Borsic-aluminum, using six laminate configurations and testing in both tension and compression. Coupons were used for tensile tests and sandwich beams and coupons tested in an IITRI compression fixture were used for compression tests.

For the previous four works, experimental results for unidirectional boron-aluminum with 50 percent fiber volume fraction were fairly consistent. All authors reported longitudinal moduli of 30 to 33 Msi and transverse moduli of 12 to 18 Msi. Ultimate tensile strengths ranged from 150 ksi to 180 ksi for [0] specimens and [90] specimens exhibited ultimate strengths ranging from 10 to 14 ksi. In reference

[8], results from cyclic tension and cyclic compression tests showed [0], [90] and $[\pm 45]_s$ laminates to load linearly to the point of the highest previous stress whereas the $[0/\pm 45]_s$ and $[(0/90)_2]_s$ laminates exhibited nonlinear behavior prior to the previous highest stress.

Many compression test methods for composite materials have been used by various researchers. Perhaps the most popular has been the sandwich beam used by Kreider and Marciano [6], Garrett et al [3], and Herakovich et al [8]. However, several other schemes have been used for compression testing of metal matrix composites, those being the IITRI coupon specimen used by Herakovich et al, the tube specimen used by Knoell [9], and coupon compression specimens using a Montgomery Templin grip by Adsit and Forest [10]. In all cases the elastic properties reported were consistent, but maximum stresses varied from a low of 180 ksi to a maximum of 350 ksi. Much of the scatter in maximum stresses depended upon the test specimen; the sandwich beam yielding the highest results. The buckling failure mode, exhibited by some compression tests, results in maximum stresses which are lower than the material ultimate values. The buckling phenomenon and the variation in strength values with test method indicates that a thorough investigation of compression test methods for composite materials would be desirable.

Another area of investigation in the metal matrix realm has been the effect of matrix, fiber, and fabrication procedures on the mechanical properties of the composite. In references [11] through [14] the results of tensile tests on boron-aluminum were reported, showing the

effects of different combinations of composite constituents (matrix and fiber) and temper conditions. Dolowy and Taylor [11] used unidirectional boron-aluminum with 6061 matrix to study the influence of thermal and mechanical conditioning on longitudinal and transverse tensile strengths. By using a T6 heat treatment on the in-situ matrix, strength increases of 10 percent in the longitudinal direction and 20 percent in the transverse direction were realized; however, the increase in transverse strength was much lower than the 100 percent increase which occurs with pure 6061 aluminum. A discussion of the effect of heat treating on residual stresses and interfacial bonds between fiber and matrix was included in this work. Large residual stresses are generated during the water quench of the heat treating procedure, but these stresses are significantly reduced during the thermal aging. It was also hypothesized that permanent damage to the interface could be produced during the solution treatment and water quench. It is important to note that T6 conditioning increased the linear elastic range of the unidirectional composite even though heat treating apparently generates damage at the fiber matrix interface.

Prewo and Kreider [12] investigated the transverse tensile properties of boron-aluminum composites using different matrix materials, different fibers, and different temper conditions. Of primary importance to this work was the fact that regardless of the matrix or fiber type, heat treating to a T6 condition consistently increased the ultimate transverse strength 50 to 100 percent.

Swanson and Hancock [13] have reported results from tensile tests on [0], off-axis [30], and [90] laminates incorporating various heat treatments into the testing program. The boron-aluminum laminates were heat treated to a T6 condition and a modified T6 condition, where after the T6 conditioning the specimen was exposed to a -196°C environment for four minutes; also, specimens in the "as received" or F condition were tested. For all three laminates, heat treating the in-situ matrix of the specimen increased the yield stress of the specimen as well as the ultimate strength. Laminates exposed to cryogenic temperatures exhibited lower yield stresses and strengths than the specimens which were only heat treated; however, these stress values were higher than those exhibited by the F condition laminates.

Prewo and Kreider [14] published a second paper on boron and Borsic fiber reinforced aluminum composites where 5.6 mil fibers were used with various aluminum alloys and volume fractions of boron; the unidirectional material was tested in longitudinal and transverse tension. Values of elastic moduli in transverse tension were reported to be greater than 20 Msi indicating the fiber contributed significantly to the stiffness since the elastic modulus of aluminum is 10 Msi. Some specimens were heat treated to a T6 condition and, as previously reported, the yield stress and strength were increased. Increasing the fiber volume fraction increased the elastic modulus of transverse boron-aluminum but did not affect the strength of the material. For longitudinal tensile tests, the elastic modulus was found to increase with increasing fiber volume fraction. By heat treating to a T6 condition,

the linear elastic range was increased; however, it was not clear if ultimate strengths were affected by heat treating. Ultimate tensile strengths increased with higher fiber volume fraction.

The X-ray exposure technique described by Cullity [15] was used by Prewo and Kreider to determine the residual stresses on the surface of boron-aluminum; the tensile residual stresses were determined to be 16 ksi in F condition specimens and 30 ksi in T6 condition specimens.

Alfred et al [16] have studied the elastic and plastic Poisson's ratio as a function of strain. It was shown that Poisson's ratio for unidirectional material can be computed by a rule of mixtures relationship and that the plastic Poisson's ratio is higher than the elastic Poisson's ratio.

Several researchers have developed computer programs to model the stress-strain behavior of boron-aluminum. Chamis and Sullivan [17] use a finite element analysis to predict initial tangent properties for boron-aluminum angle-ply laminates. The analysis uses laminate theory and accounts for nonlinear matrix behavior and residual strains. Ramsey et al [18] use lamination theory to predict the stress-strain behavior of boron-aluminum laminates. The results from the analysis were compared with those of tensile tests and shown to compare favorably. Renieri and Herakovich [19] have developed a finite element analysis to predict the stress-strain behavior of composite laminates. The analysis includes thermal loading, axial loadings, temperature and strain dependent properties, and edge effects. Balanced, symmetric laminates of Borsic-aluminum were analyzed using the finite element program and

compared with existing theories and experimental data.

As indicated by the papers reviewed herein, much work has been done to determine the mechanical properties of metal matrix composite materials; however, the experimental work has been primarily limited to uniaxial loading and a limited amount of shear testing. From the analytical viewpoint, several models have been developed to predict material properties and stress-strain response. However, the viability of any model can only be assessed after it has been compared with experimental results. One objective of this present work is to provide more complete experimental data for the nonlinear behavior of boron-aluminum.

3. THEORY

The development of new theories to predict engineering properties and mechanical behavior of composite materials has been an integral part of advances in the field. Composite materials have been studied from the macromechanical and the micromechanical viewpoints. The laminate analysis theories have been developed by considering the composite on the macro level and from micromechanics has come concepts such as the rule of mixtures. In this chapter both laminate analysis and micromechanics are used to develop analytical predictions for engineering properties and residual thermal stresses. Many details of the development of the theories have been omitted; a similar textbook account can be found in Reference [20].

3.1 Laminate Analysis

A composite laminate can be defined as a consolidated group of lamina, each lamina having its own individual lamina properties. The laminate analysis ideology uses this concept as the foundation for the development of the stress-strain relations for a composite laminate.

3.1.1 Lamina Stress-Strain Relations

Since the lamina is the foundation for laminate analysis, it is necessary to first write the general stress-strain equations for a lamina. Assuming that a lamina is a homogeneous, orthotropic material, the lamina stress-strain relation in natural coordinates is:

$$\begin{Bmatrix} \sigma_1 \\ \sigma_2 \\ \tau_{12} \end{Bmatrix} = \begin{bmatrix} Q_{11} & Q_{12} & 0 \\ Q_{12} & Q_{22} & 0 \\ 0 & 0 & Q_{66} \end{bmatrix} \begin{Bmatrix} \varepsilon_1 \\ \varepsilon_2 \\ \gamma_{12} \end{Bmatrix} \tag{3.1}$$

The components of the stiffness matrix, Q, are defined in terms of engineering constants.

It is necessary to relate the stresses and strains, not only in the natural coordinate system of the lamina, but also in a coordinate system convienent to the composite laminate. This is accomplished by transforming the stresses and strains to the arbitrary coordinate system by a rotation through the angle theta (θ) between the lamina coordinate system and the laminate coordinate system. The transformed stress-strain relation is:

$$\begin{Bmatrix} \sigma_x \\ \sigma_y \\ \tau_{xy} \end{Bmatrix} = \begin{bmatrix} \bar{Q}_{11} & \bar{Q}_{12} & \bar{Q}_{16} \\ \bar{Q}_{12} & \bar{Q}_{22} & \bar{Q}_{26} \\ \bar{Q}_{16} & \bar{Q}_{26} & \bar{Q}_{66} \end{bmatrix} \begin{Bmatrix} \varepsilon_x \\ \varepsilon_y \\ \gamma_{xy} \end{Bmatrix} \tag{3.2}$$

where the $\bar{Q}$ matrix is defined as

$$[\bar{Q}] = [T]^{-1}[Q][T] \tag{3.3}$$

and [T] is the transformation matrix.

3.1.2 Laminate Constitutive Equation

The laminate constitutive equation is developed from the lamina relations by integrating over the thickness of the laminate to get the

resultant forces and moments on the laminate.

The strain on a lamina of the laminate is defined by the strain at the midplane plus the strain resulting from bending curvature. The inplane strain on a lamina is:

$$\begin{Bmatrix} \varepsilon_x \\ \varepsilon_y \\ \gamma_{xy} \end{Bmatrix} = \begin{Bmatrix} \varepsilon_x^\circ \\ \varepsilon_y^\circ \\ \gamma_{xy}^\circ \end{Bmatrix} + Z \begin{Bmatrix} \kappa_x \\ \kappa_y \\ \kappa_{xy} \end{Bmatrix} \tag{3.4}$$

where $\{\varepsilon^\circ\}$ are the midplane strains and $\{\kappa\}$ are the middle surface curvatures.

The general stress-strain relation for a lamina becomes

$$\begin{Bmatrix} \sigma_x \\ \sigma_y \\ \tau_{xy} \end{Bmatrix} = \begin{bmatrix} \bar{Q}_{11} & \bar{Q}_{12} & \bar{Q}_{16} \\ \bar{Q}_{12} & \bar{Q}_{22} & \bar{Q}_{26} \\ \bar{Q}_{16} & \bar{Q}_{26} & \bar{Q}_{66} \end{bmatrix} \left(\begin{Bmatrix} \varepsilon_x^\circ \\ \varepsilon_y^\circ \\ \gamma_{xy}^\circ \end{Bmatrix} + Z \begin{Bmatrix} \kappa_x \\ \kappa_y \\ \kappa_{xy} \end{Bmatrix} \right) \tag{3.5}$$

The resultant forces and moments are computed by integration of the stresses in each lamina of the entire laminate. Integrating (3.5), the constitutive equations for a laminate become (in condensed notation):

$$\begin{Bmatrix} N_x \\ N_y \\ N_{xy} \end{Bmatrix} = \sum_{k=1}^{N} [\bar{Q}]_k \left\{ \int_{Z_{k-1}}^{Z_k} \begin{Bmatrix} \varepsilon_x^\circ \\ \varepsilon_y^\circ \\ \gamma_{xy}^\circ \end{Bmatrix} dZ + \int_{Z_{k-1}}^{Z_k} \begin{Bmatrix} \kappa_x \\ \kappa_y \\ \kappa_{xy} \end{Bmatrix} Z dZ \right\} \tag{3.6}$$

and

$$\begin{Bmatrix} M_x \\ M_y \\ M_{xy} \end{Bmatrix} = \sum_{k=1}^{N} [\bar{Q}]_k \left\{ \int_{Z_{k-1}}^{Z_k} \begin{Bmatrix} \varepsilon_x^\circ \\ \varepsilon_y^\circ \\ \gamma_{xy}^\circ \end{Bmatrix} Z dZ + \int_{Z_{k-1}}^{Z_k} \begin{Bmatrix} \kappa_x \\ \kappa_y \\ \kappa_{xy} \end{Bmatrix} Z dZ \right\} \quad (3.7)$$

where the summation is over all N plies of the laminate. Carrying out the integration, the equations become

$$\{N\} = [A]\{\varepsilon^\circ\} + [B]\{\kappa\} \quad (3.8)$$

$$\{M\} = [B]\{\varepsilon^\circ\} + [D]\{\kappa\}. \quad (3.9)$$

where

$$A_{ij} = \sum_{k=1}^{N} (\bar{Q}_{ij})_k (Z_k - Z_{k-1})$$

$$B_{ij} = \frac{1}{2} \sum_{k=1}^{N} (\bar{Q}_{ij})_k (Z_k^2 - Z_{k-1}^2)$$

$$D_{ij} = \frac{1}{3} \sum_{k=1}^{N} (\bar{Q}_{ij})_k (Z_k^3 - Z_{k-1}^3) \text{ with } i,j = 1,2,6$$

3.1.3 Laminate Engineering Constants

The laminate engineering constants for a symmetric laminate are determined assuming inplane loading in the direction relating to the desired constant. The constitutive equation for a symmetric laminate then becomes:

$$\begin{Bmatrix} N_x \\ N_y \\ N_{xy} \end{Bmatrix} = \begin{bmatrix} A_{11} & A_{12} & A_{16} \\ A_{12} & A_{22} & A_{26} \\ A_{16} & A_{26} & A_{66} \end{bmatrix} \begin{Bmatrix} \varepsilon_x^\circ \\ \varepsilon_y^\circ \\ \gamma_{xy}^\circ \end{Bmatrix} \tag{3.10}$$

Writing midplane strains in terms of resultant forces yields

$$\begin{Bmatrix} \varepsilon_x^\circ \\ \varepsilon_y^\circ \\ \gamma_{xy}^\circ \end{Bmatrix} = \begin{bmatrix} A_{11}^{-1} & A_{12}^{-1} & A_{16}^{-1} \\ A_{12}^{-1} & A_{22}^{-1} & A_{26}^{-1} \\ A_{16}^{-1} & A_{26}^{-1} & A_{66}^{-1} \end{bmatrix} \begin{Bmatrix} N_x \\ N_y \\ N_{xy} \end{Bmatrix} \tag{3.11}$$

Where the coefficient matrix is the inverse of the A matrix in (3.10). The average stresses on the laminate are defined as

$$\begin{Bmatrix} \bar{\sigma}_x \\ \bar{\sigma}_y \\ \bar{\tau}_{xy} \end{Bmatrix} = \frac{1}{2H} \begin{Bmatrix} N_x \\ N_y \\ N_{xy} \end{Bmatrix} \tag{3.12}$$

where H is the laminate half-thickness.

From (3.11) and (3.12) with $\bar{\sigma}_x$ not equal to zero and all other stresses equal to zero, the midplane axial strain becomes

$$\varepsilon_x^\circ = 2H\, A_{11}^{-1}\, \bar{\sigma}_x \tag{3.13}$$

Defining Young's Modulus as the axial stress per unit axial strain, the stiffness becomes

$$F_x = \frac{\bar{\sigma}_x}{\varepsilon_x^\circ} = \frac{\bar{\sigma}_x}{2HA_{11}^{-1}\bar{\sigma}_x} = \frac{1}{2HA_{11}^{-1}} \tag{3.14}$$

Similarly, E_y and G_{xy} are:

$$E_y = \frac{1}{2HA_{22}^{-1}} \tag{3.15}$$

$$G_{xy} = \frac{1}{2HA_{66}^{-1}} \tag{3.16}$$

Poisson's ratio being defined as the ratio of two coordinate strains yields

$$\nu_{xy} = -\frac{\varepsilon_y^\circ}{\varepsilon_x^\circ} = -\frac{A_{12}^{-1}N_x}{A_{11}^{-1}N_x} = \frac{A_{12}^{-1}}{A_{11}^{-1}} \tag{3.17}$$

and

$$\nu_{yx} = -\frac{\varepsilon_x^\circ}{\varepsilon_y^\circ} = -\frac{A_{12}^{-1}N_y}{A_{22}^{-1}N_y} = \frac{A_{12}^{-1}}{A_{22}^{-1}} \tag{3.18}$$

3.1.4 Laminate Thermal Analysis

The assumptions used in development of laminate theory still hold when thermal effects are to be considered; that is, all lamina are to be considered homogeneous orthotropic layers. Thermal stresses then arise in a composite laminate due to the mismatch in thermal expansion (or contraction) of individual lamina with differing ply orientations.

Thermal strains arise from changes in temperature and are thus defined for a lamina to be

$$\begin{Bmatrix} \varepsilon_1 \\ \varepsilon_2 \\ \frac{1}{2}\gamma_{12} \end{Bmatrix} = \begin{Bmatrix} \alpha_1 \\ \alpha_2 \\ 0 \end{Bmatrix} \Delta T \tag{3.19}$$

where α_1 and α_2 are coefficients of thermal expansion in the material principal coordinates and ΔT denotes temperature change. The stress on the lamina, if the lamina is completely restrained, is related to the thermal strains by the stiffness matrix [Q].

$$\begin{Bmatrix} \sigma_1 \\ \sigma_2 \\ \tau_{12} \end{Bmatrix} = \begin{bmatrix} Q_{11} & Q_{12} & 0 \\ Q_{12} & Q_{22} & 0 \\ 0 & 0 & Q_{66} \end{bmatrix} \begin{Bmatrix} \alpha_1 \\ \alpha_2 \\ 0 \end{Bmatrix} \Delta T \tag{3.20}$$

Transformation of the thermal stresses and coefficients of thermal expansion yields the general expression for thermal stress and strain.

$$\begin{Bmatrix} \sigma_x \\ \sigma_y \\ \sigma_{xy} \end{Bmatrix} = \begin{bmatrix} \bar{Q}_{11} & \bar{Q}_{12} & \bar{Q}_{16} \\ \bar{Q}_{12} & \bar{Q}_{22} & \bar{Q}_{26} \\ \bar{Q}_{16} & \bar{Q}_{26} & \bar{Q}_{66} \end{bmatrix} \begin{Bmatrix} \alpha_x \\ \alpha_y \\ \alpha_{xy} \end{Bmatrix} \Delta T \tag{3.21}$$

The equivalent thermal force for a symmetric laminate is determined by integrating over the thickness of the laminate, yielding

$$\{N\} = \Delta T \int_{-H}^{H} [\bar{Q}]_k \{\alpha\}_k dZ \tag{3.22}$$

Substituting for {N} from (3.10) and carrying out the integration, gives

$$\{N\} = [A]\{\varepsilon^{\circ}\}^{T} = \Delta T \sum_{k=1}^{N} [\bar{Q}]_k \{\alpha\}_k (Z_k - Z_{k-1}) \tag{3.23}$$

where $\{\varepsilon^{\circ}\}^{T}$ is the equivalent thermal midplane strain. Rearranging,

$$\{\varepsilon^{\circ}\}^{T} = [A]^{-1} \Delta T \sum_{k=1}^{N} [\bar{Q}]_k \{\alpha\}_k (Z_k - Z_{k-1}) \tag{3.24}$$

and defining $\{\bar{\alpha}\}$ as the laminate coefficient of thermal expansion gives

$$\{\bar{\alpha}\} = [A]^{-1} \sum_{k=1}^{N} [\bar{Q}]_k \{\alpha\}_k (Z_k - Z_{k-1}) \tag{3.25}$$

Of primary importance to this work are the residual thermal stresses developed during the curing process. Defining ΔT^{C} as the temperature differential between operating temperature and the temperature during the curing cycle at which the consolidated composite starts to develop thermal stresses, the expression for residual stresses in a laminate can be developed. The residual thermal strain in the k^{th} ply is

$$\{\varepsilon\}_k^{R} = \Delta T^{C}[\{\bar{\alpha}\} - \{\alpha\}_k] \tag{3.26}$$

where the average midplane residual strain is

$$\{\varepsilon^{\circ}\}^{R} = \Delta T^{C}\{\bar{\alpha}\} \tag{3.27}$$

The residual stress on a ply is determined by substituting (3.26) into (3.2)

$$\{\sigma\}_k^{R} = [\bar{Q}]_k(\{\bar{\alpha}\} - \{\alpha\}_k)\Delta T^{C} \tag{3.28}$$

The stresses due to curing and applied load in a lamina are

determined by adding the stresses due to applied load and curing. From equations (3.2), (3.4), and (3.28), the stress in the k^{th} ply is

$$\{Q\}^k = [\bar{Q}]^k(\{\varepsilon^\circ\} + \Delta T^C\{\bar{\alpha}\text{-}\alpha^k\}) \tag{3.29}$$

or

$$\{\sigma\}^k = [\bar{Q}]^k([A]^{-1}\{N\} + \{\bar{\alpha}\text{-}\alpha^k\}\Delta T^C) \tag{3.30}$$

3.2 Micromechanics of a Lamina

The micromechanical viewpoint for composite material analysis examines the lamina as a heterogeneous material having a fiber and matrix with different mechanical properties. The properties of the lamina are then determined from the fiber and matrix properties. Comparison of mechanical properties predicted by micromechanics with experimental results have shown that some of the predictions compare better than others.

3.2.1 Stiffness Properties of a Lamina

The various stiffness properties of a composite lamina can be predicted by the so called rule of mixtures, the resulting relations are presented here.

The stiffness for a composite lamina parallel to the fibers, E_1, is

$$E_1 = E_f V_f + E_m V_m \tag{3.31}$$

where E_f, V_f and E_m, V_m are the respective fiber and matrix stiffness and volume fraction.

The stiffness perpendicular to the fibers of a lamina is a function of the fiber and matrix stiffnesses and volume fractions

$$E_2 = \frac{E_f E_m}{V_m E_f + V_f E_m} \tag{3.32}$$

The major Poisson's ratio, ν_{12}, is determined from the Poisson's ratios of the matrix and fiber by the rule of mixtures concept,

$$\nu_{12} = V_m \nu_m + V_f \nu_f \tag{3.33}$$

where ν_m and ν_f are matrix and fiber Poisson's ratios, respectively.

The shear modulus, G_{12}, is

$$G_{12} = \frac{G_m G_f}{V_m G_f + V_f G_m} \tag{3.34}$$

which is the same type expression as that for E_2 except G_m is the shear modulus of the matrix and G_f is the shear modulus of the fiber.

3.2.2 Thermal Stresses

Curing residual stresses also develop in a composite lamina due to the different coefficients of thermal expansion of the fiber and matrix. For a composite lamina residual stresses in the fiber and matrix are:

$$\sigma_m^R = E_m(\alpha_x - \alpha_m)\Delta T^C \tag{3.35}$$

and

$$\sigma_f^R = E_f(\alpha_x - \alpha_f)\Delta T^C \tag{3.36}$$

where α_x, α_m, and α_f are the coefficients of thermal expansion of the lamina, matrix, and fiber, respectively. From equilibrium considerations and (3.35) and (3.36) the average coefficient of thermal expansion parallel to fibers in the lamina is

$$\alpha_x = \frac{E_m V_m \alpha_m + E_f V_f \alpha_f}{E_f V_f + E_m V_m} \tag{3.37}$$

and substituting into (3.35) and (3.36),

$$\sigma_m^R = \frac{E_f E_m V_f}{E_m V_m + E_f V_f} (\alpha_f - \alpha_m)\Delta T^C \tag{3.38}$$

and

$$\sigma_f^R = \frac{E_f E_m V_m}{E_m V_m + E_f V_f} (\alpha_m - \alpha_f)\Delta T^C \tag{3.39}$$

4. EXPERIMENTAL PROGRAM

4.1 Introduction

An extensive experimental program was conducted to investigate the stress-strain behavior of boron-aluminum including different temper conditions, various laminate configurations, and five different static test types. The program involved six different laminate configurations: [0], [90], $[\pm 45]_s$, $[0/\pm 45/0]_s$, $[0/\pm 45]_s$, and $[\pm 45/0]_s$. The latter two laminates were chosen to investigate the effect of stacking sequence. The five different tests were: tension, cyclic tension, compression, cyclic compression, and cyclic tension-compression. In addition to the various laminates and loading conditions, three types of heat treatments were used to alter the condition of the aluminum matrix and the residual stress state of the boron-aluminum laminate. The three temper conditions were: "as fabricated" or F, T6, and a modified T6.

4.2 Specimens

4.2.1 Materials

The constituents of the boron-aluminum composite were .0056 inch diameter boron fibers and 6061 aluminum alloy matrix. The boron-aluminum was made using standard diffusion bonding procedures by Amercom, Inc. The consolidated boron-aluminum was received from the manufacturer in 12 x 20 inch panels ready to be cut into test specimens. The speci-

mens were cut by the Materials Development Section of NASA Langley Research Center using a diamond impregnated cutting wheel; rough edges of the specimens were then filed by hand. The fiber volume fraction was determined for each panel and it was found to vary between 47 and 48 percent. The strength of the boron fibers was determined by the post-bending procedure, a standard method for fiber strength determination. The fixture has posts of different radii which are used to determine the fiber strength by successively bending the fibers around the posts in order of decreasing radius. The fiber strength is then related to the radius of the post at which it fails. The smallest radius post on the fixture produced a stress in the fiber of 542 ksi. None of the fibers tested broke on posts which had larger radii, and only 15 percent of the fibers failed when being bent around the smallest radius post. It was therefore concluded that the average fiber strength was greater than 542 ksi.

4.2.2 Tension and Cyclic Tension Specimens

The specimen design for the tension and cyclic tension tests was that described by the ASTM Standard, D 3039-71T [2]. An example of a tension specimen is shown in Figure 1. The specimen nominally measured 10 inches long by 1.0 inch wide. Each end of the specimen had bonded on each side a 0.1 inch thick, tapered fiberglass tab (the bonding agent was EA-934 room temperature curing adhesive) with a five inch gage

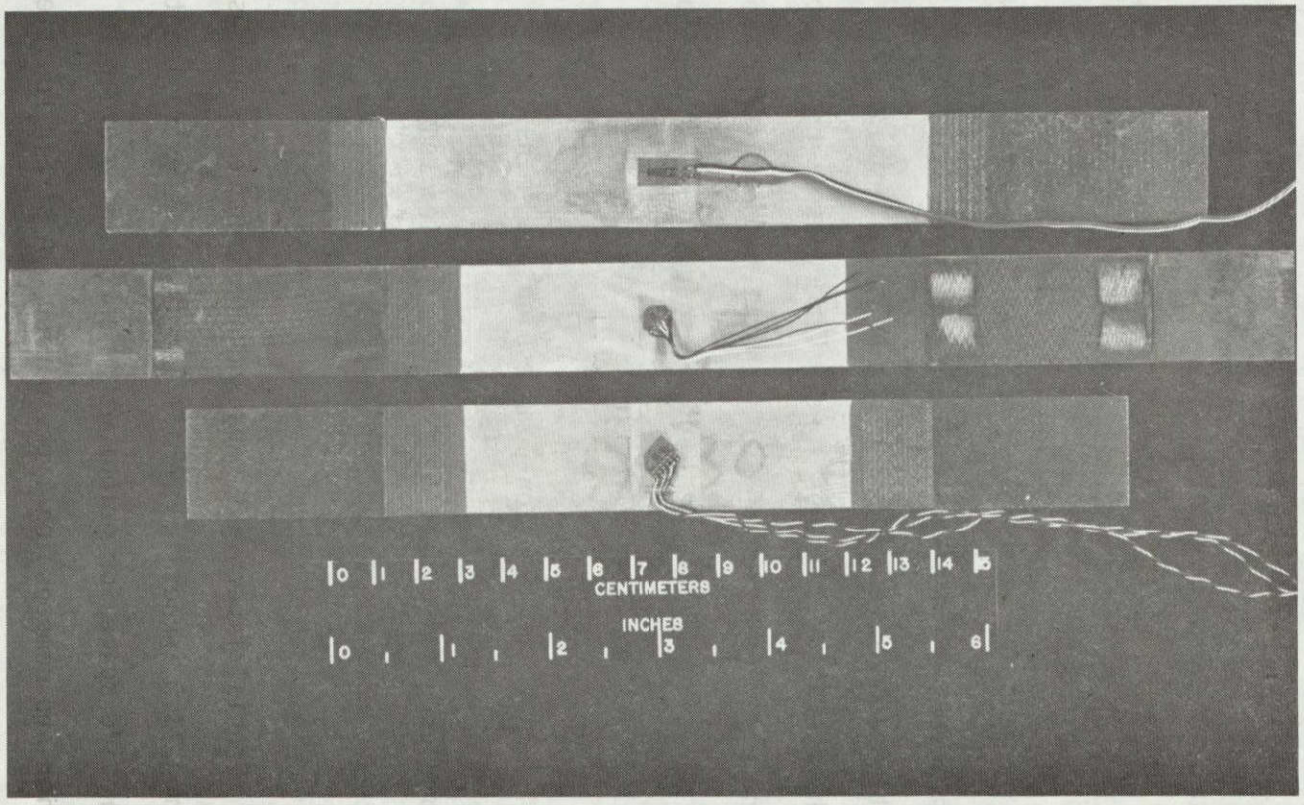

Figure 1. Example of specimen used for tension (top), tension-compression (middle) and compression (bottom) tests.

section remaining between the end tabs. On one side of the specimen, a strain rosette was bonded to the boron-aluminum measuring strain in directions 0°, 90°, and 45° to the loading axis. On the opposite side of the specimen a single gage was mounted measuring axial strain.

4.2.3 Compression and Cyclic Compression Specimens

The compression specimen used for this work is shown in Figure 1. The specimen had the same specimen design as that used by Grimes et al [22] in their investigation of resin matrix composite materials. The specimen is 1.0 inch wide and 8.5 inches long. Fiberglass tabs are bonded to the ends leaving a gage section of 3.5 inches. A small strain rosette was mounted to one side of the specimen with gages measuring deformation at 0°, 90°, and 45° to the load direction.

4.2.4 Cyclic Tension-Compression Specimens

The specimen used for cyclic tension-compression tests was again the same as used by Grimes. A typical specimen is shown in Figure 1. The boron-aluminum portion of the specimen was 8.5 inches in length and 1.0 inch wide. Special fiberglass tabs and steel spacers were used to make the specimen 11.0 inches in overall length. The extra length was necessary to provide space for gripping the specimen in order to facilitate both tension and compression type loading. A strain rosette was used to measure strain in the same manner as with the compression specimen.

4.3 Procedure for Heat Treating, Cleaning, and Cryogenic Exposure

The specimens alloted for each test type were divided into three groups representing different temper conditions. As mentioned previously, the three groups were boron-aluminum in the F or "as fabricated" condition, boron-aluminum with the aluminum matrix in a T6 heat treatment, and the third group was developed by adding the additional step to the T6 heat treatment procedure of placing the specimen in liquid nitrogen (-320° F) after heat treating. This step was performed to change the residual stress state in the laminate by cryogenic exposure.

As a first step toward heat treating, the entire group of specimens was cleaned by a standard aluminum cleaning process. This was necessary to remove any grease or residue which might react with the aluminum or boron at elevated temperature. The procedure used to clean the material was to place the specimens in a six percent solution of sodium hydroxide with water at room temperature for one minute, then into deionized water for two minutes. The next step was to put the same specimens in a solution of 48 percent nitric acid, four percent hydrofluoric acid, and 48 percent water at room temperature for five to ten seconds, and then rinse the specimens in deionized water for two minutes. Finally, the material was dipped in alcohol and blown dry. The cleaning procedures produced a stable oxide on the aluminum surface which acted as a protective coating for the aluminum alloy and boron fibers.

The procedure used for heat treating the boron-aluminum specimens was basically the same as that used when heat treating aluminum alloy plates. The boron-aluminum specimens were put in an oven at 980° F for 30 minutes and then quenched in distilled water at room temperature. The quenched specimens were then annealed at 350° F for eight hours. The resulting boron-aluminum specimen had an aluminum alloy matrix with a T6 heat treatment designation. When heat treating the specimens, extreme caution was taken to maintain precise temperatures and clean specimens. These precautions were necessary to guard against chemical reactions of the boron or aluminum with other elements enhanced by the high temperature environment. The modified T6 or T6N type of temper condition was formed by placing a specimen heat treated to a T6 condition into liquid nitrogen (-320° F) for five minutes.

4.4 Test Procedures

4.4.1 Tension and Compression Tests

The monotonic tension, cyclic tension, monotonic compression, and cyclic compression tests were performed on a 120,000 pound Baldwin Testing machine. Strain and load data were acquired using the Beckman Data Acquisition System at NASA Langley Research Center.

4.4.1.1 Tension and Cyclic Tension Tests

The tension and cyclic tension tests were performed according to the standards set forth in the tentative method of test for "Tensile

Properties of Oriented Fiber Composites" [21]. The load path for the cyclic tension tests of a laminate depended upon the results of the monotonic tension tests of that laminate. Some laminates were loaded to 25 percent of ultimate, 50 percent, 75 percent, and finally to failure; other laminates were tested with five cycles of loading with the maximum loads of the cycles being 20 percent, 40 percent, 60 percent, and 80 percent of predicted ultimate and then loading to failure.

4.4.1.2 Compression and Cyclic Compression Tests

The compression specimens were tested using a side-support steel testing fixture (Figure 2) to prevent premature failure by buckling. The surfaces of the side-support fixture adjacent to the compression specimen were sprayed with a Teflon lubricant to prevent the transfer of load into the fixture by friction. The fixture was then bolted together using 30 inch-pounds of torque on each bolt. The strain rosette was located on the specimen in such a way that it was under the cut out area of the side-support fixture and the lead wires were connected to the gage through a hole in the fixture as shown in Figure 2.

Load was introduced into the compression specimen directly through the ends; no gripping was necessary for compression tests. Monotonic compression tests were run on all laminates and these results were used to determine the load path for the cyclic compression tests. As with the tensile tests, some laminates were cycled four times and others were cycled five times with incremental percentage increases in load with each cycle.

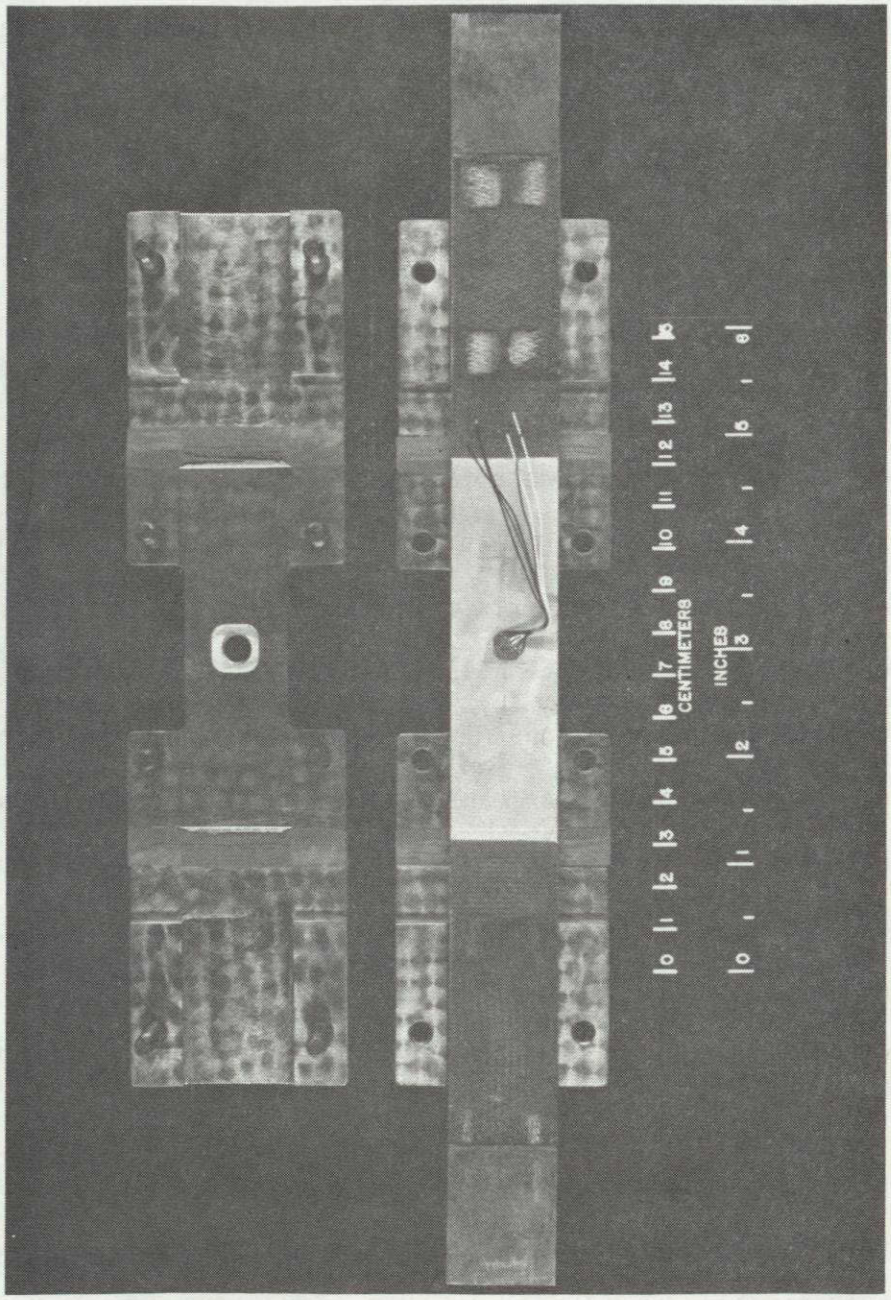

Figure 2. Steel side-support fixture used for compression and tension-compression tests. The cut out area in the center of the fixture (top) is for the strain gage.

4.4.2 Cyclic Tension-Compression Tests

An example of the cyclic tension-compression specimen and the side-support testing fixture is shown in Figure 2. Because the nature of the test involved testing in both tension and compression, it was necessary to use hydraulic grips which could apply both tensile and compressive loads to the specimen. These tests were performed using an MTS servo controlled, closed-looped tension-compression testing machine with MTS 50,000 pound hydraulic grips. Load and strain data were recorded on magnetic tape using a Vidar data acquisition system.

Ultimate strengths recorded from the monotonic compression and monotonic tension tests were used to determine the peak loads of the cycles. Usually the peak load of a cycle and the number of cycles were the same as those used for the cyclic compression and cyclic tension tests. A typical load path was to load the specimen in tension to 25 percent of tensile ultimate strength, then load in compression to 25 percent of the compressive ultimate strength, and then repeat the same procedure at 50 percent and 75 percent of the tensile and compressive ultimate strengths. Finally, the specimens were failed in tension. In some cases the cycle was reversed, introducing compressive loads first and tensile loads second; however, tensile failures were still sought.

5. RESULTS AND DISCUSSION

5.1 Introduction

This chapter presents a comparison of experimental results showing the effects of temper condition on the stress-strain behavior of the boron-aluminum laminates studied in this investigation. Stress-strain results are presented for monotonic tension and compression, cyclic tension, cyclic compression and cyclic tension-compression tests in Figures 4 through 24 and 26 through 60. Average material properties from the tests are tabulated in Tables 1 through 29.

Included in the tables of monotonic results are yield stress and strain denoted by σ_x^y and ε_x^y respectively, initial tangent modulus, E_x, and Poisson's ratio, ν_{xy}, and ultimate stresses and strains denoted with a superscript u. In addition, for the cyclic tension and cyclic compression tests, the tables present initial loading and initial unloading stiffness and Poisson's ratios for each cycle, denoted by E_x^L, E_x^{UL}, ν_{xy}^L, and ν_{xy}^{UL}, respectively. Also included are yield stresses and strains and the maximum stresses and strains (denoted by superscript m) for each cycle; the maximum values of the final cycle are the failure stresses and strains. The residual axial strain, ε_x^R, at the end of each cycle is also recorded. For the cyclic tension-compression tests, the maximum stresses and strains for both the tension and compression portions of each cycle are recorded, as are the initial loading and unloading tangent moduli.

Engineering properties as determined from the [0], [90], and

$[\pm 45]_s$* laminates are used in a laminate analysis program to predict engineering constants for the $[0/\pm 45/0]_s$, $[0/\pm 45]_s$, and $[\pm 45/0]_s$ laminates. These values are compared with experimental results.

As mentioned in Section 4.4.1.2, a side-supported compression specimen (Figure 2) was chosen for the compression and cyclic tension-compression tests. Results from these tests have indicated that this specimen is not completely satisfactory. The stress-strain diagrams and strain gages mounted on the side-support fixture indicate that, at the beginning of the test, some of the load is transferred into the fixture. A strain gage mounted on the side-support fixture measured a strain of 30 microinches at the very beginning of the test; this strain reading remained constant for the remainder of the test. Simple calculations predict this strain to be equivalent to a 600 pound reduction in the load applied to the specimen. This 600 pound reduction in load is reflected by the stress-strain diagram where the initial stiffness of the specimen was of the order 10^9 psi as compared to 10^7 psi for moduli of most composite laminates. That part of the stress-strain curve associated with loading of the fixture was ignored when tabulating results, and elastic moduli were computed from the adjacent portion of the curve. However, the compression and tension-compression curves presented in this report show the data exactly as it was recorded; no alterations have been made to account for loading of the fixture.

* used for determination of shear modulus of unidirectional material [23]

The effect of the side-support fixture is reflected by the initial portion of the stress-strain diagram for monotonic compression tests; the cyclic compression stress-strain diagrams show the fixture loading at the beginning of each cycle and unloading at the beginning of the unloading portion of each cycle. The effect of the fixture on the tension-compression stress-strain diagrams is also reflected in each cycle, but the fixture is loaded at the initial unloading portion of the tensile curve and unloaded when the compression load is initially reduced.

The transfer of load into the fixture affects the stress-strain diagrams by shifting part of the curve by an amount equivalent to the load in the fixture. Because the actual data from the test are presented in the figures, it was decided to present yield stress and strength data directly from the figures without adjusting the numbers. Thus, the yield stress and maximum stress results for the compression, compression-compression, and tension-compression tests differ from the actual values by an amount equivalent to the load in the fixture. Since this load was a constant for the entire test the trends exhibited by the data are not altered.

Comparison of the failure stresses from the compression tests with results reported in the literature [3,6,8,9,10] indicates that this side-support specimen results in lower compressive strengths than other reported values. The average compressive strength for all the tests of unidirectional material was 256 ksi; typical strength values reported in

the literature are 350 ksi or higher. Coupled with the fact that the strength was low compared to other reported results is the fact that all of the specimens tested in compression failed outside of the gage section. Usually, failure occurred at the end of the taper of the fiberglass tab by shearing of the laminate as shown in Figure 3; it is likely that failure occurred in this area because of insufficient lateral support. Another failure mode was brooming of the ends of the specimen.

Even though the side-support fixture takes load at the beginning of a compression test, the stress-strain data provides much valuable information. The low ultimate stresses did not present a major problem, as the major objective of this work was to investigate the nonlinear behavior of boron-aluminum.

A second problem associated with the design of the specimen was evident during the tension-compression tests. When testing the [0] and $[0/\pm45/0]_s$ laminates, the large tensile loads applied to the specimens caused debonding of the boron-aluminum from the fiberglass tabs. Usually this occurred before the test had progressed into the final cycle of the desired load path. In some cases new tabs were put on the specimen and the test was started at the cycle during which the debonding had occurred. In other cases the specimen was merely loaded in tension to failure. It is obvious that after the specimen debonded the continuous strain history was no longer available for additional tests since new strain gages were required.

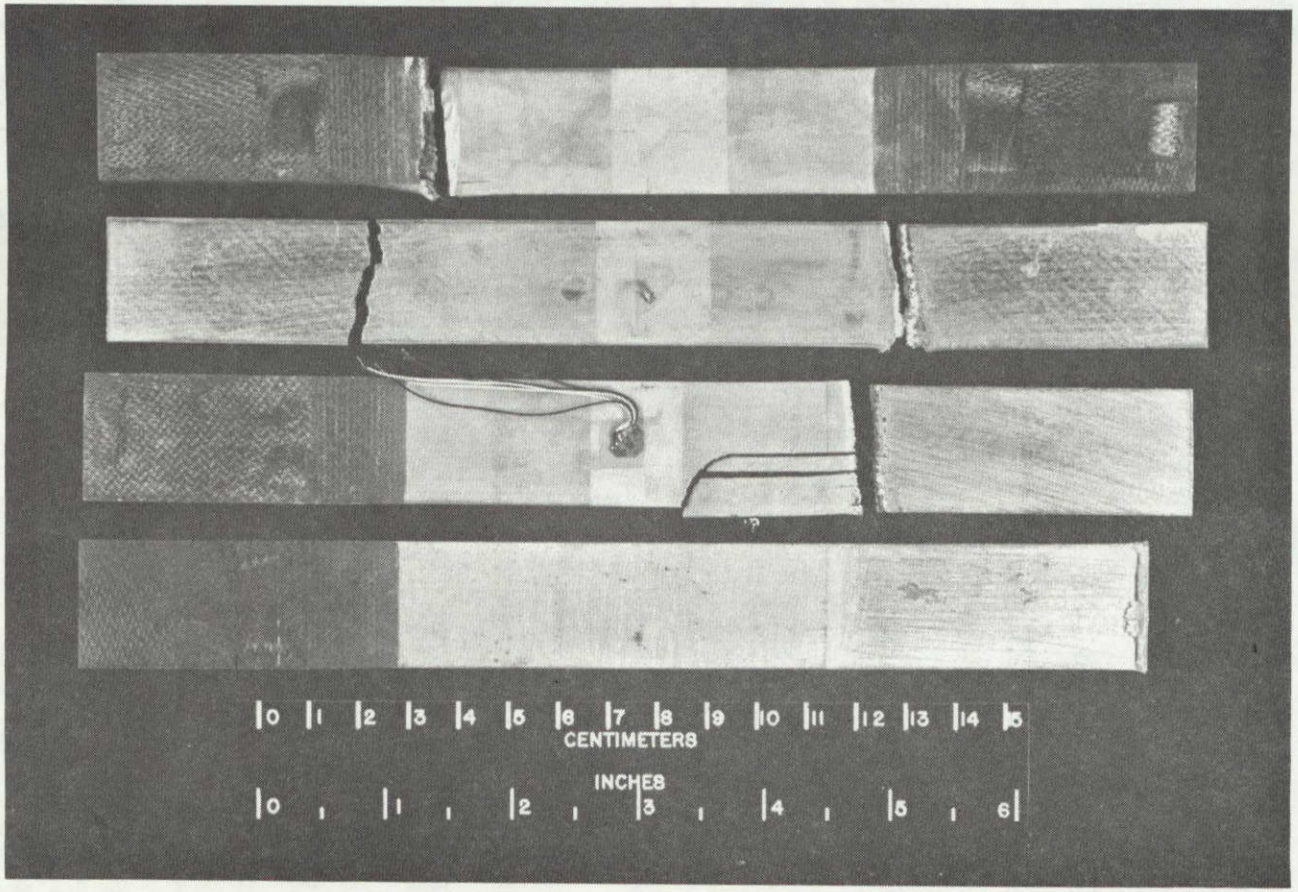

Figure 3. Examples of failed compression specimens exhibiting different failure modes. The top specimen shows the typical failure at the end of the tab. The second and third examples show compression failure and subsequent tensile failure from recoil of the specimen. The final specimen exhibits the brooming failure mode.

reduced, and strain hardening of the aluminum matrix increases the linear elastic range of the matrix. As a direct result of these changes, the linear region of the tensile stress-strain curve of the [0] laminate is increased. Table 1 shows results indicating that the yield stress is changed significantly by cryogenic exposure of the [0] laminate for all three heat treatments.

Figure 4 shows the variation of the tensile stress-strain curves for [0] boron-aluminum after various temper conditionings, and Table 1 lists numerical results from the tests.

The elastic moduli for the tensile tests did not change significantly with temper conditon, it ranged from 32.2 Msi to 33.7 Msi. The rule of mixtures modulus prediction for a fiber modulus of 58 Msi and a matrix modulus of 10 Msi is 32.8 Msi, which compares well with experimental results. Varying the temper condition from the F condition increased the yield stress of the unidirectional material but reduced the strength. The average yield stress for the F condition specimens was 29.0 ksi as compared to 43.0 ksi for the T4 condition specimens and 80.4 ksi for the T6 condition specimens. The yielding of the unidirectional material is primarily due to the nonlinear behavior of the aluminum matrix. The experimental yield stress values are as expected since T6 condition aluminum has the highest yield stress, F condition (the F condition from diffusion bonding closely resembles an "overaged" temper condition) aluminum the lowest yield stress, and T4 condition aluminum an intermediate value. The cyrogenic exposure of the F, T4, and T6 condition material further increased the yield stresses to 69.3

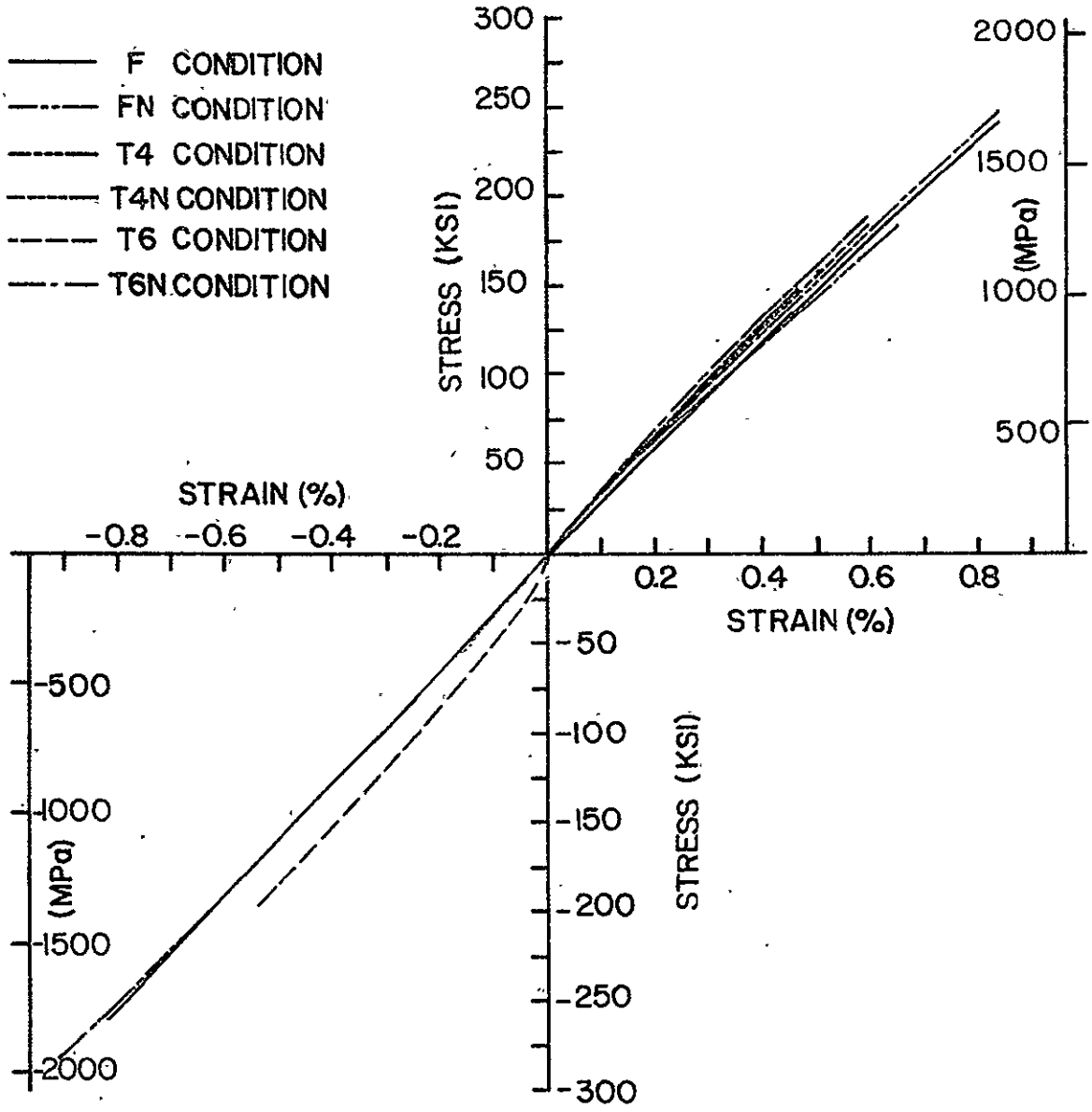

FIGURE 4. COMPARISON OF $[0_8]$ B/Al LAMINATE WITH DIFFERENT TEMPER CONDITIONS IN TENSION AND COMPRESSION.

TABLE 1

INFLUENCE OF TEMPER CONDITION ON THE TENSILE STRESS-STRAIN BEHAVIOR OF UNIDIRECTIONAL BORON-ALUMINUM

TEMPER CONDITION	E_x (Msi)	ν_{xy}	σ_x^y (ksi)	ε_x^y (%)	σ_x^u (ksi)	ε_x^u (%)	ε_y^u (%)
F	33.0	- *	29.0	0.094	253.	0.886	-0.246
FN	32.9	0.218	69.3	0.214	231.	0.783	-0.207
T4	33.1	0.251	43.0	0.133	192.	0.671	-0.196
T4N	32.2	0.233	90.6	0.284	162.	0.534	-0.124
T6	33.7	0.237	80.4	0.243	185.	0.613	-0.145
T6N	33.1	0.213	117.1	0.356	176.	0.556	-0.132

*Transverse strain data was not available

ksi, 90.6 ksi, and 117.1 ksi, respectively as explained previously in this section.

A significant decrease in strength, as compared to the F condition material, was exhibited by the unidirectional material which had been heat treated. A portion of this decrease can be attributed to increases in the residual stress due to heat treating; however, the magnitude of the decrease in strength cannot be entirely due to higher residual stresses. It is possible that part of the strength reduction is due to fiber degradation and interfacial bond damage which developed during the heat treating and the reduced ultimate strain of T4 and T6 condition aluminum. The strength results also indicate that cryogenic exposure of the specimens further decreased the failure stress because of the reduced axial compressive residual stress in the fibers.

The influence of temper condition on the compressive stress-strain behavior of unidirectional boron-aluminum is shown in Figure 4; Table 2 contains the associated numerical results. The stress-strain curve up to approximately 15 ksi was not used in tabulating results because load was being transferred into the fixture. The elastic moduli were computed from the portion of the curve above 15 ksi up to the yield stress; the modulus values for the F, T6, and T6N condition were 31.5 Msi, 34.3 Msi, and 31.6 Msi, respectively. Assuming that compression specimens did not yield in the initial portion of the curve up to 15 ksi, the modulus results from the unidirectional monotonic tension and compression tests do not exhibit higher moduli in compression than in tension as reported in Reference 8.

TABLE 2

INFLUENCE OF TEMPER CONDITION ON THE COMPRESSIVE STRESS-STRAIN BEHAVIOR OF UNIDIRECTIONAL BORON-ALUMINUM

TEMPER CONDITION	E_x (Msi)	ν_{xy}	σ_x^y * (ksi)	ε_x^y (%)	σ_x^u * (ksi)	ε_x^u (%)	ε_y^u (%)
F	31.5	0.282	-69.3	-0.204	-280.	-0.888	0.275
T6	34.3	0.202	-170.2	-0.450	-202.	-0.539	0.128
T6N	31.6	0.197	-54.0	-0.159	-277.	-0.890	0.245

* Fixture influence

Unlike the [0] laminate tension tests where the yield stress was increased 50 to 100 percent by cryogenic exposure, the compression tests show the T6N condition specimens to have a yield stress which is one third that of the T6 condition specimens. The cryogenic exposure reduces reduces the residual axial compressive stress in the fibers and decreases the tensile axial residual stress in the matrix reducing the compressive linear elastic range of the matrix and thus the composite.

Maximum stresses and strains are listed in Table 2, but they are not believed to be the true strengths of the [0] laminates, for the reasons discussed in section 5.1.

5.2.2 Cyclic Tests

5.2.2.1 Tension

Figures 5, 7, and 9 show the typical stress-strain behavior of [0] boron-aluminum under tensile cyclic loading and Table 3 contains the numerical results for F condition, T4N condition, and T6N condition specimens, respectively. Specimens were not available for use with a T6 condition, so as a third case specimens with a T4N condition were tested. The maximum nominal stresses for the first three cycles were 44 ksi, 88 ksi, and 132 ksi; all cyclic tension tests on unidirectional boron-aluminum were cycled at these maximum stress levels.

For the F condition laminate (Figure 5), the specimen yields on the first cycle of loading at 20.2 ksi; on the second cycle the yield stress is approximately the same as the maximum stress of the previous cycle indicating some strain hardening occurred, upon unloading during the

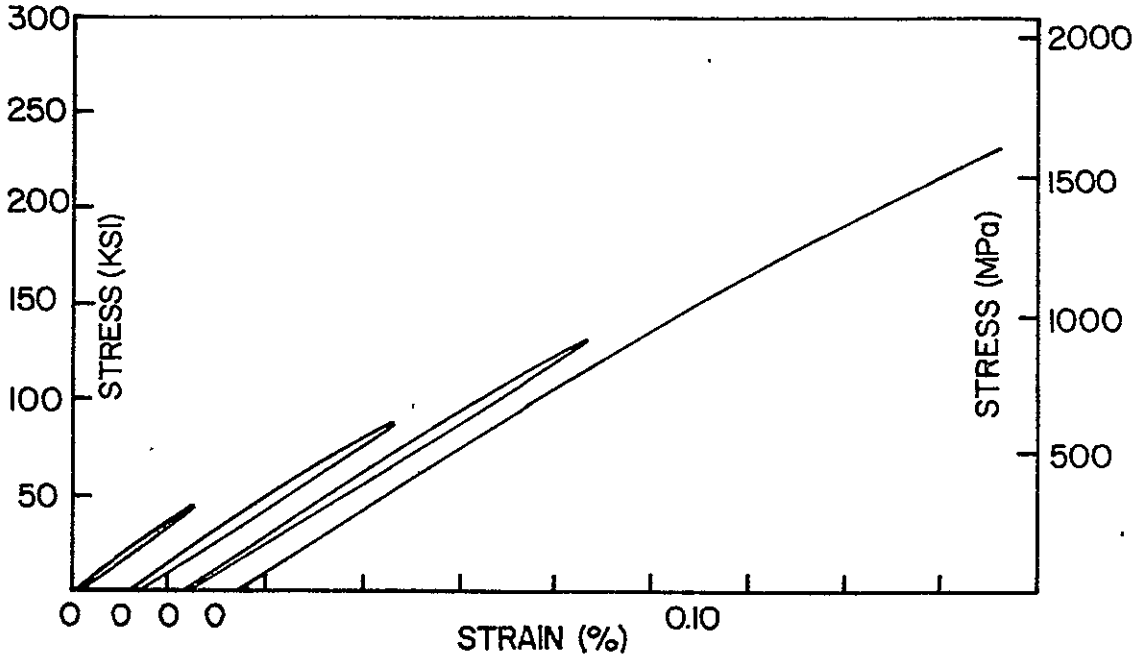

FIGURE 5. CYCLIC TENSION STRESS-STRAIN DIAGRAM FOR F CONDITION $[0_8]$ B/Al LAMINATE.

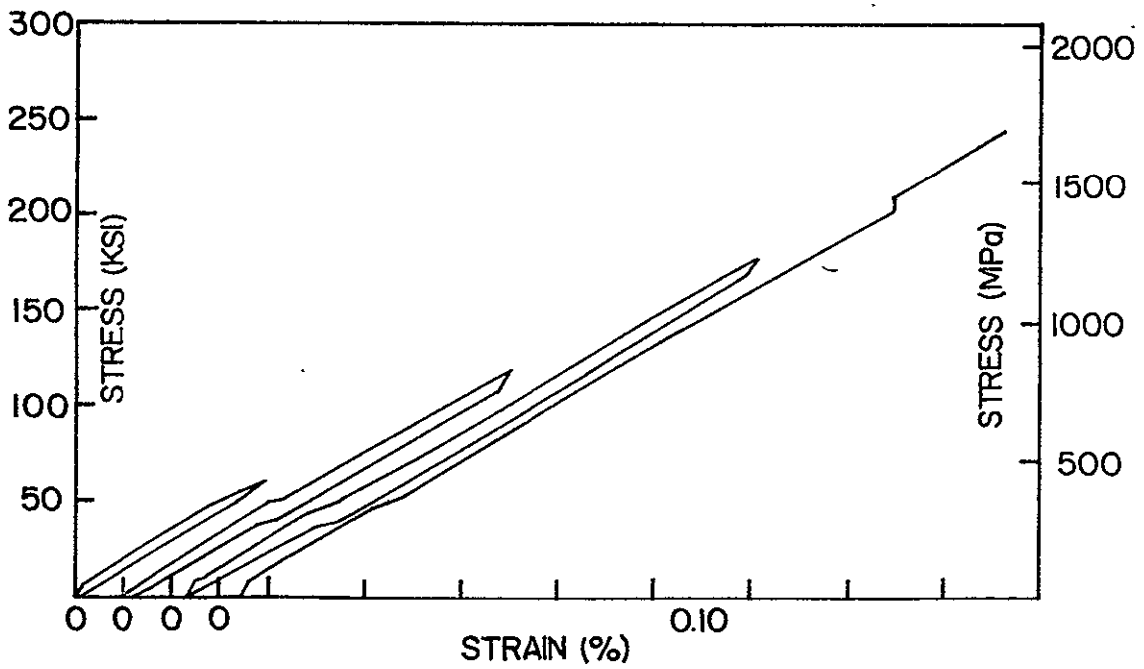

FIGURE 6. CYCLIC COMPRESSION STRESS-STRAIN DIAGRAM FOR F CONDITION $[0_6]$ B/Al LAMINATE.

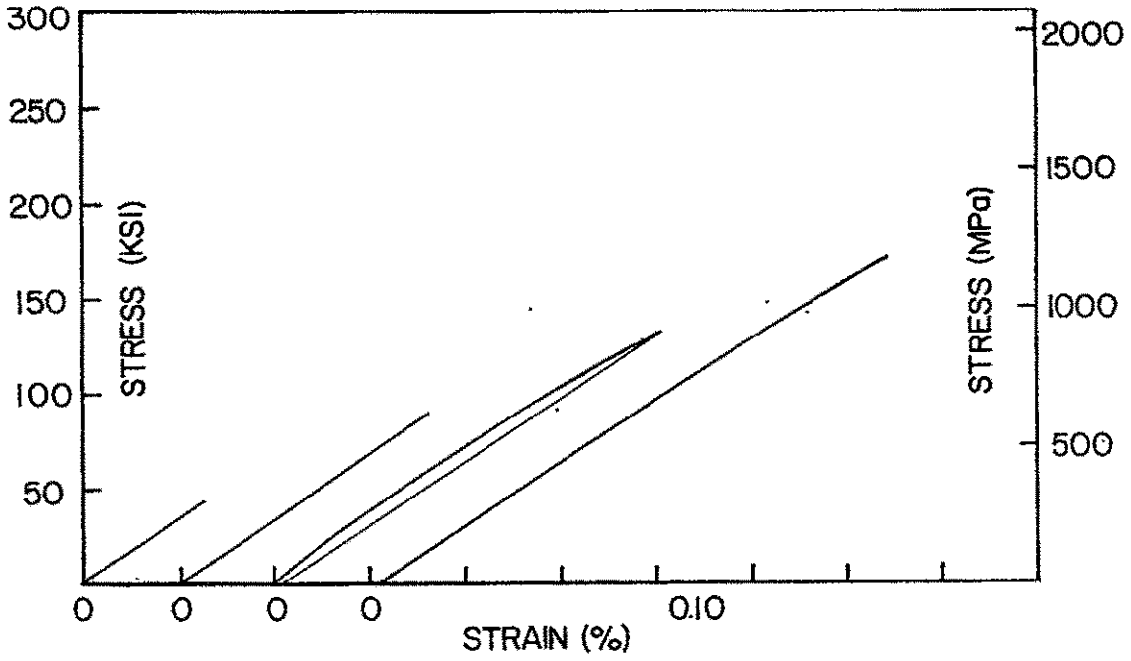

FIGURE 7. CYCLIC TENSION STRESS-STRAIN DIAGRAM FOR $[0_8]$ B/Al LAMINATE, MODIFIED T4 CONDITION.

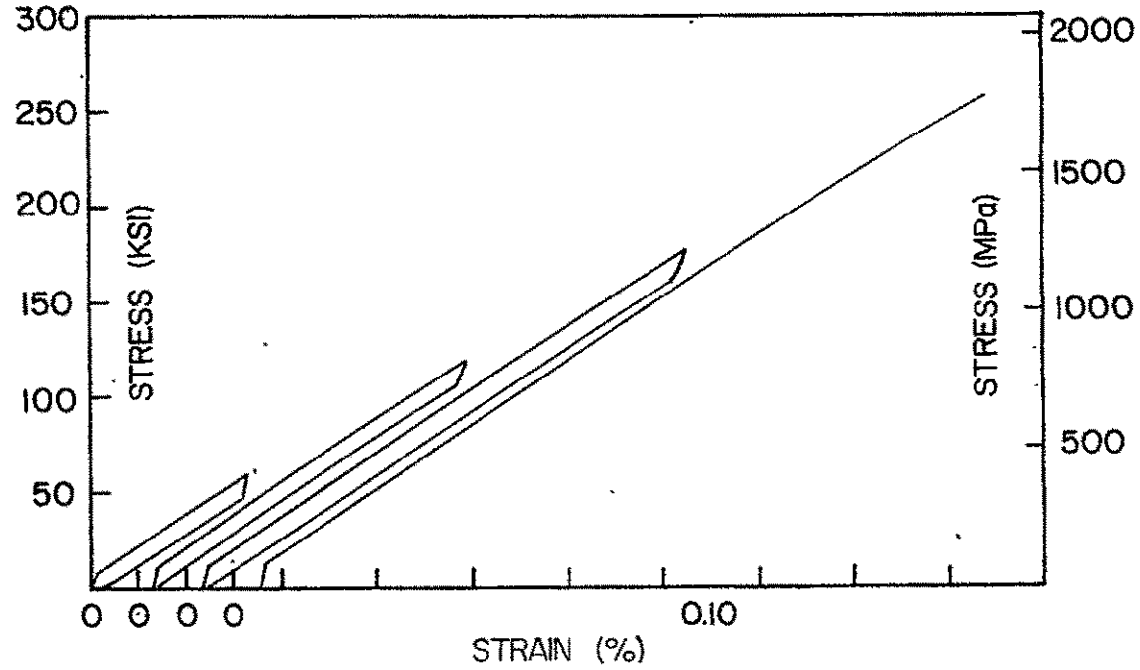

FIGURE 8. CYCLIC COMPRESSION STRESS-STRAIN DIAGRAM FOR $[0_6]$ B/Al LAMINATE, T6 CONDITION.

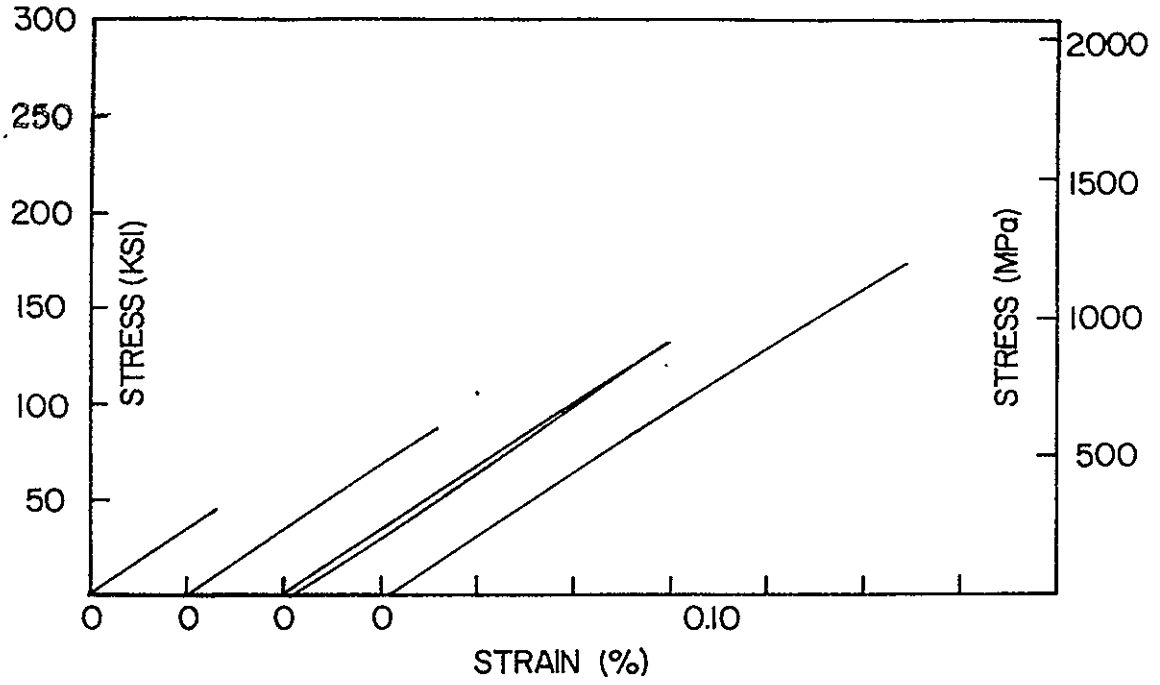

FIGURE 9. CYCLIC TENSION STRESS-STRAIN DIAGRAM FOR $[0_8]$ B/Al LAMINATE, MODIFIED T6 CONDITION.

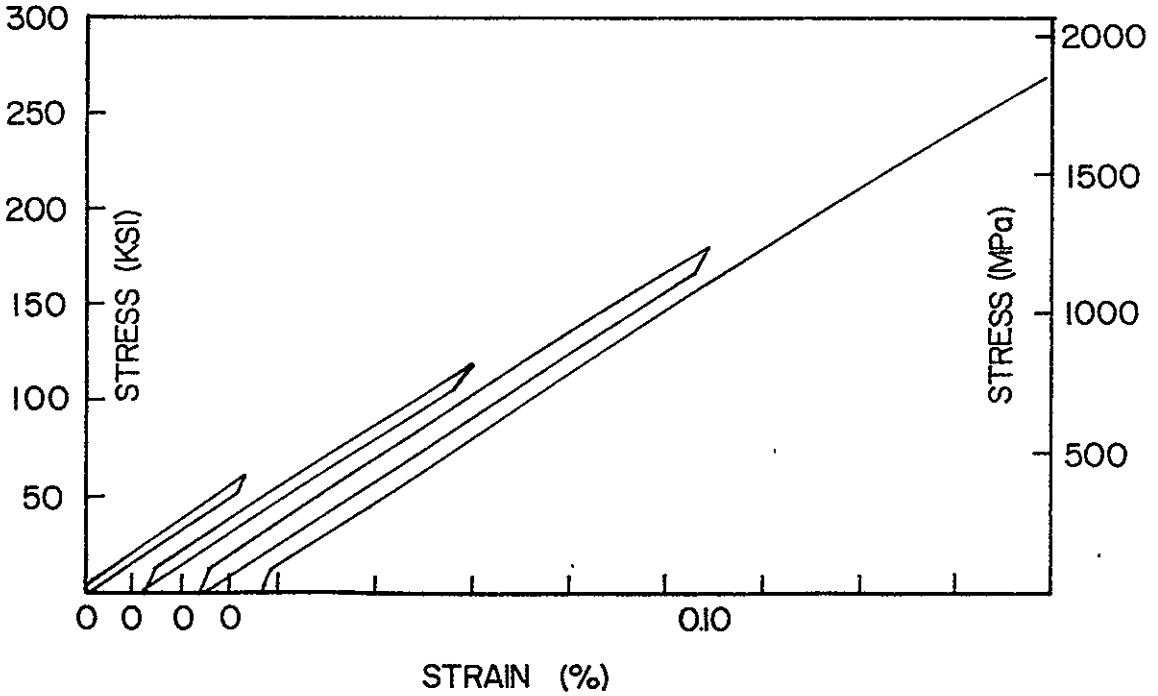

FIGURE 10. CYCLIC COMPRESSION STRESS-STRAIN DIAGRAM FOR $[0_6]$ B/Al LAMINATE, MODIFIED T6 CONDITION.

TABLE 3

INFLUENCE OF TEMPER CONDITION ON THE CYCLIC TENSION STRESS-STRAIN BEHAVIOR OF UNIDIRECTIONAL BORON-ALUMINUM

TEMPER CONDITION	CYCLE	E_x^L (Msi)	E_x^{UL} (Msi)	ν_{xy}^L	ν_{xy}^{UL}	σ_x^y (ksi)	ε_x^y (%)	σ_x^m (ksi)	ε_x^m (%)	ε_y^m (%)	ε_x^R (%)
F	I	36.0	34.4	0.281	0.229	20.2	0.056	43.6	0.132	-0.039	0.006
	II	34.0	33.5	0.239	0.245	46.3	0.144	88.6	0.286	-0.084	0.016
	III	33.7	33.2	0.239	0.239	65.3	0.216	132.2	0.436	-0.129	0.021
	IV	33.6	-	0.243	-	67.0	0.224	235.3	0.813	-0.238	-
T4N	I	33.0	34.4	0.212	0.220	-	-	44.2	0.131	-0.032	0.000
	II	32.7	33.7	0.214	0.213	-	-	88.5	0.265	-0.063	0.000
	III	33.5	33.4	0.214	0.221	98.0	0.299	132.7	0.409	-0.100	0.009
	IV	33.4	-	0.214	-	136.1	0.423	171.0	0.543	-0.135	-
T6N	I	32.0	33.8	0.238	0.234	-	-	44.5	0.133	-0.033	0.000
	II	33.7	34.0	0.231	0.231	-	-	89.1	0.268	-0.064	0.000
	III	33.6	33.9	0.231	0.233	-	-	133.5	0.405	-0.098	0.000
	IV	33.6	-	0.230	-	138.8	0.425	174.2	0.545	-0.138	-

second cycle the stress-strain diagram exhibits linear behavior from the maximum stress of the cycle down to 22 ksi a range of approximately 66 ksi. The yield stress on the third cycle was 65 ksi and for the unloading portion the linear region extended from the maximum stress over a region of 65 ksi. On the fourth cycle the yield stress was 67 ksi and the specimen failed at 235 ksi. The results of this test and similar tests on F condition [0] boron-aluminum indicate that at linear range of 65 to 70 ksi is the maximum attainable by cycling in tension.

The stiffness and Poisson's ratio of the unidirectional material was computed for the initial loading portion and the initial unloading portion of each cycle. The moduli for the F condition specimens exhibited a decreasing modulus as the magnitude of the cycles was increased; the modulus on the first cycle was 36.0 Msi and the modulus on the final cycle was 33.6 Msi.

The typical cyclic tension stress-strain behavior of unidirectional boron-aluminum with a T4N temper condition is shown in Figure 7. The specimen did not yield during the first two cycles, and the unloading was linear for both cycles. On the third cycle the specimen yielded at 98.0 ksi; on the fourth cycle the yield stress was 136.1 ksi, approximately the same stress as the maximum stress of the third cycle.

The cyclic stress-strain behavior of the T6N condition material is shown in Figure 9, numerical results are also in Table 3. The specimen loaded and unloaded linearly for the first three cycles, but the fourth and final cycle yielded at a stress of 138.8 ksi and failed at 174.2 ksi. Modulus values for loading and unloading ranged from 32.0 Msi to

34.0 Msi and Poisson's ratio ranged from 0.238 to 0.230; the modulus and Poisson's ratio data did not exhibit any pattern.

Comparison of the cyclic tension stress-strain diagrams for specimens having different temper conditions is consistent with the data from the monotonic tests; that is, heat treating the F condition unidirectional material resulted in higher yield stress and lower strength, and cryogenic exposure produced even higher yield stress and slight reductions in strength. The additional information gained from the cyclic tests characterized the strain hardening behavior of the specimens. The F condition material initially yielded at a lower stress level than the specimens with stronger matrix, and further cycling developed a linear range of 65-70 ksi during both the loading and unloading portions of the cycles. The heat treated specimens yielded at higher stress levels than the F condition material; the T6N condition material did not yield until the final cycle and hence its strain hardening behavior is not determined. However, the T4N condition specimen did yield on the third cycles, unloaded linearly, and on the fourth cycle did not yield until the highest previous stress level.

5.2.2.2 Compression Tests

The typical compressive, cyclic stress-strain behavior of unidirectional boron-aluminum with an F, T6, and T6N condition is shown in Figures 6, 8, and 10; numerical results are in Table 4. Specimens representing the three temper conditions were successively cycled to 60 ksi; 120 ksi, 180 ksi; and finally to failure.

TABLE 4

INFLUENCE OF TEMPER CONDITION ON THE CYCLIC COMPRESSION STRESS-STRAIN BEHAVIOR OF UNIDIRECTIONAL BORON-ALUMINUM

TEMPER CONDITION	CYCLE	E_x^L (Msi)	E_x^{UL} (Msi)	ν_{xy}^L	ν_{xy}^{UL}	σ_x^{y} * (ksi)	ε_x^y (%)	σ_x^{m} * (ksi)	ε_x^m (%)	ε_y^m (%)	ε_x^R (%)
F	I	31.9	31.5	0.196	0.185	-	-	-59.7	-0.198	0.033	-0.005
	II	31.6	31.8	0.194	0.232	-66.2	-0.223	-119.1	-0.403	0.093	-0.014
	III	31.6	32.4	0.197	0.232	-123.5	-0.417	-178.1	-0.610	0.156	-0.016
	IV	31.3	-	0.192	-	-112.7	-0.383	-252.8	-0.837	0.249	-
T6	I	32.7	32.8	0.227	0.225	-	-	-59.5	-0.163	0.035	-0.013
	II	33.8	33.1	0.226	0.222	-	-	-118.7	-0.342	0.075	-0.015
	III	33.3	33.7	0.221	0.230	-150.0	-0.437	-177.8	-0.526	0.120	-0.024
	IV	33.3	-	0.221	-	-184.1	-0.546	-258.4	-0.792	0.199	-
T6N	I	33.1	32.9	0.211	0.212	-	-	-59.9	-0.168	0.036	-0.005
	II	33.4	33.4	0.212	0.219	-86.3	-0.249	-120.2	-0.353	0.081	-0.012
	III	33.3	33.5	0.218	0.212	-123.4	-0.363	-179.0	-0.545	0.134	-0.028
	IV	33.3	-	0.214	-	-190.5	-0.583	-282.0	-0.889	0.239	-

* Fixture influence

The F condition specimens showed very unusual behavior as seen from Figure 6. At approximately the same stress level on both the loading and unloading portion of each cycle the curve showed a sudden slope change and then returned to the previous slope. On the fourth cycle the specimen showed a sharp increase in slope at a stress level of 210 ksi. This phenomenon was unique to the F condition unidirectional material; no explanation is offered for this behavior, but it would seem likely that it is related to specimen and fixture design rather than material behavior.

Neglecting the initial -15 ksi of the stress-strain curve where the fixture was taking load and the sudden change in slope, the F condition cyclic compression specimens behaved very similar to the F condition cyclic tension specimen. The modulus values ranged from 31.3 Msi to 32.4 Msi and Poisson's ratio varied from 0.185 to 0.232. The F condition material did not yield on the first cycle; on the second cycle it yielded at -66.2 ksi and unloaded linearly; on the third cycle it yielded at approximately the highest stress level of the previous cycle, -123.5 ksi and unloaded nonlinearly with a linear range of 110 ksi. On the fourth cycle it yielded at approximately the same stress level, -112,7 ksi and finally failed at -252.8 ksi.

The typical cycle compression stress-strain behavior of a T6 condition unidirectional boron-aluminum specimen is shown in Figure 8. The T6 condition material did not yield on the first two cycles and on the third yielded at -150.0 ksi; on the fourth and final cycle it yielded at -184.1 ksi near the previous highest stress level. Modulus values for

loading and unloading varied from 32.7 Msi to 33.8 Msi. Small residual strains were recorded at the end of the first two cycles; these strains are not believed to represent any permanent deformation, rather they would appear to be due to the side-support fixture or experimental error.

Figure 10 shows the cycle compression stress-strain behavior of T6N condition unidirectional boron-aluminum. The moduli and Poisson's ratios of the cycles (Table 4) ranged from 32.9 Msi to 33.5 Msi and 0.211 to 0.219, respectively. Yielding of the T6N condition did not occur until the second cycle at -86.3 ksi. On the third and fourth cycles, the yield stress was approximately the maximum stress of the previous cycle, in all cases the unloading portion of the curve was linear.

The cyclic compression results for the unidirectional boron-aluminum are consistent with the results of the monotonic compression tests. As with the monotonic tests, the T6 condition specimens had a higher yield stress than the T6N condition specimens. Similar to the cyclic tension tests, the yield stress of the F condition cyclic compression specimen did not increase with each cycle, instead a linear range of 110 ksi to 125 ksi was exhibited by both the loading and unloading portion of the cycles. Peculiar to the F condition cyclic compression specimens was the abrupt slope change of each test at approximately the same stress level. As with all of the compression data, ultimate stresses and strains are reported, but peculiarities of the fixture invalidate these results as material properties.

5.2.2.3 Cyclic Tension - Compression Tests

Typical cyclic tension-compression stress-strain curves for F, T6 and T6N condition unidirectional boron-aluminum are shown in Figures 11, 12, and 13 and Table 5. The typical load path for the tension-compression tests was to load in tension to 60 ksi, then to -60 ksi in compression, then increase the stress level to 120 ksi and 180 ksi following the same tension, compression path for the second and third cycles, and finally fail the specimen in tension on the fourth cycle. For the F and T6 condition specimens, three complete cycles were run on the specimens and on the fourth cycle the fiberglass tabs debonded from the boron-aluminum while in tension. The T6N condition specimen was tested through two complete cycles and on the third cycle the tabs debonded. The concluding cycles for all three specimens were pure tension loading to failure. For some of these final tensile cycles, failure did not occur because the load required to fail the specimens was out of the load range of the machine.

The cyclic tension-compression stress-strain behavior of the F condition material (Figure 11, Table 5) yields additional information to clarify the nonlinear loading and unloading behavior of the F condition unidirectional material tested in tension and compression; the material exhibits a Baushinger effect [24], that is upon loading into the inelastic region in tension, the compressive yield stress is reduced. On the first cycle of the F condition specimen tension-compression test, the tensile yield stress is 35.3 ksi which corresponds well with the mono-

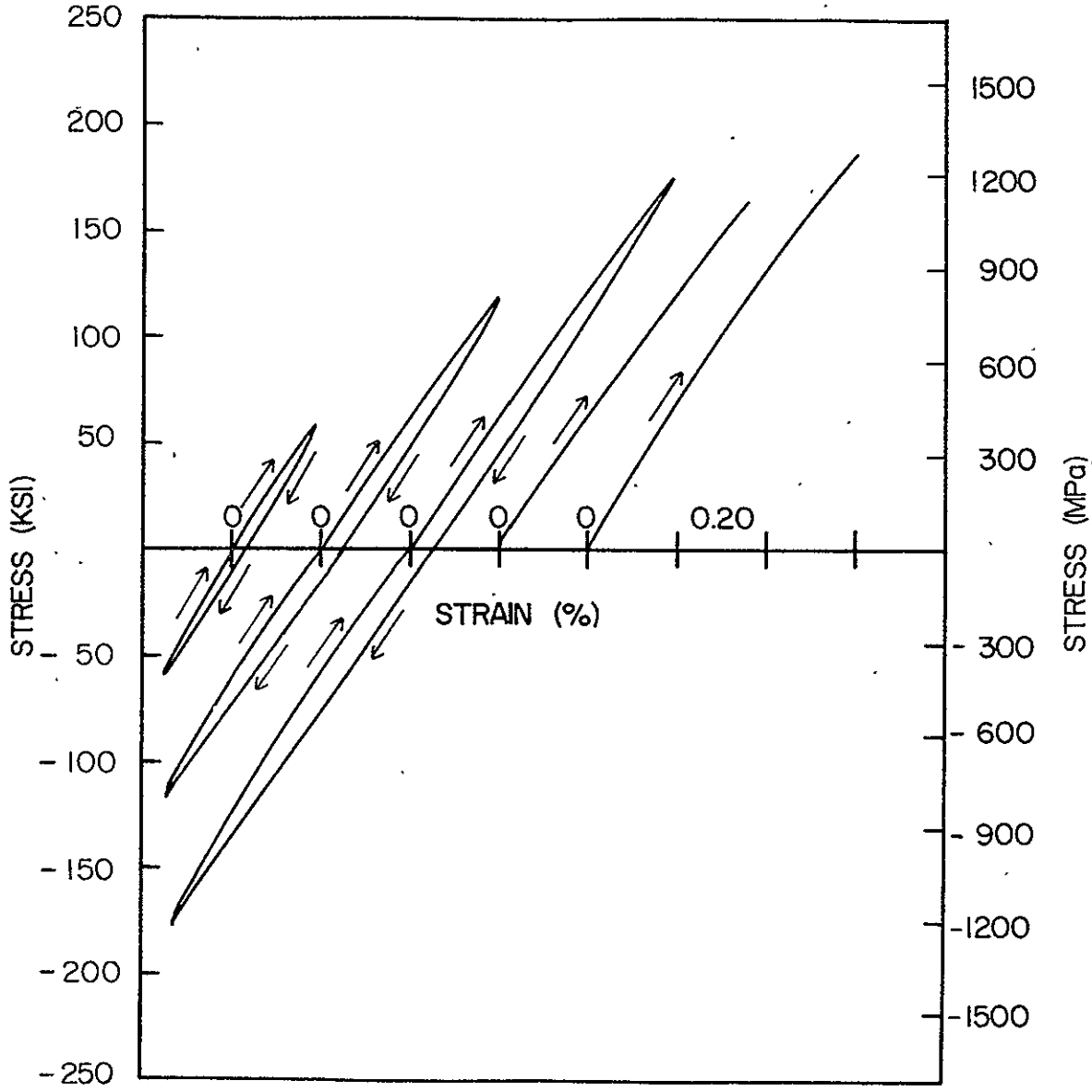

FIGURE 11. CYCLIC TENSION-COMPRESSION STRESS-STRAIN DIAGRAM FOR $[0_6]$ B/Al LAMINATE, F CONDITION.

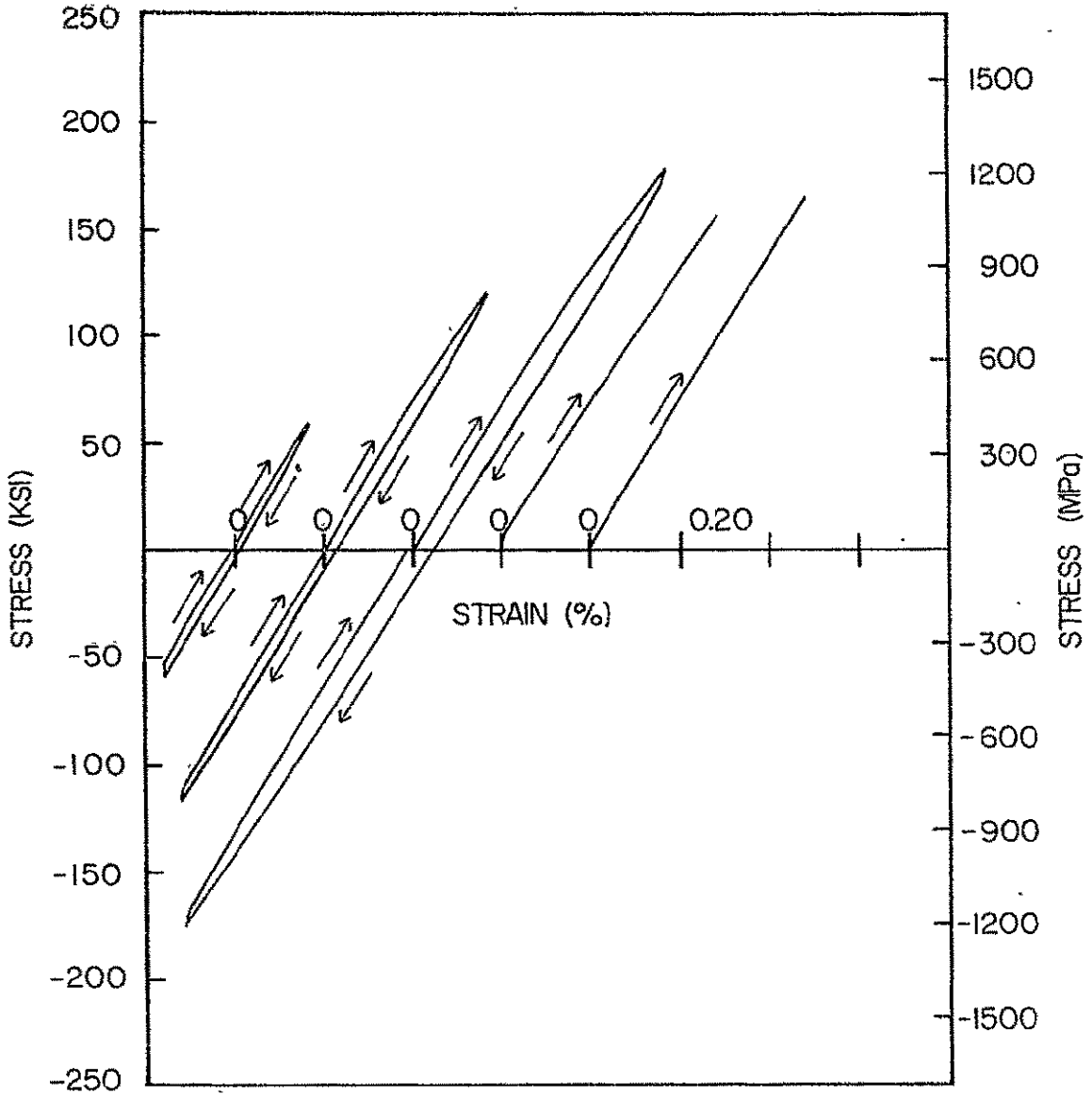

FIGURE 12. CYCLIC TENSION–COMPRESSION STRESS-STRAIN DIAGRAM FOR $[0_6]$ B/Al LAMINATE, T6 CONDITION.

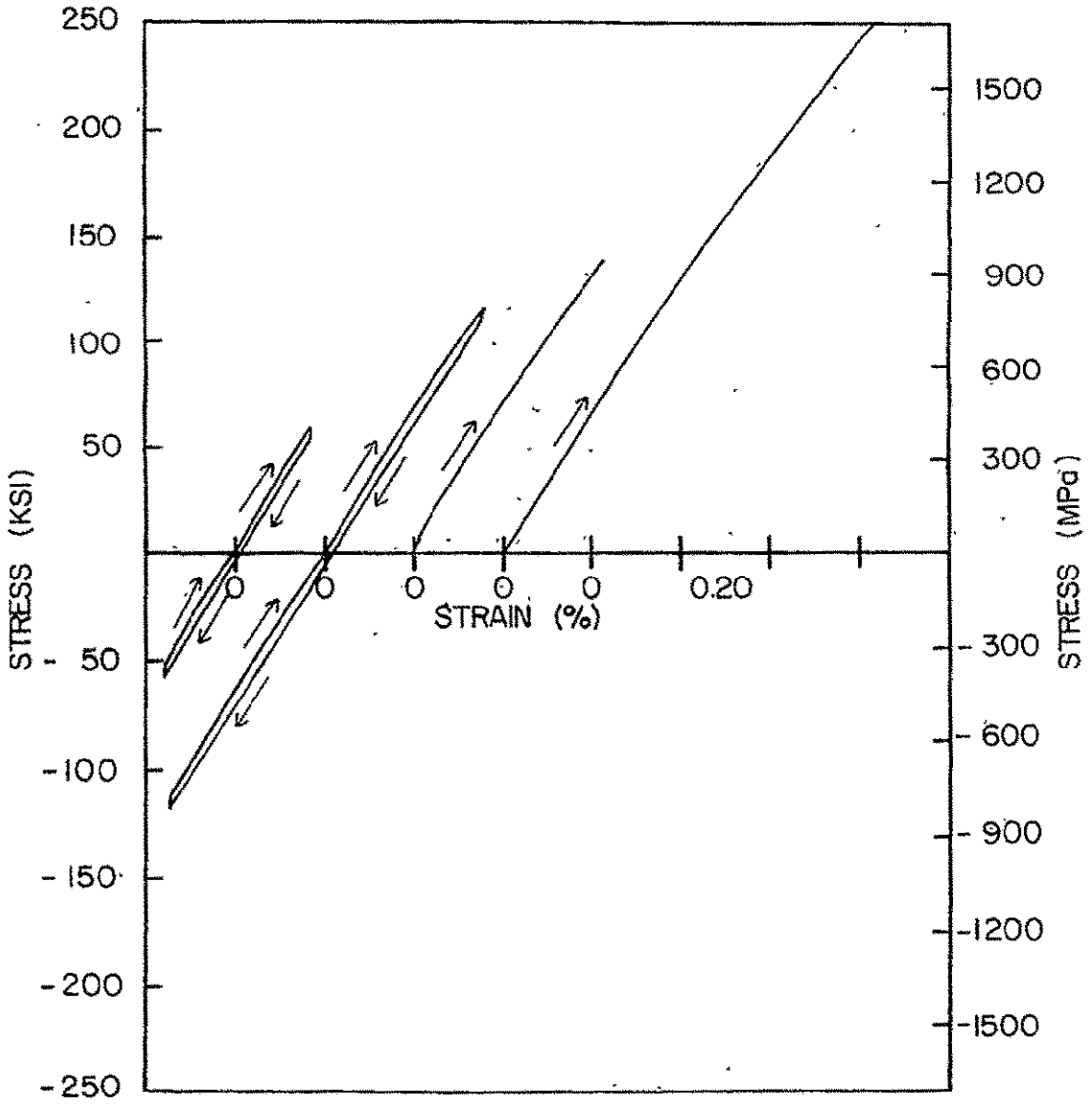

FIGURE 13. CYCLIC TENSION-COMPRESSION STRESS-STRAIN DIAGRAM FOR $[0_6]$ B/Al LAMINATE, T6N CONDITION.

TABLE 5

INFLUENCE OF TEMPER CONDITION ON THE TENSION-COMPRESSION STRESS-STRAIN BEHAVIOR OF UNIDIRECTIONAL BORON-ALUMINUM

TEMPER CONDITION	CYCLE	E_x^L (Msi)	E_x^{UL} (Msi)	σ_x^{m*} (ksi)	ε_x^m (%)	ε_y^m (%)	ε_x^R (%)
F	I-T	30.9	34.1	58.8	0.184	-0.045	0.040
	I-C	34.1	34.1	-58.5	-0.152	0.032	-0.033
	II-T	32.9	33.6	119.1	0.392	-0.105	0.036
	II-C	29.9	35.1	-119.5	-0.349	0.080	-0.005
	III-T	33.3	33.8	177.5	0.592	-0.162	0.056
	III-C	30.2	35.7	-177.9	-0.530	0.139	-0.009
	IV-T	28.8	-	174.9	0.628	-0.141	-
	V-T	34.7	-	187.3	0.585	-0.152	-
T6	I-T	33.8	34.4	60.0	0.168	-0.038	0.013
	I-C	34.4	34.4	-60.1	-0.163	0.032	-0.007
	II-T	34.2	34.2	119.2	0.362	-0.091	0.031
	II-C	34.2	36.2	-119.3	-0.326	0.061	-0.002
	III-T	33.3	33.8	177.8	0.564	-0.150	0.054
	III-C	32.8	35.2	-178.2	-0.508	0.109	-0.003
	IV-T	32.5	-	159.2	0.553	-0.125	-
	V-T	34.2	-	107.9	0.331	-0.065	-
	VI-T	33.3	-	165.0	0.487	-0.092	-
	VII-T	33.4	-	158.9	0.534	-	-
T6N	I-T	33.7	33.7	59.4	0.169	-0.038	0.006
	I-C	33.7	33.7	-59.1	-0.167	0.033	-0.008
	II-T	33.7	33.2	118.4	0.355	-0.079	0.012
	II-C	33.2	34.1	-118.5	-0.347	0.075	-0.013
	III-T	30.8	-	142.4	0.479	-0.092	-
	IV-T	32.8	-	255.1	0.759	-0.192	-

* Fixture influence

tonic tensile tests; however, on the compression side of the curve the yield stress is 34.0 ksi, almost half of the yield stress recorded from the monotonic compression tests. Upon unloading from the maximum compressive stress of the first cycle into tension on the second cycle, the stress-strain curve is linear up to 40.7 ksi, a range of approximately 100 ksi. This linear elastic range of 100 ksi is maintained for the remainder of the test. Upon loading in compression on the second and third cycles and loading in tension on the fourth cycle, the modulus decreases to approximately 29.5 Msi; this is a result of the fact that the specimen is loaded beyond the linear elastic range and it is responding inelastically to load. The rule of mixtures with the matrix being perfectly plastic gives a stiffness of 28.8 Msi and the experimental stiffness is 29.5 Msi, a 2 percent variation.

On the fourth cycle of the test, the fiberglass tabs debonded from the specimen, and on the fifth cycle the specimen was failed in tension at 187.3 ksi.

The T6 condition specimen (Figure 12, Table 5) responded linearly during the first cycle and on the second cycle the tensile yield stress was 51.5 ksi and unloading was linear from the maximum tensile stress to the maximum compressive stress. The unloading portion of the compression curve was linear also. On the third cycle the specimen yielded in tension at 119.8 ksi, the highest previous stress level, and then unloaded into compression until it yielded at -38.7 ksi, a range of 217 ksi. As with the F condition specimen, the compressive yield stress was lower in the third cycle as compared to the second indicating that the

material exhibits a Baushinger effect.

On the fourth cycle the specimen was to be failed in tension; however, the tabs debonded from the specimen. New tabs and strain gages were put on the specimen, and on the fifth cycle the tabs debonded again; it was then decided to test the specimen without fiberglass tabs. On the sixth cycle the maximum load of the machine did not fail the specimen and finally on the seventh cycle the specimen failed at 158.9 ksi. The fifth and sixth cycles have been omitted from Figure 12, but the numerical results are reported in Table 5. For both of these cycles the specimens loaded linearly to maximum load without yielding.

The first two cycles of the tension-compression behavior of T6N boron-aluminum (Figure 13, Table 5) were successively run without debonding; however, on the third cycle the tabs debonded, and on the fourth cycle the specimen was loaded to failure in tension. The specimen did not yield during the first three cycles of the test and on the fourth cycle it yielded at 139.7 ksi.

5.2.3 Conclusions

Two basic observations can be made from the tests on unidirectional boron-aluminum: heat treating and cryogenic exposure of the laminate affected the yield stress in tension and compression, and cycling the laminate either in tension, compression or combined tension-compression establishes a maximum linear elastic range which is not altered by further cycling.

As expected, the experimental results from the test have shown that

increasing the yield stress of the aluminum matrix by heat treating the laminate changes the residual stress state in the laminate and increases the yield stress for tensile tests and decreases it for compression tests.

The cyclic tension and cyclic compression tests of the F condition unidirectional material showed that a linear elastic range of 65 to 70 ksi is established by cycling in tension and a range of 110 to 125 ksi is created by cycling in compression. The cyclic tension and compression tests on the T6 and T6N condition material behaved differently from the F condition material; the initial yield stress was higher and the unloading portion of the curve was linear.

The tension-compression tests provided enough information to indicate that the material exhibits a Baushinger effect after a maximum linear elastic range has been created by cyclic loading. The F condition created a smaller linear range than the heat treated material. Results from the tension-compression test on the T6 condition specimen show that the yield surface expands isotropically until the maximum linear elastic range is established and then the material shows the Baushinger effect.

5.3 The [90] Laminate

5.3.1 Monotonic Tension and Compression Tests

The influence of temper condition on the tensile and compressive stress-strain behavior of transverse boron-aluminum is shown in Figure 14 and Tables 6 and 7. The initial tangent moduli of the tension and

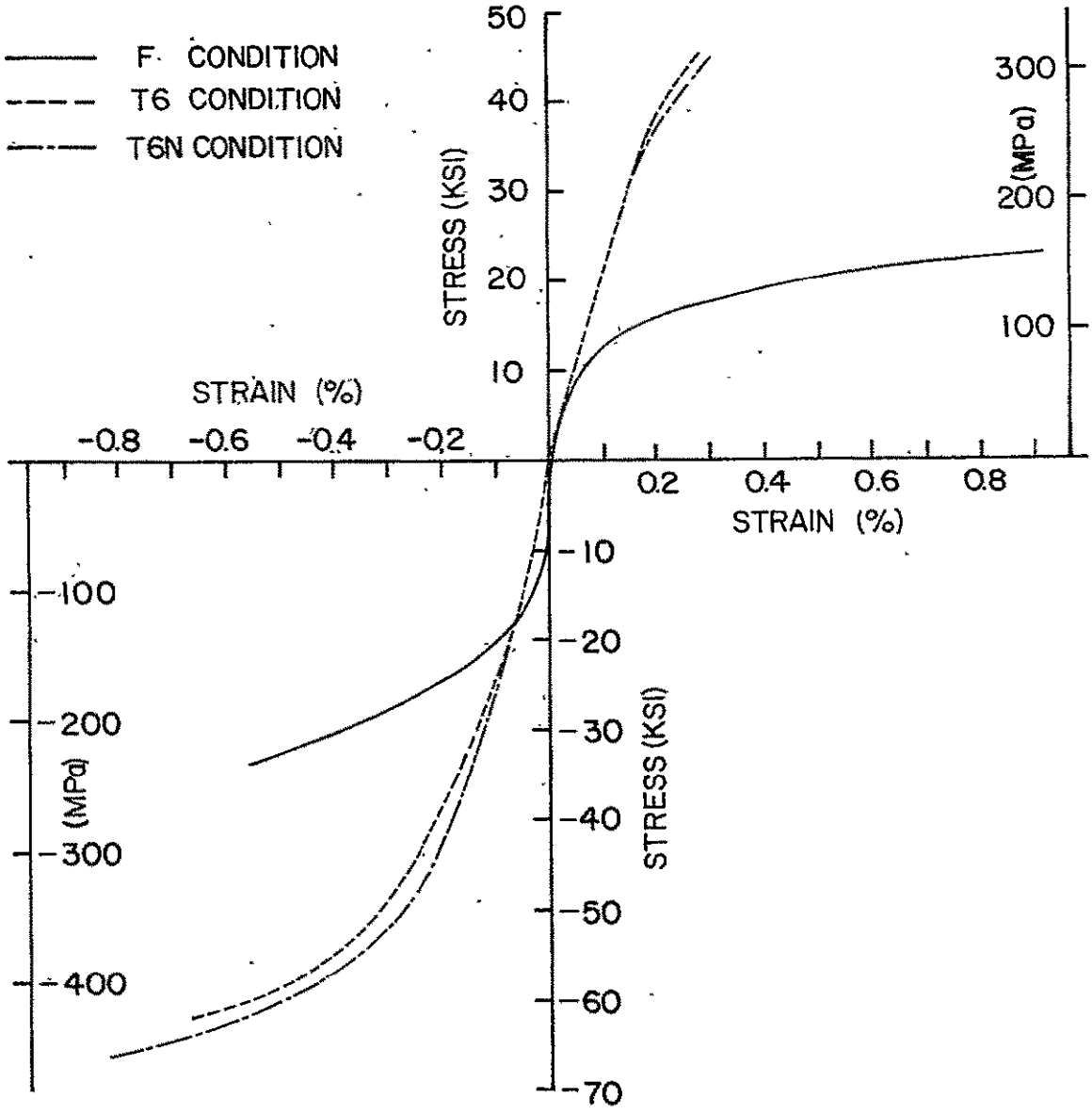

FIGURE 14. COMPARISON OF $[90_8]$ B/Al LAMINATE WITH DIFFERENT TEMPER CONDITIONS IN TENSION AND COMPRESSION.

TABLE 6

INFLUENCE OF TEMPER CONDITION ON THE TENSILE STRESS-STRAIN BEHAVIOR OF [90] BORON-ALUMINUM

TEMPER CONDITION	E_x (Msi)	ν_{xy}	σ_x^y (ksi)	ε_x^y (%)	σ_x^u (ksi)	ε_x^u (%)	ε_y^u (%)
F	20.4	0.104	7.10	0.040	22.2	0.822	-0.010
T6	21.3	0.124	26.56	0.127	46.2	0.286	-0.022
T6N	19.9	0.045	25.88	0.134	45.8	0.300	-0.031

TABLE 7

INFLUENCE OF TEMPER CONDITION ON THE COMPRESSIVE STRESS-STRAIN BEHAVIOR OF [90] BORON-ALUMINUM

TEMPER CONDITION	E_x (Msi)	ν_{xy}	σ_x^{y*} (ksi)	ε_x^y (%)	σ_x^{u*} (ksi)	ε_x^u (%)	ε_y^u (%)
F	21.4	-	-	-	-39.2	-0.735	0.035
T6	19.5	0.124	-21.45	-0.095	-64.6	-0.912	0.047
T6N	20.8	0.138	-29.21	-0.126	-62.9	-0.707	0.052

* Fixture influence

compression tests varied from 19.5 Msi to 21.4 Msi, and the variation was independent of the type of test (i.e. tension or compression). The rule of mixtures transverse modulus prediction using a fiber modulus of 58 Msi, matrix modulus of 10 Msi and fiber volume fraction of 47.5 percent gives a transverse composite modulus of 16.5 Msi which is approximately 25 percent lower than the experimental values. It should also be noted that the transverse modulus of the composite is approximately double that of aluminum.

The yield stress values from the tension and compression tests on the T6 and T6N condition specimens were significantly greater than yield stress of the F condition specimens. However, the yield stresses of the T6 and T6N condition were nearly the same in tension, but the compressive yield stresses of the T6 and T6N condition specimens were -21.4 ksi and -29.2 ksi, respectively. The yield stress and strain were not reported for the F condition compression tests because the influence by the fixture altered the initial portion of the stress-strain curve. The strength of the transverse boron-aluminum was increased 100 percent in tension and 50 percent in compression by heat treatment, but the strength values in compression are not the true strength for the material as mentioned in Section 5.1. Both the yield stress increase and strength increase of the T6 and T6N condition material, as compared to the F condition material, indicate that the properties of the matrix have a considerable influence on the transverse stress-strain behavior of boron-aluminum.

There was a large variation in the ultimate strain data depending

upon the temper condition and the type of test. The tension test results showed the largest failure strain, 0.822 percent, for the F condition material, and the T6 and T6N condition specimens had approximately the same failure strains, 0.286 percent and 0.300 percent, respectively. The compressive failure strains for the various temper conditions exhibited the opposite trend, the F condition material had the lowest failure strain and the T6 and T6N condition specimens had the highest. The compressive failure strains, however, are believed to be lower than the true failure strains of the transverse composite laminate for reasons discussed in section 5.1.

5.3.2 Cyclic Tests

5.3.2.1 Tension and Compression

Typical tension-tension behavior of transverse boron-aluminum with the F, T6, and T6N temper conditions is shown in Figures 15, 17, and 19, respectively, and compression-compression behavior is shown in Figure 16, 18, and 20.

The test results from the cyclic tension (Table 8) and cyclic compression (Table 9) were consistent with the monotonic tension and compression test results. The additional information gained from the cyclic tests concerned the strain hardening behavior of the transverse material. For both the cyclic tension and cyclic compression tests the material loaded and unloaded linearly, if the stress level was not above the yield stress. When the specimens were loaded above the yield stress, unloading was linear. The loading portion of the following

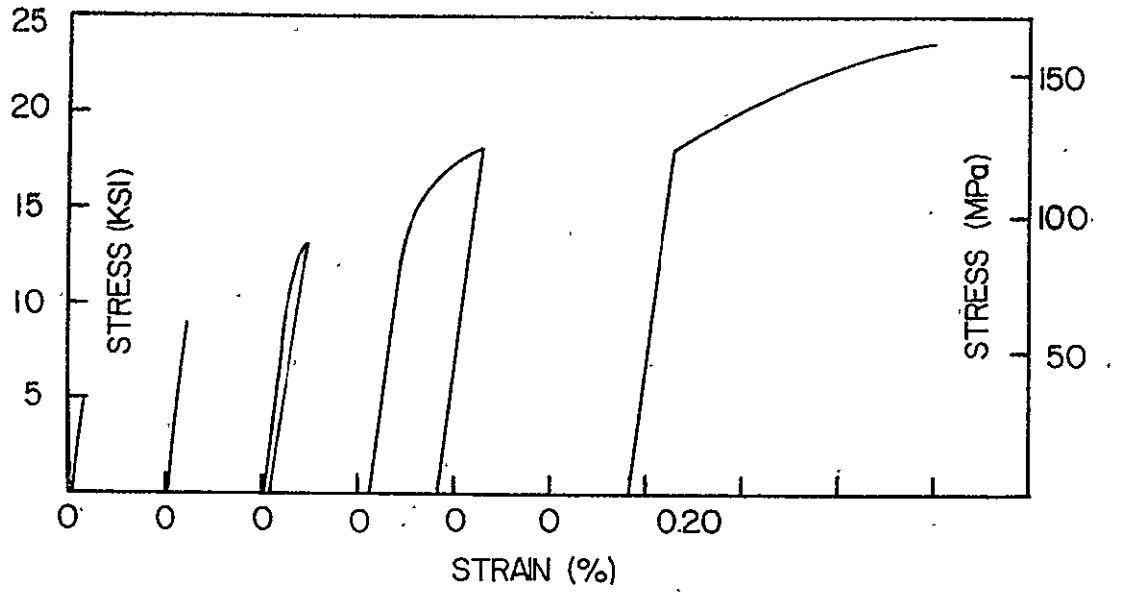

FIGURE 15. CYCLIC TENSION STRESS-STRAIN DIAGRAM FOR $[90_8]$ B/Al LAMINATE, F CONDITION.

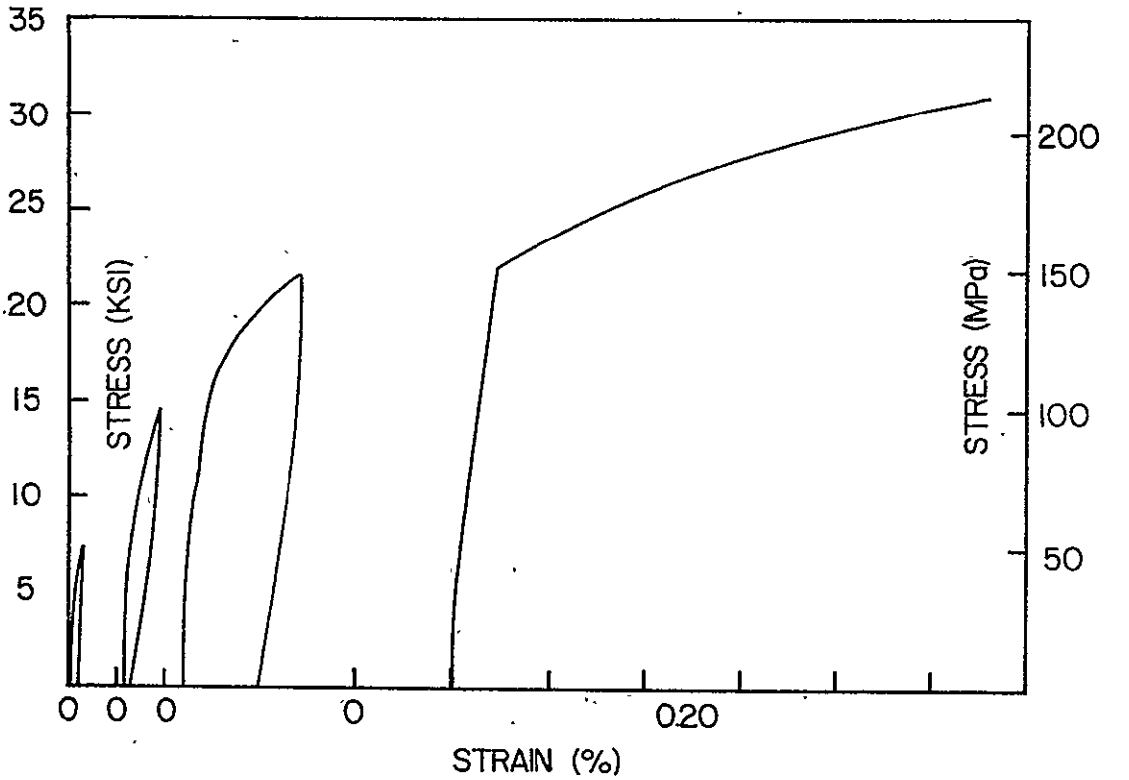

FIGURE 16. CYCLIC COMPRESSION STRESS-STRAIN DIAGRAM FOR $[90_8]$ B/Al LAMINATE F CONDITION.

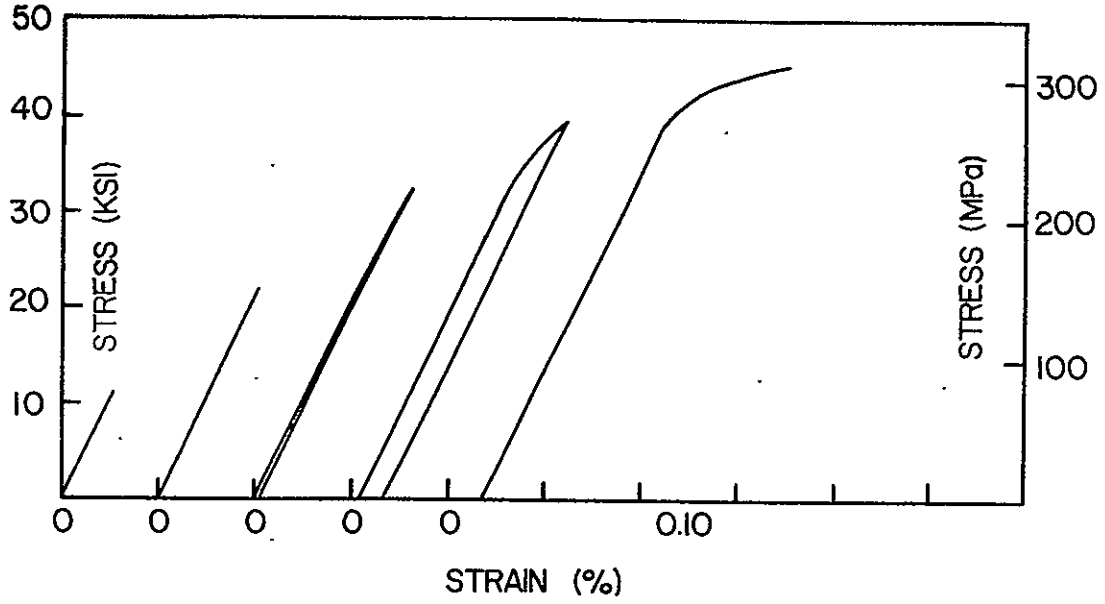

FIGURE 17. CYCLIC TENSION STRESS-STRAIN DIAGRAM FOR $[90_8]$ B/Al LAMINATE, T6 CONDITION.

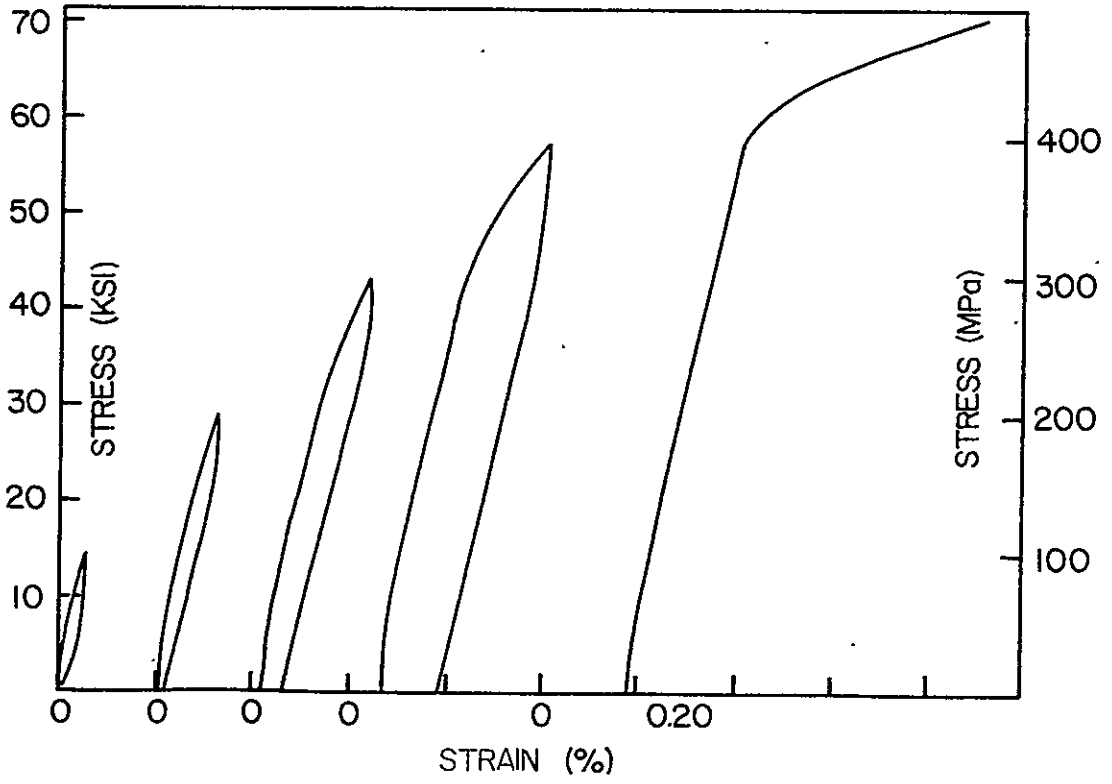

FIGURE 18. CYCLIC COMPRESSION STRESS-STRAIN DIAGRAM FOR $[90_8]$ B/Al LAMINATE, T6 CONDITION.

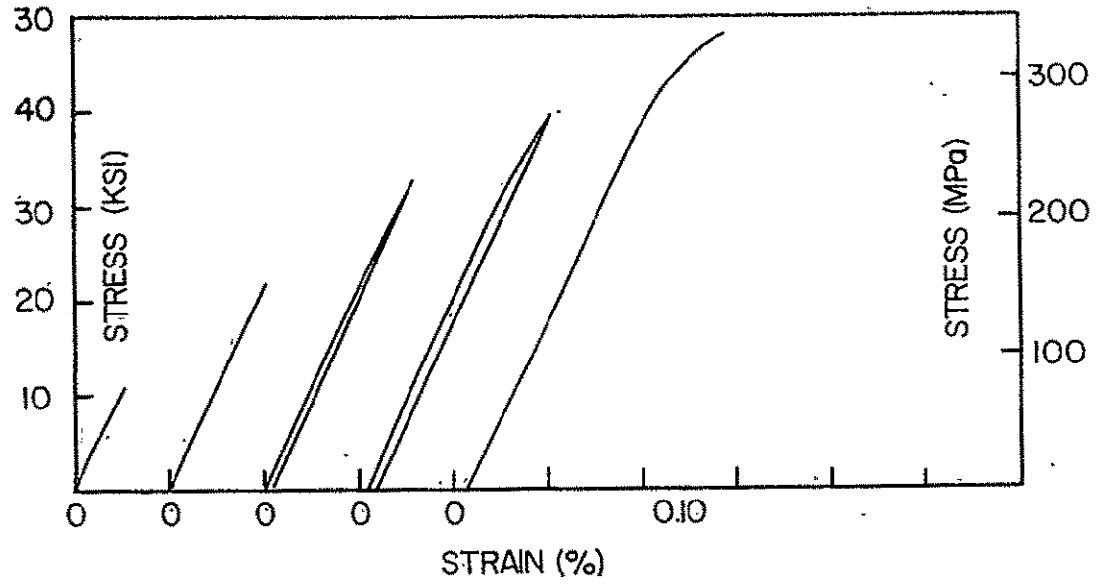

FIGURE 19. CYCLIC TENSION STRESS-STRAIN DIAGRAM FOR $[90_8]$ B/Al LAMINATE, MODIFIED T6 CONDITION.

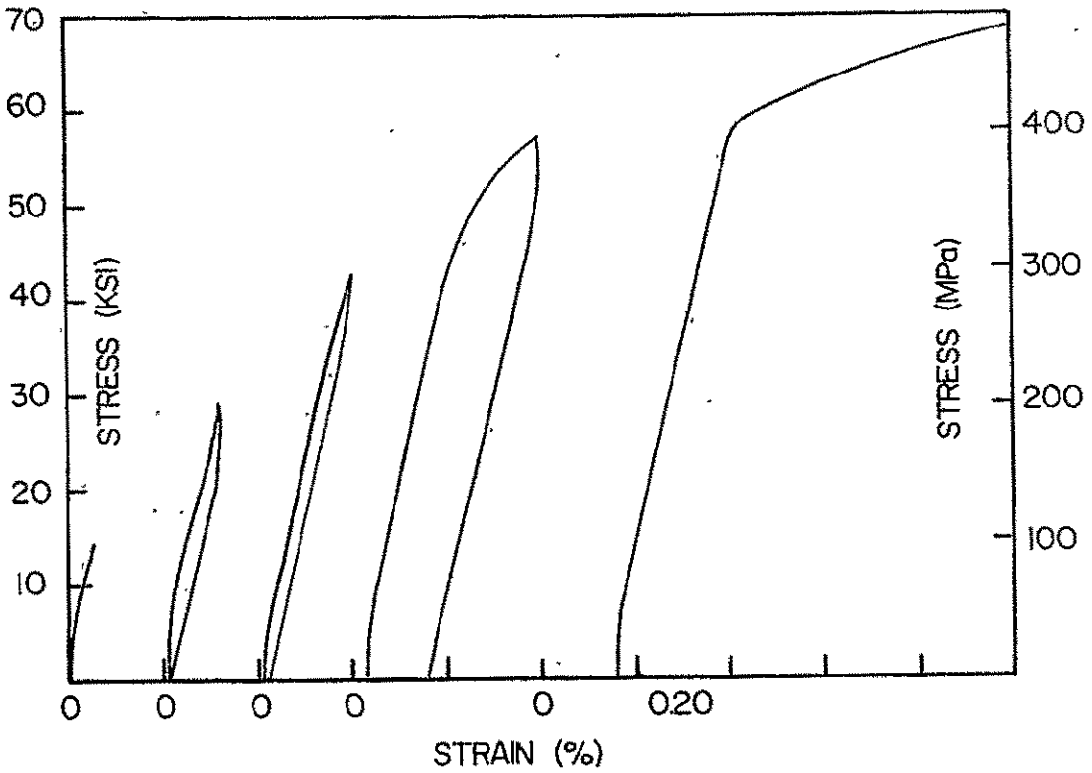

FIGURE 20. CYCLIC COMPRESSION STRESS-STRAIN DIAGRAM FOR $[90_8]$ B/Al LAMINATE, MODIFIED T6 CONDITION.

TABLE 8

INFLUENCE OF TEMPER CONDITION ON THE CYCLIC TENSION STRESS-STRAIN BEHAVIOR OF [90] BORON-ALUMINUM

TEMPER CONDITION	CYCLE	E_x^L (Msi)	E_x^{UL} (Msi)	ν_{xy}^L	ν_{xy}^{UL}	σ_x^y (ksi)	ε_x^y (%)	σ_x^m (ksi)	ε_x^m (%)	ε_y^m (%)	ε_x^R (%)
F	I	20.1	23.1	0.123	0.123	-	-	4.7	0.023	-0.004	0.002
	II	21.2	22.1	0.123	0.130	-	-	8.9	0.045	-0.006	0.003
	III	21.4	21.8	0.126	0.138	9.5	0.050	13.6	0.094	-0.008	0.029
	IV	20.6	20.4	0.130	0.135	13.6	0.097	18.1	0.259	-0.011	0.168
	V	20.3	-	0.136	-	17.6	0.257	23.5	0.786	-0.121	-
T6	I	21.1	22.2	0.106	0.119	-	-	10.9	0.052	-0.006	0.001
	II	21.0	20.9	0.116	0.116	-	-	21.8	0.104	-0.013	0.001
	III	21.0	21.4	0.119	0.114	26.6	0.133	32.4	0.162	-0.018	0.007
	IV	20.8	20.5	0.121	0.120	32.8	0.171	39.6	0.224	-0.021	0.032
	V	20.5	-	0.120	-	37.5	0.219	45.5	0.356	-0.020	-
T6N	I	21.6	21.6	0.125	0.132	-	-	10.8	0.050	-0.006	0.000
	II	21.3	21.8	0.134	0.128	-	-	21.8	0.103	-0.013	0.002
	III	21.4	21.7	0.130	0.130	25.6	0.129	32.4	0.160	-0.020	0.008
	IV	21.3	21.9	0.133	0.130	33.4	0.173	39.5	0.205	-0.026	0.018
	V	21.9	-	0.144	-	39.3	0.214	48.1	0.288	-0.033	-

TABLE 9

INFLUENCE OF TEMPER CONDITION ON THE CYCLIC COMPRESSION STRESS-STRAIN BEHAVIOR OF [90] BORON-ALUMINUM

TEMPER CONDITION	CYCLE	E_x^L (Msi)	E_x^{UL} (Msi)	ν_{xy}^L	ν_{xy}^{UL}	σ_x^{y} * (ksi)	ε_x^y (%)	σ_x^{m} * (ksi)	ε_x^m (%)	ε_y^m (%)	ε_x^R (%)
F	I	14.1	-	0.144	0.220	-	-	-7.4	-0.025	0.002	-0.012
	II	12.9	20.1	0.131	0.141	-9.5	-0.041	-14.5	-0.084	0.010	-0.034
	III	20.9	19.1	0.137	0.129	-15.2	-0.090	-21.7	-0.284	0.019	-0.202
	IV	20.2	-	0.130	-	-21.1	-0.288	-31.1	-1.317	0.013	-
T6	I	21.1	21.6	0.141	0.129	-	-	-14.3	-0.051	0.007	-0.009
	II	22.1	21.6	0.145	0.137	-16.3	-0.059	-28.8	-0.127	0.017	-0.022
	III	22.2	21.8	0.143	0.140	-29.4	-0.132	-43.1	-0.235	0.031	-0.066
	IV	22.1	22.7	0.143	0.135	-43.5	-0.241	-57.4	-0.410	0.044	-0.183
	V	22.5	-	0.138	-	-55.2	-0.406	-70.6	-0.921	0.067	-
T6N	I	19.5	21.4	0.117	0.112	-	-	-14.4	-0.055	0.006	-0.010
	II	21.2	21.1	0.124	0.119	-	-	-28.7	-0.125	0.016	-0.012
	III	21.4	21.1	0.119	0.130	-33.2	-0.148	-42.9	-0.206	0.027	-0.027
	IV	21.2	21.7	0.129	0.129	-43.1	-0.207	-57.2	-0.399	0.045	-0.159
	V	21.3	-	0.131	-	-57.8	-0.408	-69.0	-1.018	0.064	-

* Fixture influence

cycle was linear up to a stress level equivalent to the maximum stress of the previous cycle and then resumed nonlinear behavior. As with the monotonic tests, the initial yield stresses and strains varied according to the temper condition of the material and whether the test was tensile or compressive. It is important to note that the initial loading and initial unloading portions of each cycle of the compression curves (approximately 5-10 ksi) have a very high slope due to the load in the fixture.

5.3.2.3 Cyclic Tension-Compression Tests

Figures 21-23 show the respective cyclic tension-compression diagrams for [90] boron-aluminum with F, T6, and T6N temper conditions. The numerical results from these tests are presented in Table 10. The problem of load transfer into the fixture on each cycle of the test caused extreme difficulty in determining yield stresses and modulus values.

Results from the F condition [90] specimen (Figure 21) show (as did the results from the F condition [0] laminate) that the yielding phenomenon resemble a Baushinger effect with the compressive yield stress being reduced due to yielding in tension. Since the [90] laminate is very much matrix dependent, the material behavior is similar to that of the matrix, as expected. For the F condition transverse material the first cycle of loading produced no yielding; on the second cycle the specimen yielded at 10 ksi in tension, and upon unloading into compression the yield stress was linear for a range of 17.5 ksi down to

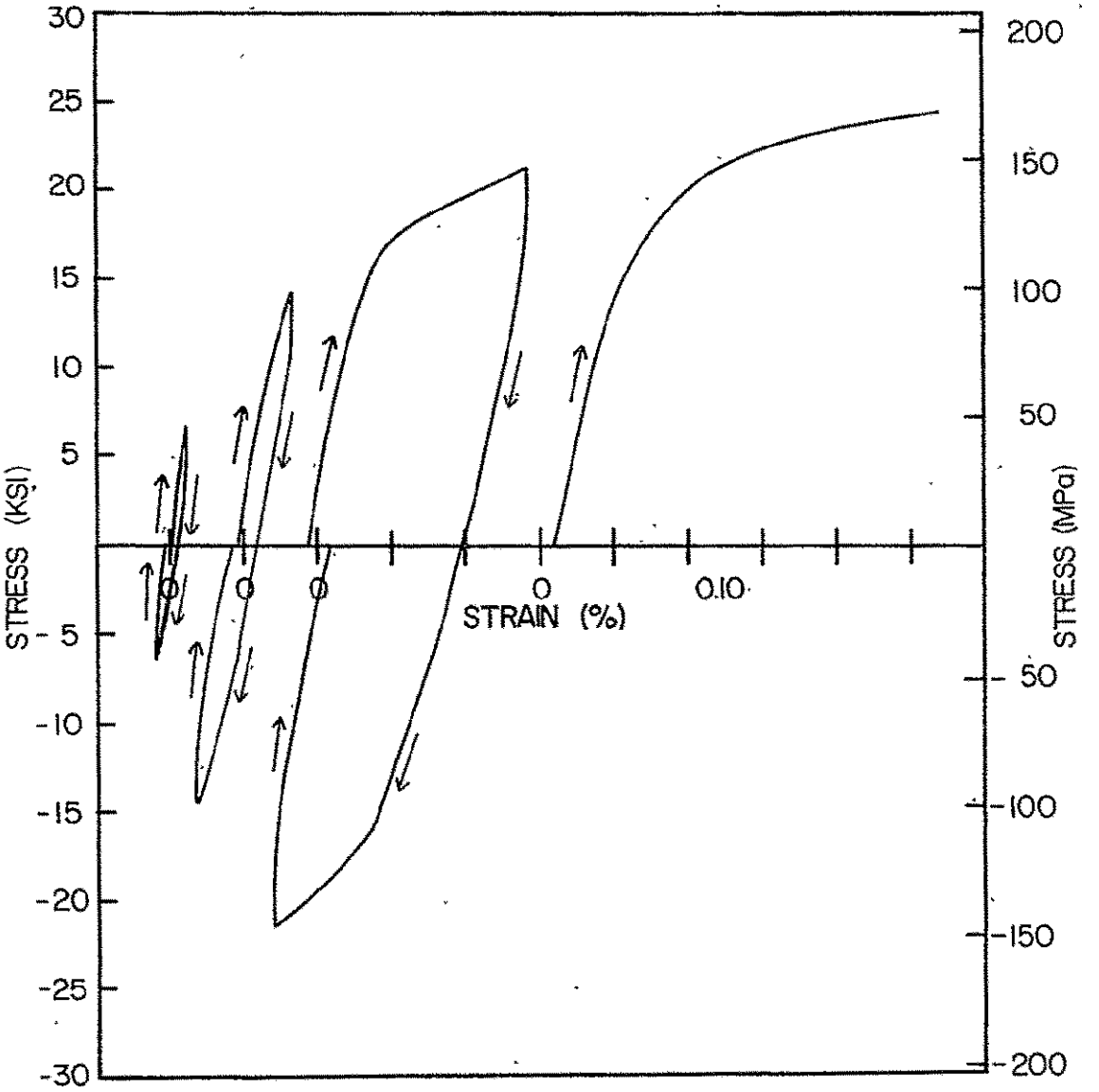

FIGURE 21. CYCLIC TENSION COMPRESSION STRESS-STRAIN DIAGRAM FOR $[90_8]$ B/Al LAMINATE, F CONDITION.

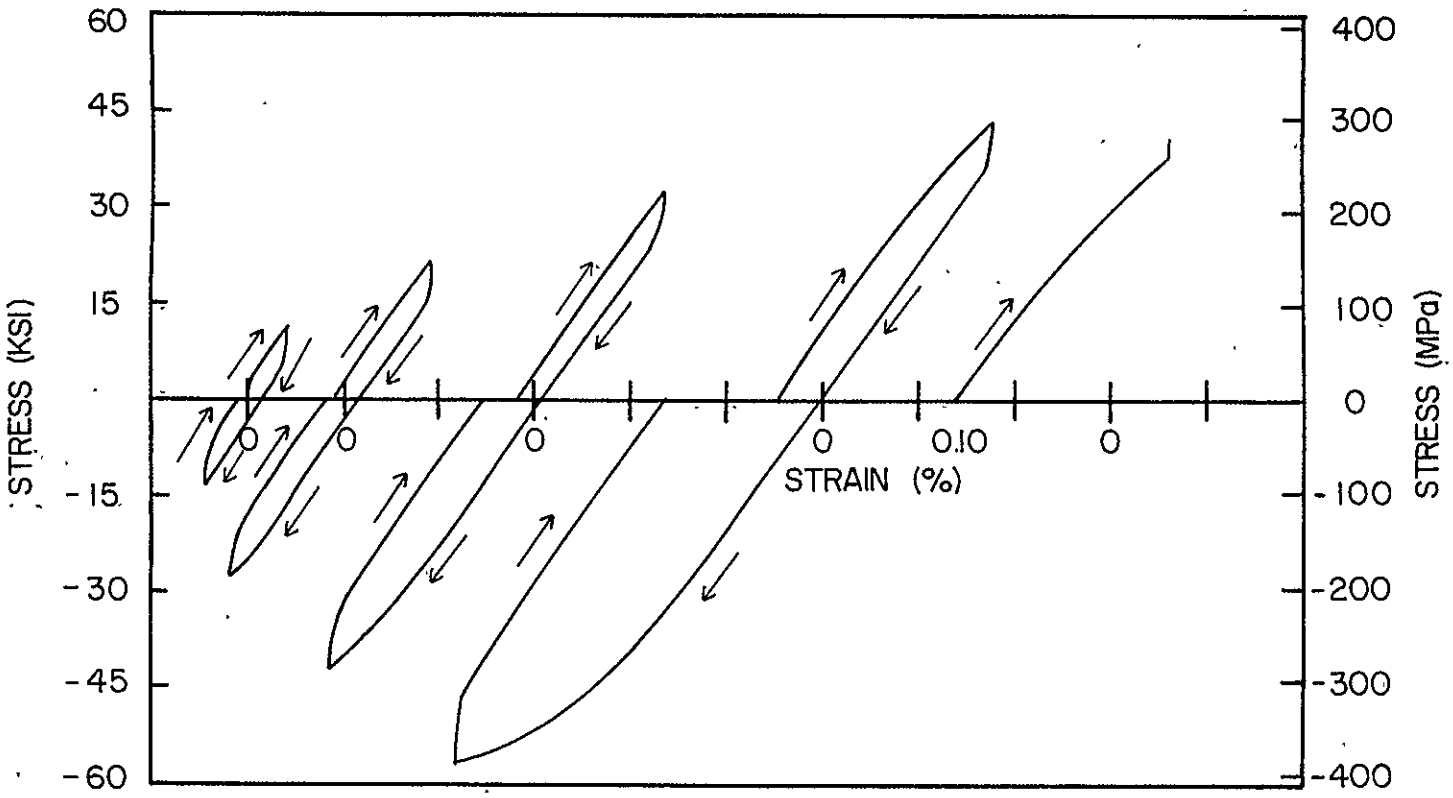

FIGURE 22. CYCLIC TENSION-COMPRESSION STRESS-STRAIN DIAGRAM FOR $[90_8]$ B/Al LAMINATE, T6 CONDITION.

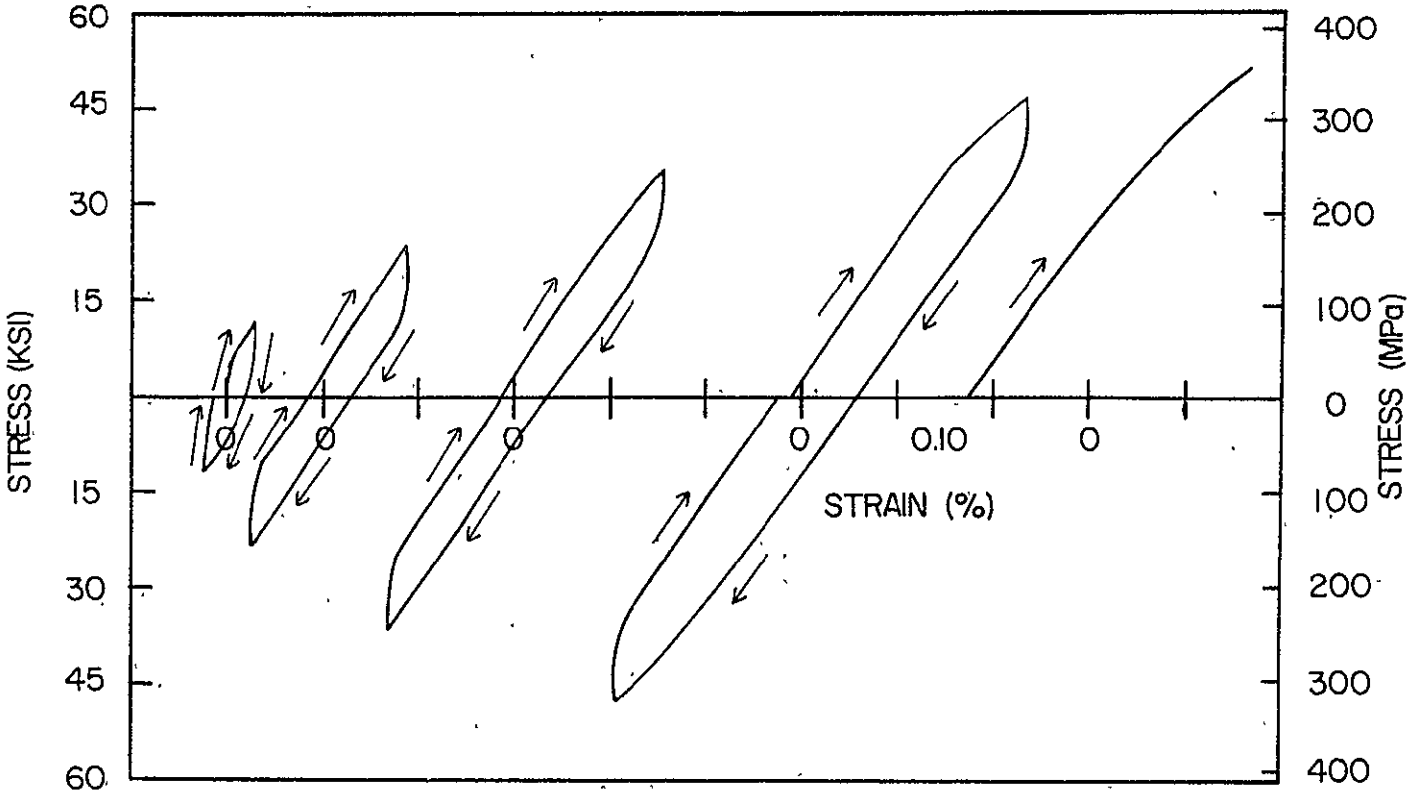

FIGURE 23. CYCLIC TENSION-COMPRESSION STRESS-STRAIN DIAGRAM FOR $[90_6]$ B/Al LAMINATE, MODIFIED T6 CONDITION.

TABLE 10

INFLUENCE OF TEMPER CONDITION ON THE TENSION-COMPRESSION STRESS-STRAIN BEHAVIOR OF [90] BORON-ALUMINUM

TEMPER CONDITION	CYCLE	E_x^L (Msi)	E_x^{UL} (Msi)	σ_x^{m*} (ksi)	ε_x^m (%)	ε_y^m (%)	ε_x^R (%)
F	I-T	22.0	23.8	6.8	0.023	-0.004	0.014
	I-C	23.8	-	-6.7	-0.021	0.003	-0.009
	II-T	21.6	21.6	14.4	0.032	-0.008	0.020
	II-C	21.6	21.6	-14.3	-0.064	0.012	-0.017
	III-T	18.6	19.9	21.4	0.282	-0.011	0.198
	III-C	15.9	19.9	-21.4	-0.060	0.026	0.018
	IV-T	20.3	-	27.2	0.543	-0.010	-
T6	I-T	20.8	21.6	11.4	0.042	-0.004	0.013
	I-C	21.6	20.8	-13.8	-0.048	0.008	-0.010
	II-T	22.3	21.9	22.0	0.092	-0.009	0.013
	II-C	21.9	21.5	-22.7	-0.119	0.019	-0.019
	III-T	21.6	21.8	32.4	0.135	-0.012	0.009
	III-C	21.8	22.5	-42.3	-0.213	0.034	-0.053
	IV-T	21.2	20.8	43.4	0.180	-0.012	0.000
	IV-C	20.8	22.0	-56.9	-0.382	0.057	-0.161
	V-T	19.5	-	44.4	0.091	-0.001	-
T6N	I-T	-	-	11.9	0.031	-0.005	0.024
	I-C	-	-	-11.6	-0.022	0.004	-0.014
	II-T	22.9	22.6	23.8	0.089	-0.013	0.028
	II-C	22.6	22.6	-23.6	-0.077	0.011	-0.015
	III-T	22.1	22.1	35.8	0.152	-0.022	0.033
	III-C	22.1	22.1	-35.7	-0.130	0.019	-0.017
	IV-T	21.7	21.1	47.4	0.237	-0.030	0.062
	IV-C	21.1	21.7	-47.5	-0.195	0.028	-0.026
	V-T	13.2	-	51.7	0.268	-0.032	-

* Fixture influence

-3.1 ksi, lower than -9.5 ksi, the initial yield stress reported from the F condition cyclic compression test. The yield stress on the third cycle was again 10 ksi but the linear range was increased to 24.3 ksi; the unloading portion of the curve was linear from the maximum tensile stress, 21.4 ksi, to zero load and then behaved nonlinearly to the maximum compressive stress. The specimen loaded linearly from the maximum compressive stress of the third cycle to 6.3 ksi in tension on the fourth cycle, the linear range was 27.7 ksi. These results do not indicate that a constant linear range is established by cyclic loading of the specimen, nor do they show conclusively the linear range is increased by loading above the yield stress. However, the results show that cycling into the nonlinear region in tension reduces the compressive yield stress and vice versa.

The T6 condition specimen (Figure 22) exhibited a yielding phenomenon different than that of the F condition specimen. The specimen did not yield during the first cycle or the tensile portion of the second cycle but it did yield in compression at -22.7 ksi, the magnitude of the maximum tensile stress of the second cycle. On the third cycle the specimen did not yield in tension but yielded in compression at -30.8 ksi increasing the linear range to 63.2 ksi. After yielding in compression on the third cycle, the loading proceeded well into the nonlinear region, and on the fourth cycle the specimen yielding in tension at 24.1 ksi, exhibiting approximately the same linear range as the third cycle. For the first three cycles the yielding phenomenon resembled isotropic hardening with the yield stress, be it tensile or compressive,

corresponding to the maximum previous stress. The reduced tensile yield stress on the fourth cycle deviates from the isotropic hardening behavior and the fact that the linear range is approximately the same for two consecutive cycles indicates that a maximum linear range has been established. The linear range from the maximum tensile stress to the compressive yield stress in compression on the fourth cycle was 71 ksi, and from the maximum compression stress of the fourth cycle to the tensile yield stress on the fifth the linear range was 74 ksi. Two different yield phenomenon are occurring during the test. For the first three cycles the yield behavior resembles isotropic hardening, and on the final three cycles the Baushinger effect best characterizes the behavior.

The T6N condition specimen (Figure 23) behaved similar to the T6 condition laminate. The T6N specimen yielded first in tension at 25.9 ksi on the third cycle, the highest previous stress, and did not yield in compression on the third cycle but the linear range was increased to 72 ksi from 50 ksi. On the fourth cycle the tensile yield stress increased to 37.8 ksi, the same stress level as the maximum stress of the previous cycle, the linear range was 74 ksi. The yield stress in compression for the fourth cycle was lowered to -21.9 ksi and the linear range was not changed. The tensile yield stress was lowered to 19.5 ksi on the fifth cycle and the linear range decreased slightly to 67 ksi.

One very important difference between the tests of the T6 and T6N condition specimens was the levels to which the specimens were loaded in compression. The maximum compressive stress of the cycles for the test

on the T6 specimens were higher than those for the T6N specimens. This difference in the load history did not change the fundamental yield behavior. The T6 and T6N condition specimens hardened isotropically for the first few cycles and then maintained a relatively constant linear range for the remainder of the test.

5.3.3 Conclusions

As with the [0] laminate, two major conclusions can be drawn from the results of the tests on the [90] boron-aluminum laminate. Heat treating the material significantly changes the mechanical response and the yielding phenomenon is dependent on whether the specimen has been heat treated.

The strengthening of the matrix of the [90] laminate by heat treating increased the yield stress and strength of the composite. Yield stresses were increased 100 to 400 percent and the strength was increased 50 to 100 percent for both the tension and compression tests. Also the tensile failure strains were reduced by heat treating the material.

The nonlinear behavior of the laminate depended upon the heat treatment of the specimen. The cyclic tension and cyclic compression tests unloaded linearly after yielding on the loading portion of the cycle. The subsequent cycle's yield stress was equivalent to the maximum previous stress. However, the cyclic tension-compression tests showed that the results from the cyclic tension and cyclic compression tests did not completely characterize the nonlinear behavior of the material. As with the cyclic tension and cyclic compression tests,

results from the tension-compression tests indicate that the linear range of the stress-strain curve is increased by loading into the inelastic region.

The F condition specimen behaved in a Baushinger manner, that is the linear elastic range was increased with each cycle but the associated yield stress was reduced. The T6 and T6N condition specimens behaved differently from the F condition specimen. The yield surface expanded by isotropic hardening for the first few cycles and then maintained a constant linear range for the remainder of the test. Also the load history of the T6 and T6N condition was different and fundamentally the yield behavior was not changed.

5.4 The $[\pm 45]_s$ Laminate

5.4.1 Monotonic Tension and Compression Tests

The influence of temper condition on the tensile and compressive behavior of the $[\pm 45]_s$ boron-aluminum laminate is shown in Figure 24 and comparison of the numerical results are shown in Tables 11 and 12. The precipitation hardening of the aluminum matrix by heat treating effected the mechanical response of the laminate in much the same way as it altered the behavior of the [90] laminate.

As indicated in Table 11, the tensile modulus values were very similar for all three temper conditions with an average value of 21 Msi; the laminate analysis program predict a modulus of 20.7 Msi. The compression moduli for the T6 and T6N specimens were approximately the same as the tensile values (Table 12); however, the compression tests on

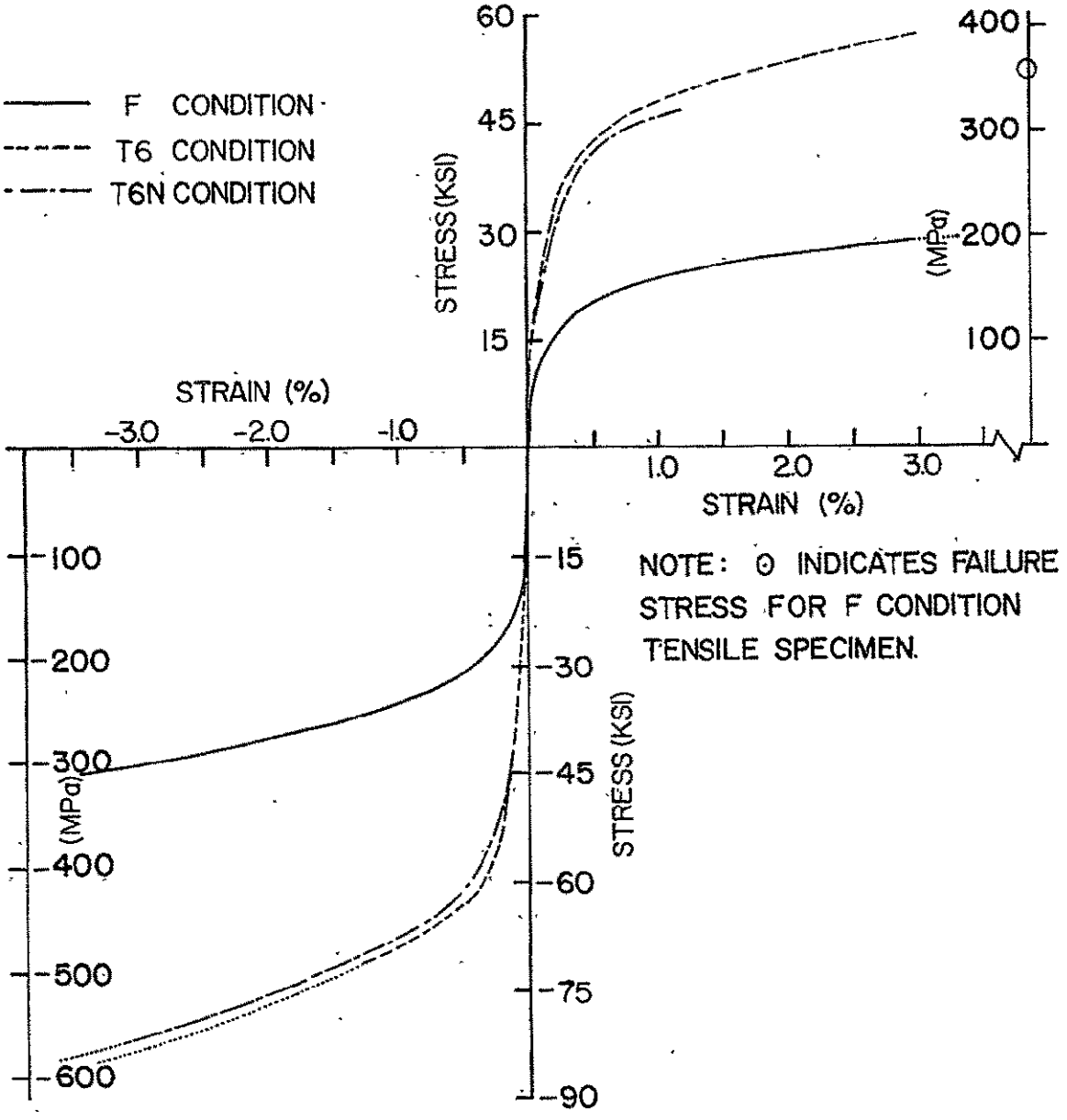

FIGURE 24. COMPARISON OF $[\pm 45]_s$ B/Al LAMINATE WITH DIFFERENT TEMPER CONDITIONS IN TENSION AND COMPRESSION.

TABLE 11

INFLUENCE OF TEMPER CONDITION ON THE TENSILE STRESS-STRAIN BEHAVIOR OF $[\pm 45]_s$ BORON-ALUMINUM

TEMPER CONDITION	E_x (Msi)	ν_{xy}	σ_x^y (ksi)	ε_x^y (%)	σ_x^u (ksi)	ε_x^u (%)	ε_y^u (%)
F	21.3	0.365	5.78	0.029	51.8	~23.0	~-19.0
T6	21.3	0.312	17.98	0.093	55.6	2.726	-2.044
T6N	20.5	0.332	16.82	0.085	47.0	0.952	-0.600

TABLE 12

INFLUENCE OF TEMPER CONDITION ON THE COMPRESSIVE STRESS-STRAIN BEHAVIOR OF $[\pm 45]_s$ BORON-ALUMINUM

TEMPER CONDITION	E_x (Msi)	ν_{xy}	$\sigma_x^{y\,*}$ (ksi)	ε_x^y (%)
F	18.5 *	-	-	-
T6	21.2	0.353	-42.86	-0.152
T6N	19.4	0.349	-36.18	-0.134

* Fixture influence

the F condition material was influenced significantly by fixture effects. The low modulus value (18.5 Msi) reported for the F condition material is from that portion of the curve where the fixture influence is no longer present; it is likely that the specimen is in the nonlinear region which explains the lower modulus value. The average modulus results presented in Tables 11 and 12 indicate that the modulus of the T6N condition specimens is lower than that of the T6 condition specimens, however, examination of the individual test results does not indicate this is always true.

The laminate analysis program predicts a Poisson's ratio of 0.354; the average experimental values (Tables 11 and 12) vary between 0.365 and 0.312. The T6 condition tension specimen had the lowest value of 0.312; all other values were above 0.33 which is in fairly good agreement with the laminate theory value.

The shear modulus, G_{12}, was determined to be 7.65 Msi using the analysis in [23], and this value was used as input data for the laminate analysis program.

The T6 condition specimens exhibited higher yield stresses than the F condition material. The tensile tests showed the average yield stresses of the F and T6 condition specimens to be 5.78 ksi and 17.98 ksi, respectively; thus, the T6 heat treatment results in an increase of approximately 300 percent. The tensile strength of the laminate was not significantly changed by heat treating; however, the failure strains were changed significantly. The T6 condition specimens failed at 2.73 percent strain. The strain of the F condition exceeded the measurable

limit of the strain gage, but projection of the stress-strain curve indicated the tensile failure strain to be approximately 23 percent.

A unique deformation characteristic associated with the F condition $[\pm 45]_s$ laminate was significant fiber rotation. The measured fiber rotation of the outer ply of a failed specimen was 10°. Figure 25 shows examples of failed F condition $[\pm 45]_s$ specimens after tensile loading. The T6 and T6N condition specimens did not exhibit significant fiber rotation.

The effect of liquid nitrogen on the tensile yield stress is not significant; however, the tensile strength was reduced by 18 percent as compared to the T6 condition. This reduction in strength indicates that the laminate has been damaged during the liquid nitrogen exposure.

No yield stress is reported for the F condition compression specimen as the influence of the fixture on the stress-strain curve extended into the nonlinear range of the curve. The T6 and T6N condition specimens had yield stresses of -42.86 ksi and -36.18 ksi, respectively. Ultimate stress and strain results are not presented because the fixture was designed to allow for strains of up to four percent and for the $[\pm 45]_s$ laminate the maximum strains exceeded this value. An example of a $[\pm 45]_s$ compression specimen exhibiting the large deformation is shown in Figure 25.

As indicated in Figure 24, the influence of cryogenic exposure on the compressive stress-strain behavior of the $[\pm 45]_s$ specimens is minor. The stress-strain curves of the T6 and T6N condition specimens follow essentially the same curve; however, the yield stress of the T6N condi-

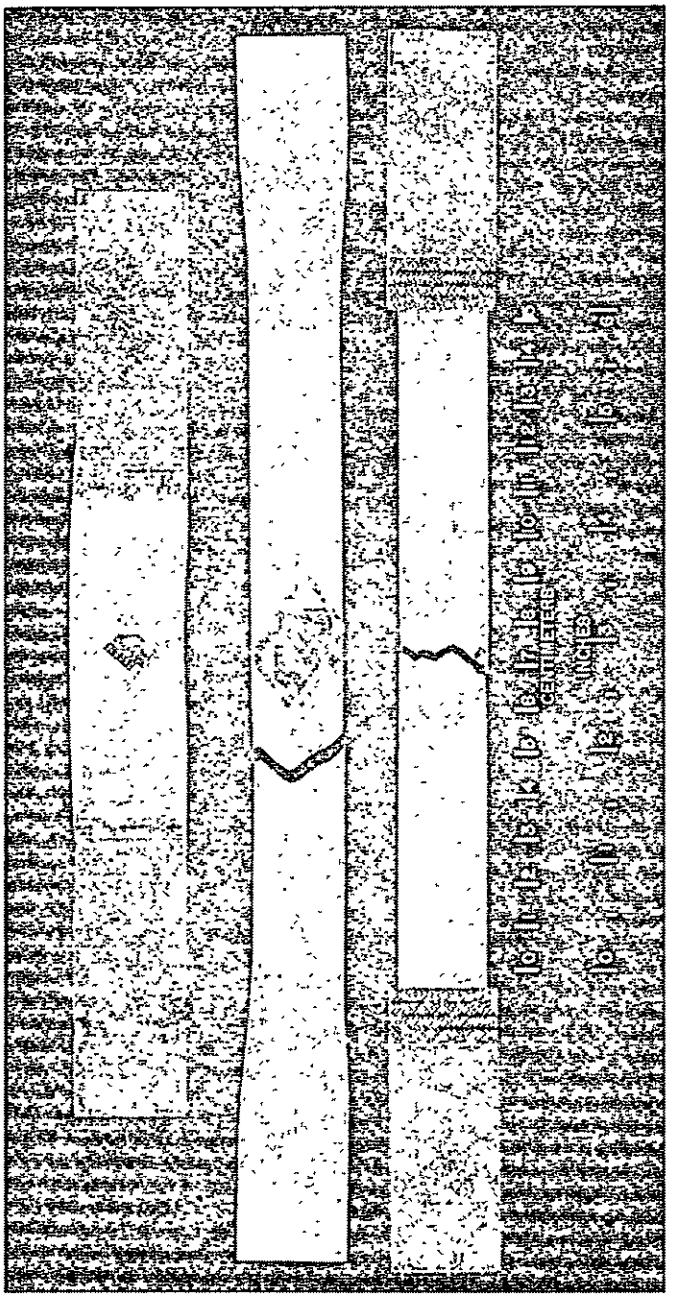

Figure 25. Examples of tested F condition $[\pm 45]_s$ specimens showing the large deformation when testing in compression (top) and tension (middle and bottom).

tion specimen is reduced relative to the T6 condition specimen.

5.4.2 Cyclic Tests

5.4.2.1 Tension and Compression

The cyclic tension and cyclic compression results were consistent with the monotonic tests in that the heat treated specimens yielded at higher stress levels and the liquid nitrogen treatment had an insignificant effect on the stress-strain behavior. Figures 26, 28, 30 show the respective cyclic tension stress-strain response of F, T6, and T6N condition $[\pm 45]_s$ boron-aluminum; Figures 27, 29, and 31 show the cyclic compression-compression response for the same three temper conditions. Tables 13 and 14 list numerical results from the tests.

The cyclic tension tests for the $[\pm 45]_s$ laminate exhibited strain hardening behavior similar to the [90] laminate; after loading beyond the elastic limit, the unloading portion of that cycle was linear and on the next cycle the response was linear up to the maximum stress of the previous cycle, beyond which the laminate responded nonlinearly. As with the monotonic tests, the ultimate strain of the F condition specimen was beyond the limit of the strain gage.

The initial modulus on the first cycle of the tension-tension tests was not affected by the temper condition with values ranging from 20.5 Msi to 21.0 Msi (Table 13). However, during cyclic loading the modulus generally exhibited a small decrease with each successive cycle. (The low modulus of the first cycle, in particular for the F condition

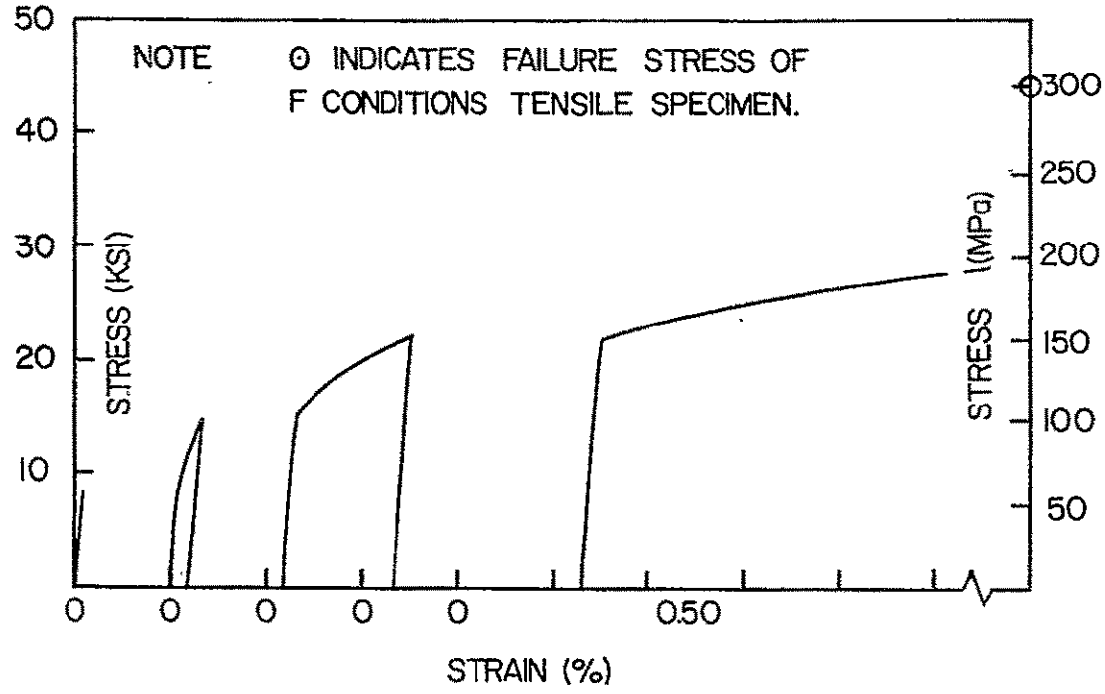

FIGURE 26. CYCLIC TENSION STRESS-STRAIN DIAGRAM FOR $[\pm 45]_s$ B/Al LAMINATE, F CONDITION.

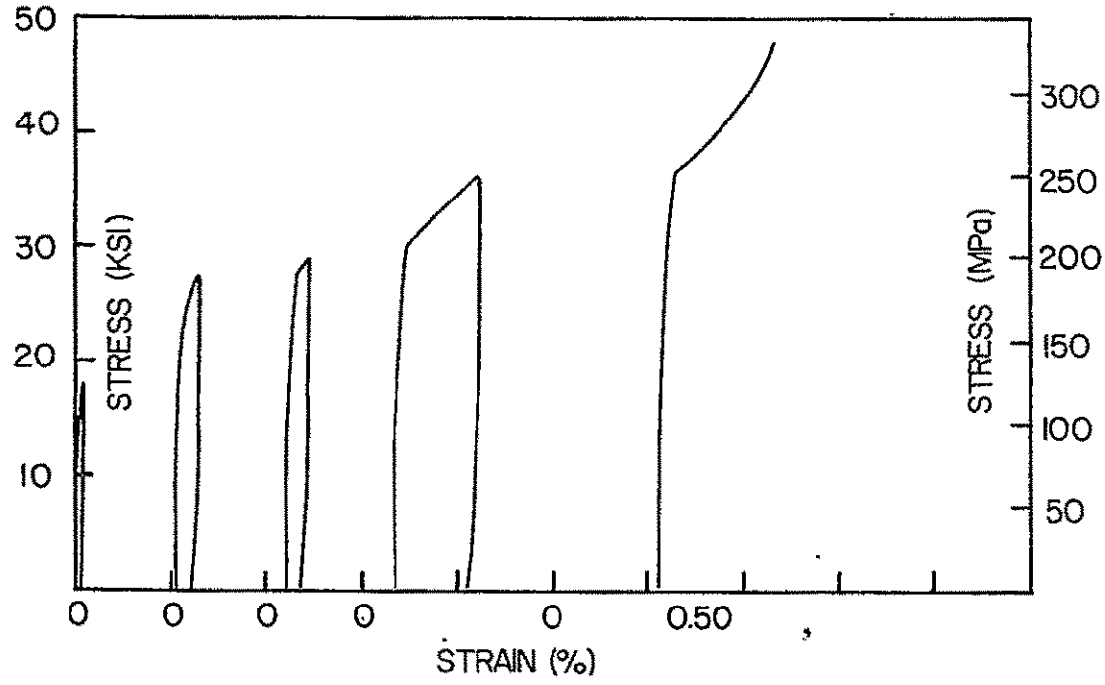

FIGURE 27. CYCLIC COMPRESSION STRESS-STRAIN DIAGRAM FOR $[\pm 45]_s$ B/Al LAMINATE, F CONDITION.

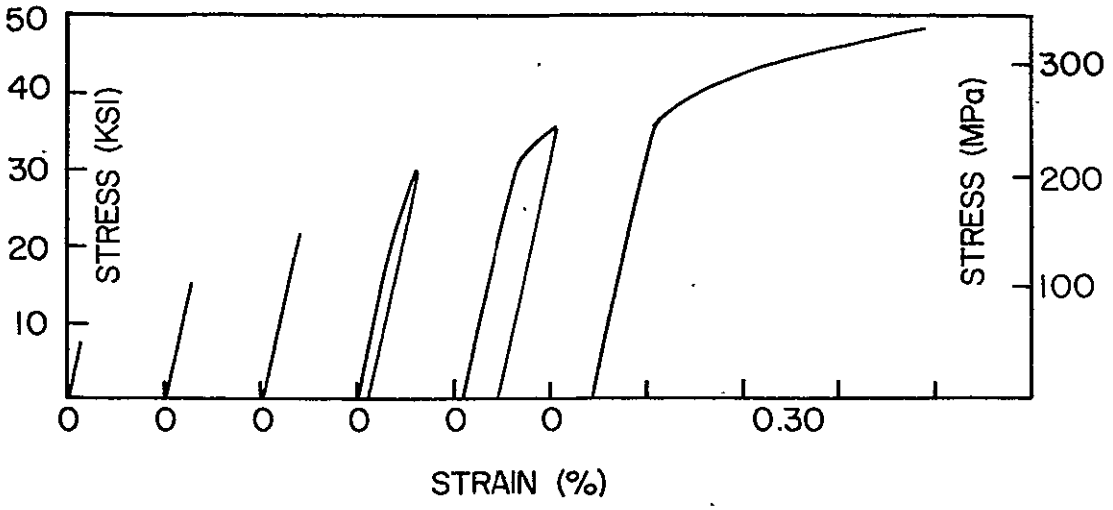

FIGURE 28. CYCLIC TENSION STRESS-STRAIN DIAGRAM FOR $[\pm 45]_s$ B/Al LAMINATE, T6 CONDITION.

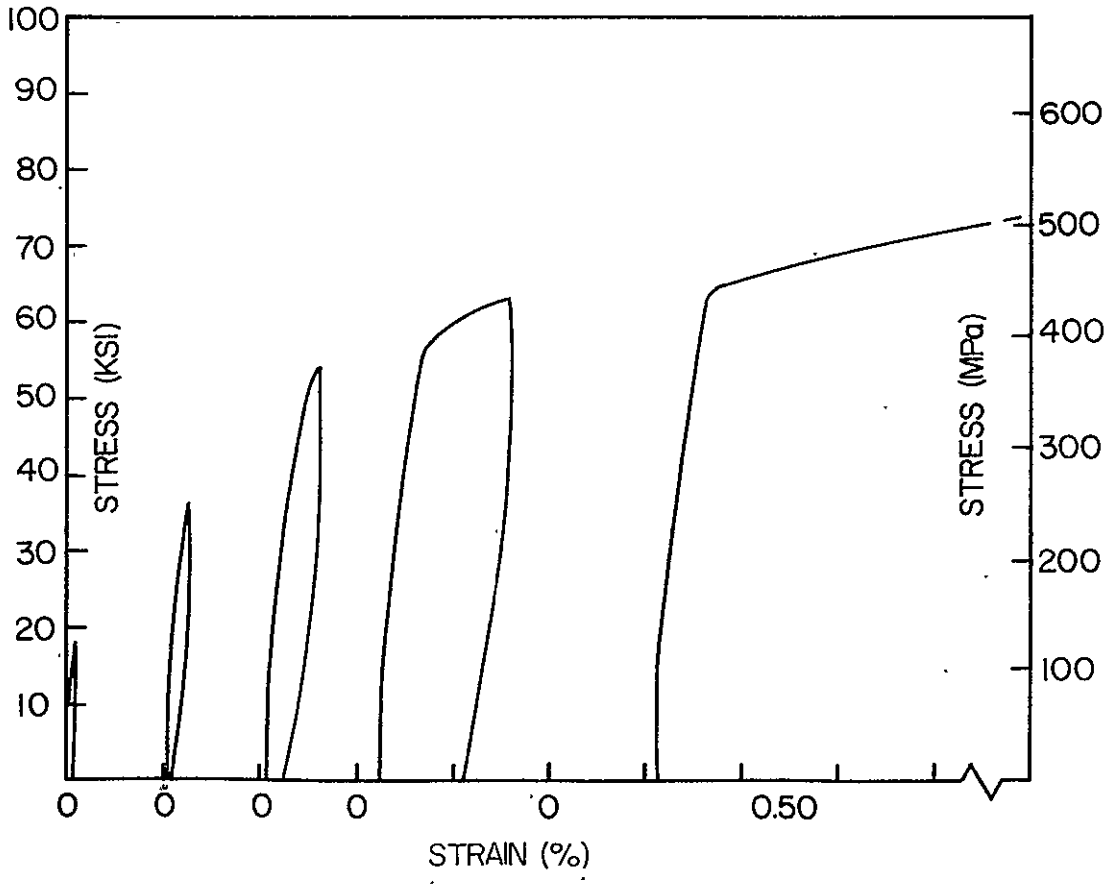

FIGURE 29. CYCLIC COMPRESSION STRESS-STRAIN DIAGRAM FOR $[\pm 45]_s$ B/Al LAMINATE, T6 CONDITION.

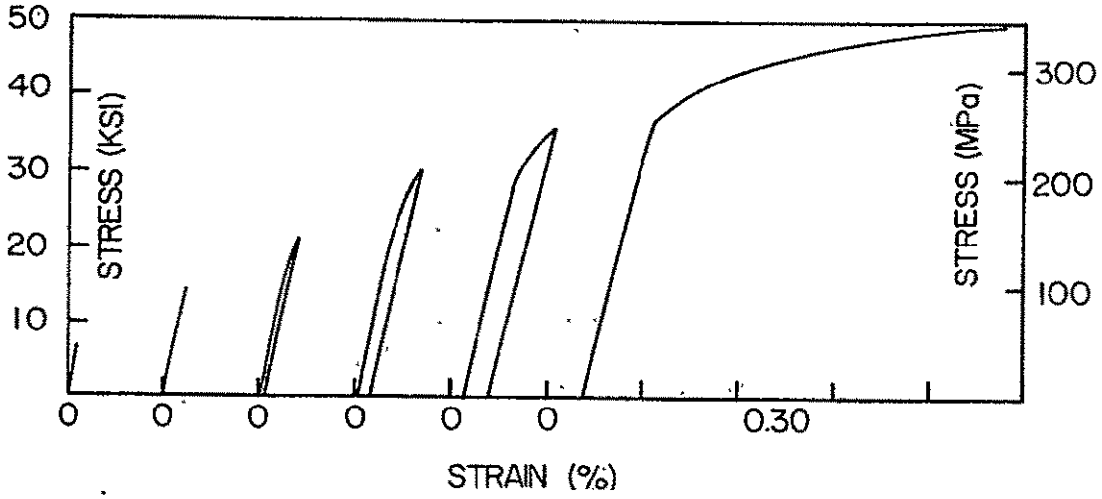

FIGURE 30. CYCLIC TENSION STRESS-STRAIN DIAGRAM FOR $[\pm 45]_s$ B/Al LAMINATE, MODIFIED T6 CONDITION.

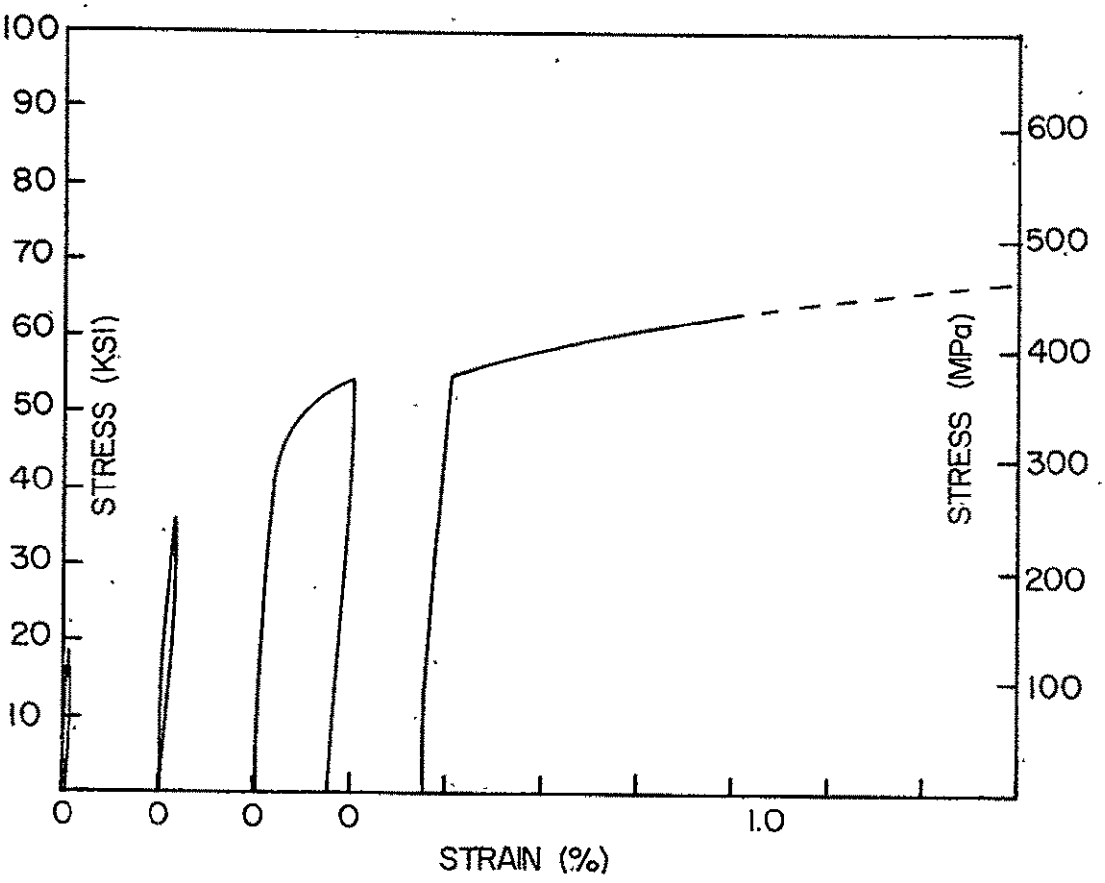

FIGURE 31. CYCLIC COMPRESSION STRESS-STRAIN DIAGRAM FOR $[\pm 45]_s$ B/Al LAMINATE, MODIFIED T6 CONDITION.

TABLE 13

INFLUENCE OF TEMPER CONDITION ON THE CYCLIC TENSION STRESS-STRAIN BEHAVIOR OF $[\pm 45]_s$ BORON-ALUMINUM

TEMPER CONDITION	CYCLE	E_x^L (Msi)	E_x^{UL} (Msi)	ν_{xy}^L	ν_{xy}^{UL}	σ_x^y (ksi)	ε_x^y (%)	σ_x^m (ksi)	ε_x^m (%)	ε_y^m (%)	ε_x^R (%)
F	I	20.5	23.7	0.448	0.421	5.1	0.024	8.0	0.040	-0.028	0.005
	II	22.5	20.6	0.390	0.367	8.0	0.042	14.5	0.163	-0.124	0.092
	III	20.0	18.7	0.375	0.385	14.5	0.167	21.7	0.760	-0.660	0.647
	IV	19.0	-	0.376	-	21.7	0.769	44.2	>3.275	<-3.2	-
T6	I	20.6	21.5	0.401	0.374	-	-	7.3	0.034	-0.015	0.000
	II	20.0	20.4	0.315	0.363	-	-	14.7	0.074	-0.024	0.002
	III	20.1	20.5	0.343	0.358	-	-	21.8	0.117	-0.041	0.010
	IV	20.0	19.8	0.360	0.353	23.2	0.128	29.3	0.185	-0.074	0.037
	V	19.5	18.9	0.349	0.358	28.6	0.183	35.8	0.318	-0.154	0.135
	VI	19.0	-	0.355	-	32.8	0.310	48.1	1.176	-0.893	-
T6N	I	21.0	21.8	0.323	0.315	-	-	7.0	0.032	-0.013	0.000
	II	20.7	21.6	0.318	0.329	-	-	14.4	0.070	-0.026	0.003
	III	21.1	19.6	0.336	0.364	14.9	0.075	21.2	0.120	-0.046	0.013
	IV	19.5	18.0	0.360	0.361	21.7	0.129	29.1	0.201	-0.081	0.043
	V	18.0	16.8	0.365	0.373	28.4	0.203	35.9	0.323	-0.152	0.121
	VI	16.9	-	0.372	-	35.1	0.324	49.2	1.447	-1.163	-

INFLUENCE OF TEMPER CONDITION ON THE CYCLIC COMPRESSION STRESS-STRAIN BEHAVIOR OF $[\pm 45]_S$ BORON-ALUMINUM

TEMPER CONDITION	CYCLE	E_x^L * (Msi)	E_x^{UL} * (Msi)	ν_{xy}^L	ν_{xy}^{UL}	σ_x^y * (ksi)	ε_x^y (%)	σ_x^m * (ksi)	ε_x^m (%)	ε_y^m (%)	ε_x^R (%)
F	I	19.7	-	0.354	-	-	-	-18.3	-0.039	0.013	-0.029
	II	-	21.9	-	0.266	-18.3	-0.042	-27.2	-0.157	0.191	-0.118
	III	27.4	23.2	0.383	0.326	-27.2	-0.163	-29.1	-0.224	0.317	-0.176
	IV	28.6	24.9	0.352	0.320	-29.1	-0.231	-36.3	-0.607	-	-0.558
	V	26.7	-	0.267	-	-36.3	-0.631	-	-	-	-
T6	I	17.4	-	0.283	-	-	-	-18.1	-0.041	0.008	-0.026
	II	18.5	20.6	0.353	0.267	-	-	-35.9	-0.132	0.039	-0.040
	III	22.5	21.2	0.297	0.311	-37.0	-0.141	-54.2	-0.311	0.131	-0.125
	IV	20.0	19.5	0.311	0.306	-53.6	-0.315	-62.6	-0.740	0.429	-0.566
	V	19.2	-	0.327	-	-61.0	-0.794	-	-	-	-
T6N	I	20.0	24.6	0.309	0.286	-	-	-18.5	-0.061	0.019	-0.023
	II	19.2	16.2	0.316	0.335	-33.4	-0.158	-36.2	-0.180	0.619	-0.037
	III	18.0	17.9	0.337	0.337	-36.4	-0.184	-53.9	-0.990	0.428	-0.784
	IV	17.4	20.0	0.342	0.449	-51.1	-1.021	-63.0	<-3.4	2.194	<-3.4
	V	-	-	-	-	-63.0	<-3.4	-	-	-	-

* Fixture influence

material, indicates that the matrix has yielded due to residual thermal stresses). This decrease in modulus is most evident in the F and T6N condition specimens.

The transfer of load into the fixture during the cyclic compression tests significantly altered the appearance of the stress-strain curves. The influence of the fixture affected the initial loading and initial unloading portion of each cycle for a range of up to 20 ksi. In some cases it was impossible to determine an accurate stiffness for a cycle, as seen from Table 14. The failure stresses and strains for the final cycle have not been reported for the reasons given in Section 5.4.1. The final cycle of the F condition specimen (Figure 27) has an increasing slope after yielding at 36.3 ksi; indicating that the fixture is influencing further deformation.

Assuming that the stress-strain response of the material is linear for that portion of the test which is influenced by the fixture, the strain hardening behavior of the material in compression is analogous to the tensile strain hardening behavior. Independent of temper condition, the specimens load linearly to the previous maximum stress and unload linearly. The T6 condition specimen showed some nonlinearity (other than fixture influence) on the unloading portions of the third and fourth cycles (Figure 29); however, all the other T6 condition cyclic compression specimens unloaded linearly.

5.4.2.2 Tension-Compression Tests

The cyclic tension-compression behavior of F, T6, and T6N condition

$[\pm 45]_s$ boron-aluminum is shown in Figures 32-34 and numerical results are presented in Table 15. In general, the transfer of load into the fixture caused severe problems in obtaining meaningful results for the $[\pm 45]_s$ laminate. This is evidenced by the large variation in modulus values for the tests (Table 15). The diagram of the cyclic test on the F condition material (Figure 32) shows spikes on the compression portion of the second and third cycles; this is due to the fixture taking most of the load associated with the spike. No real time data was available during the actual testing and the phenomenon was not observed until after all the tests were completed. The first cycle of this test has been omitted from the figure because the influence of the fixture dominated the behavior of the specimen during the entire cycle.

A discussion of the assumptions used concerning the fixture is essential to understand the conclusions made in this section. For example, in Figure 34, the tensile portion of the fourth cycle has a vertical unloading curve for approximately 20 ksi, gradually changes slope and then behaves linearly in compression. It is assumed that the portion of this cycle from the maximum tensile stress down to approximately zero load is fixture dominated and does not represent the stress-strain behavior of the composite. In addition, it is also assumed that the behavior of the $[\pm 45]_s$ laminate during this portion of the cycle is linear. These assumptions are based on results from the cyclic tension tests and reported results by other researchers.

Results from the cyclic tension-compression test on the F condition

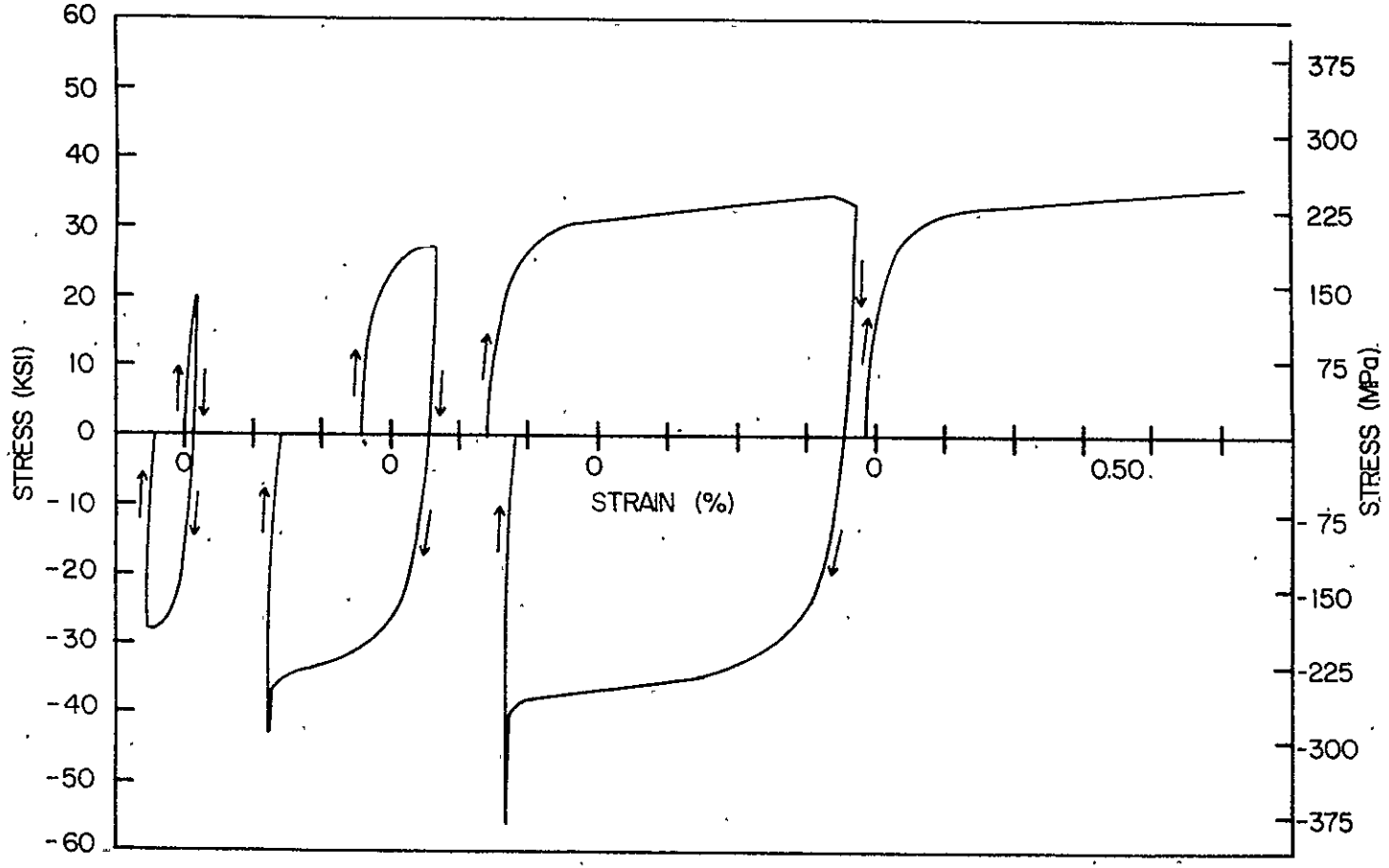

FIGURE 32. CYCLIC TENSION-COMPRESSION STRESS-STRAIN DIAGRAM FOR $[\pm 45]_s$ B/Al LAMINATE, F CONDITION.

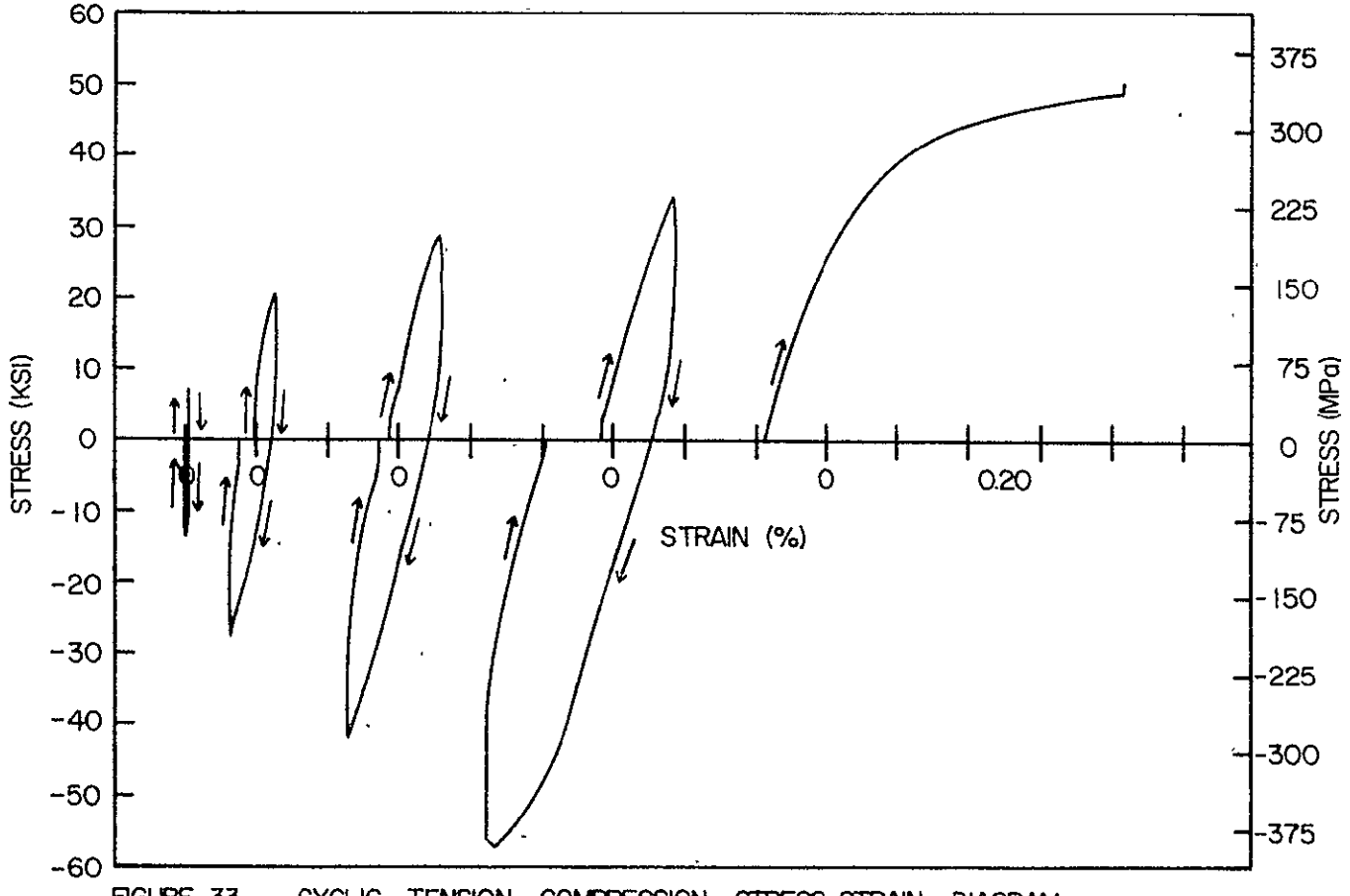

FIGURE 33. CYCLIC TENSION–COMPRESSION STRESS-STRAIN DIAGRAM FOR $[\pm 45]_s$ B/Al LAMINATE, T6 CONDITION.

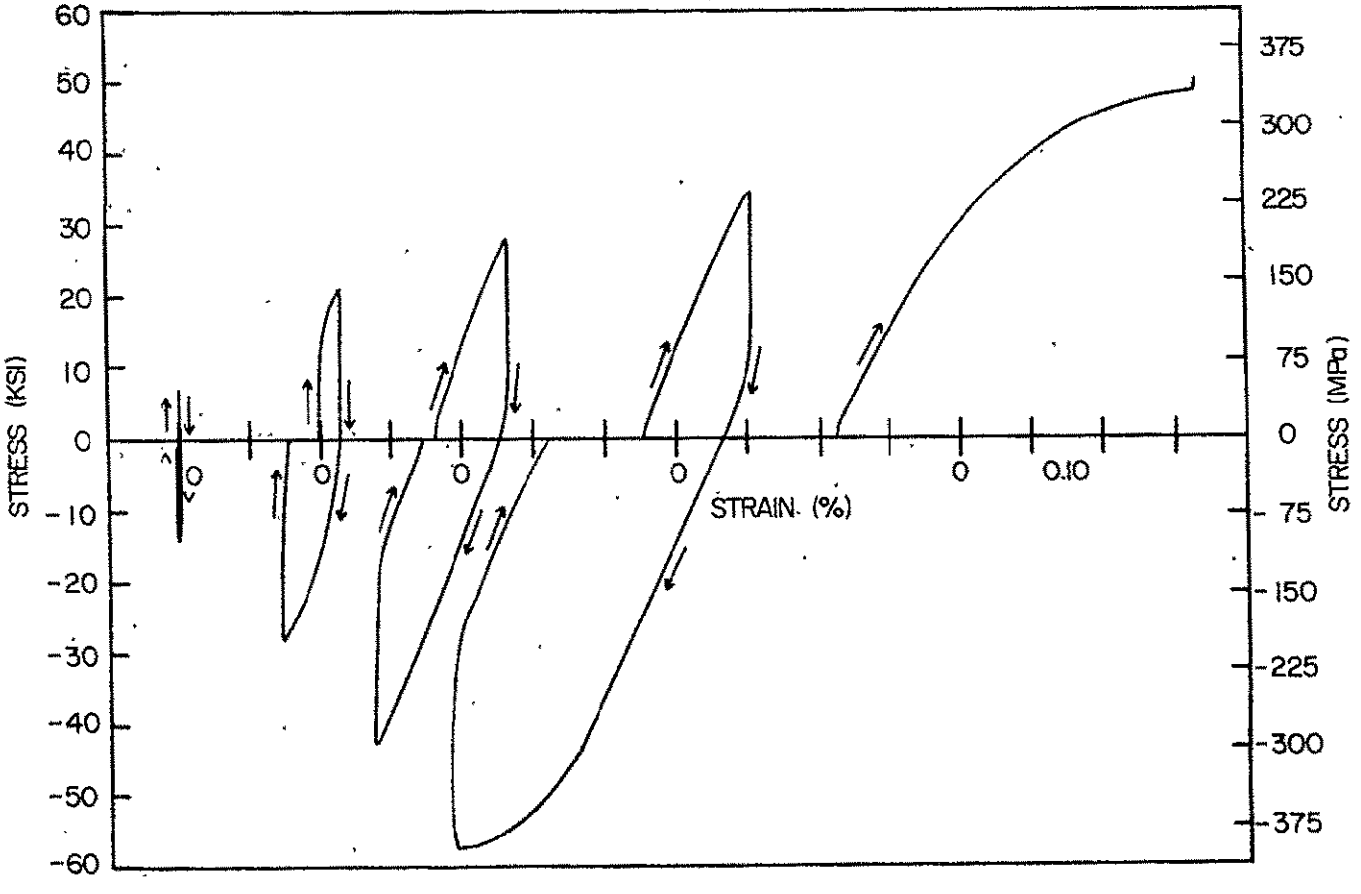

FIGURE 34 CYCLIC TENSION-COMPRESSION STRESS-STRAIN DIAGRAM FOR $[\pm 45]_s$ B/Al LAMINATE, MODIFIED T6 CONDITION.

TABLE 15

INFLUENCE OF TEMPER CONDITION ON THE TENSION-COMPRESSION STRESS-STRAIN BEHAVIOR OF $[\pm 45]_S$ BORON-ALUMINUM

TEMPER CONDITION	CYCLE	E_x^L (Msi)	E_x^{UL} (Msi)	σ_x^{m*} (ksi)	ε_x^m (%)	ε_y^m (%)	ε_x^R (%)
F	I-T	-	-	7.6	0.006	-0.005	0.006
	I-C	-	-	-13.8	-0.016	0.006	-0.012
	II-T	21.9	25.0	19.9	0.070	-0.057	0.065
	II-C	25.0	21.9	-28.2	-0.269	0.374	-0.231
	III-T	21.3	20.1	27.3	0.228	-0.183	0.282
	III-C	20.1	21.3	-43.2	-0.873	1.335	-0.814
	IV-T	21.3	21.3	34.8	1.705	-1.697	1.768
	IV-C	21.3	21.3	-56.5	-0.670	1.674	-0.601
	V-T	17.8	-	47.0	2.357	-2.374	-
T6	I-T	-	-	7.2	0.002	-0.008	0.002
	I-C	25.4	-	-13.7	-0.008	-0.006	-0.010
	II-T	23.6	25.5	20.6	0.052	-0.002	0.041
	II-C	25.5	-	-28.1	-0.075	0.011	-0.053
	III-T	23.2	21.4	28.4	0.105	-0.031	0.080
	III-C	21.4	22.1	-42.5	-0.147	0.053	-0.064
	IV-T	18.6	18.0	34.2	0.169	-0.051	0.103
	IV-C	18.0	19.9	-56.9	-0.336	0.272	-0.180
	V-T	16.3	-	50.6	0.832	-0.505	-
T6N	I-T	-	-	6.8	0.001	-0.001	0.000
	I-C	-	-	-13.9	-0.004	0.001	-0.004
	II-T	24.8	-	21.0	0.027	-0.009	0.026
	II-C	-	-	-28.3	-0.055	0.016	-0.047
	III-T	24.5	24.5	27.9	0.063	-0.020	0.053
	III-C	24.5	24.5	-42.5	-0.125	0.044	-0.058
	IV-T	23.1	21.4	34.2	0.108	-0.028	0.063
	IV-C	21.1	21.1	-57.3	-0.312	0.180	-0.181
	V-T	17.4	-	50.2	0.334	-0.085	-

* Fixture influence

material (Figure 32) show a behavior different from the [0] and [90] laminates. The [0] and [90] laminates both exhibited a Baushinger effect upon loading into the nonlinear region in tension or compression. The F condition $[\pm 45]_s$ specimen does not show this effect, rather the tensile and compressive yield stresses remain approximately the same for the entire test. The yield stress when loading in tension was between 12 - 15 ksi, and the compressive yield stress varied from -10 ksi to -12 ksi. Even though the yield stress values did not change, the linear range was increased because increasing the magnitude of the maximum previous stress increased the linear range from this stress to the yield stress in reversed loading (Figure 32). At stress levels above the yield stress, the response was more nonlinear eventually resembling perfectly plastic behavior.

The yield behavior of the T6 condition specimen (Figure 33) was very different from the behavior of the F condition material. Assuming linear response for that portion of the curve altered by the fixture taking load, the yield behavior due to loading into the nonlinear region for the first four cycles was analogous to isotropic hardening. The specimen did not yield until the second cycle when it yielded at -20 ksi. On the third and fourth cycles the specimen yielded at a stress level equivalent to the magnitude of the maximum previous stress (i.e. isotropic hardening). It is not known if the specimen hardened isotropically on the tensile portion of the fourth cycle because the previous maximum stress was greater than the maximum tensile stress of

the cycle. The tensile yield stress is not increased to the magnitude of the maximum previous stress; instead, the same linear range, 77 ksi, exhibited in the fourth cycle is maintained.

The T6N condition specimen (Figure 34) behaved precisely as the T6 condition specimen; isotropic hardening characterized the first four cycles and the yield stress on the fifth cycle was reduced to 25 ksi with a linear range from the maximum compressive stress of 82 ksi.

5.4.3 Conclusions

The stress-strain behavior of the $[\pm 45]_s$ laminate, as with [0] and [90] laminates, is altered significantly by heat treatment, however, the cryogenic exposure has no major effect on the response of the material. The monotonic tests indicate that the yield stress in tension and compression is increased substantially by heat treatment and the tensile failure strains are reduced. Cryogenic exposure did not significantly change the tensile yield stress, but the tensile strength was reduced.

Heat treating the material also changed the manner in which the laminate responded to cyclic tension-compression loading. The F condition material exhibited constant tensile and compressive yield stress for the entire test. The T6 and T6N condition specimens exhibited increasing yield stress values which corresponded to the magnitude of the previous maximum stress for the first four cycles and on the final cycle the tensile yield stress was reduced.

Regardless of the temper condition, the stiffness of the laminate was shown to reduce by cyclic loading. This was observed in the cyclic

tension tests and the cyclic tension-compression tests for the T6 and T6N condition specimens.

5.5 The $[0/\pm45/0]_s$ Laminate

5.5.1 Monotonic Tension and Compression Tests

The influence of temper condition on the tension and compression stress-strain behavior of $[0/\pm45/0]_s$ boron-aluminum is shown in Figure 35 and Tables 16 and 17. No difference could be distinguished between the tensile and compressive moduli. The average tensile modulus results ranged from 23.8 Msi to 24.3 Msi, and the compressive values ranged from 22.3 Msi to 24.1 Msi. All values are lower than the lamination theory prediction of 26.9 Msi. Thermoelastic laminate analysis predicts significant tensile residual stress in the ±45° laminae; it is likely that the ±45° laminae are stressed into the nonlinear region as a result of curing and thus the experimental modulus is lower than the analytic prediction. The Xray residual stress results from Reference 14 showed that heat treating "as received" unidirectional boron-aluminum to a T6 condition increased the axial tensile residual stress in the matrix. Heat treating the $[0/\pm45/0]_s$ laminate should increase the residual stress in the ±45° laminae for similar reasons. As a result of the higher residual stresses, the heat treated specimens will have a lower modulus; this is substantiated by the monotonic tension and tension-tension results (Tables 16 and 18).

The yield stress of the laminate was affected by heat treating and to a lesser extent cryogenic exposure. Heat treating the laminate

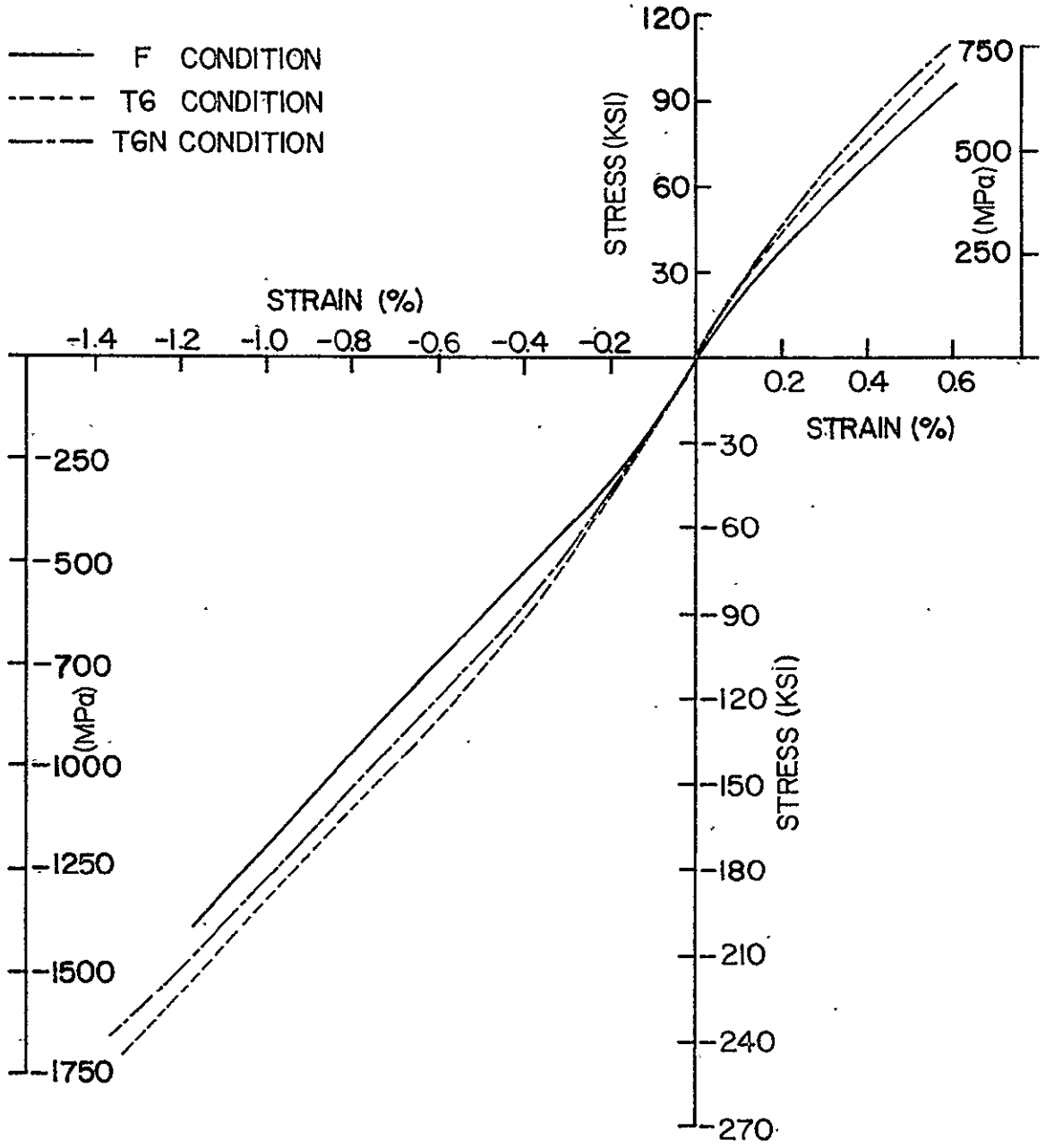

FIGURE 35. COMPARISON OF $[0/\pm45/0]_s$ B/Al LAMINATE WITH DIFFERENT TEMPER CONDITIONS IN TENSION AND COMPRESSION.

TABLE 16

INFLUENCE OF TEMPER CONDITION ON THE TENSILE STRESS-STRAIN BEHAVIOR OF $[0/\pm45/0]_s$ BORON-ALUMINUM

TEMPER CONDITION	E_x (Msi)	ν_{xy}	σ_x^y (ksi)	ε_x^y (%)	σ_x^u (ksi)	ε_x^u (%)	ε_y^u (%)
F	24.3	0.264	10.3	0.044	99.1	0.621	-0.222
T6	23.8	0.282	23.8	0.102	101.7	0.563	-0.198
T6N	23.9	0.263	24.5	0.105	109.0	0.578	-0.192

TABLE 17

INFLUENCE OF TEMPER CONDITION ON THE COMPRESSIVE STRESS-STRAIN BEHAVIOR OF $[0/\pm45/0]_s$ BORON-ALUMINUM

TEMPER CONDITION	E_x (Msi)	ν_{xy}	σ_x^{y*} (ksi)	ε_x^y (%)	σ_x^{u*} (ksi)	ε_x^u (%)	ε_y^u (%)
F	22.3	0.361	-18.9	-0.061	-209.3	-1.261	1.022
T6	24.1	0.295	-63.9	-0.259	-230.7	-1.288	0.706
T6N	23.7	0.293	-46.2	-0.180	-247.3	-1.417	0.824

* Fixture influence

increased the average tensile yield stress from 10.3 ksi for the F condition specimens to 23.8 ksi for the T6 condition material. The average compressive yield stress for the T6 condition material was -63.9 ksi as compared to -18.9 ksi for the F condition specimens. The tensile yield stress was not changed significantly by the liquid nitrogen exposure, as compared to the T6 condition value, but the compressive yield stress was reduced significantly from -63.9 ksi to -46.2 ksi (Table 17). The one major characteristic indicating that the cryogenic exposure did effect the stress-strain behavior is the fact that the tensile stress-strain curve of T6N condition specimen was shifted up as compared to T6 condition specimen's stress-strain curve (i.e. for each value of strain the T6N condition specimen had a higher stress value than T6 condition specimen). The opposite trend was exhibited by the T6N and T6 condition specimens under compression loading (i.e. each value of stress for the same strain was reduced). This shift in the stress-strain curves indicates that the liquid nitrogen changed the residual stress state in the laminate.

The T6 heat treatment had essentially no effect on the tensile strength of the laminate as compared to the F condition material; however, the liquid nitrogen exposure did increase the strength to 109.0 ksi from 101.7 ksi for the T6 condition specimens. Also associated with the T6 heat treatment is a reduction in ultimate strain; the F condition specimen had the largest failure strain, 0.621 percent, and the T6 and T6N condition specimens had smaller values of 0.563 percent and 0.578 percent, respectively.

Comparison of the compressive failure stresses of the $[0/\pm45/0]_s$, $[0]$, and $[\pm45]_s$ laminates provides more evidence that the failure stresses associated with this type of compression specimen are not the true strength of the material. The compressive failure stresses of the $[0]$ and $[0/\pm45/0]_s$ laminates were approximately the same; however, the $[\pm45]_s$ laminate exhibited much lower failure stresses than these two laminates. Neglecting interlaminar effects, it would be expected that the failure stress of the $[0/\pm45/0]_s$ specimens would be much lower than the unidirectional compressive strength since 50 percent of the laminate is of lower strength laminae. As shown by the experimental results (Tables 2, 12, 17) the $[0/\pm45/0]_s$ laminate does not have lower failure stresses than the $[0]$ laminate and it is likely the specimen design is responsible for these results.

5.5.2 Cyclic Tests

5.5.2.1 Tension

Results from the cyclic tension tests were consistent with the monotonic tension results. The initial moduli (Table 18) ranged from 23.0 Msi to 25.8 Msi, and the initial yield stresses varied with the temper condition in the same manner as the monotonic specimens. Independent of temper condition, a small reduction in modulus is exhibited on each successive cycle (Table 18). The F condition specimen's initial modulus was 25.8 Msi and the modulus on the last cycle was 23.3 Msi. The moduli of the T6 and T6N condition specimens shows a similar trend; however, the decrease is smaller. The failure stress and strain for all

TABLE 18

INFLUENCE OF TEMPER CONDITION ON THE CYCLIC TENSION STRESS-STRAIN BEHAVIOR OF $[0/\pm45/0]_s$ BORON-ALUMINUM

TEMPER CONDITION	CYCLE	E_x^L (Msi)	E_x^{UL} (Msi)	ν_{xy}^L	ν_{xy}^{UL}	σ_x^y (ksi)	ε_x^y (%)	σ_x^m (ksi)	ε_x^m (%)	ε_y^m (%)	ε_x^R (%)
F	I	25.8	25.1	0.309	0.282	10.7	0.042	21.3	0.095	-0.029	0.011
	II	24.7	23.3	0.307	0.299	21.4	0.098	42.6	0.222	-0.082	0.033
	III	24.1	22.4	0.316	0.298	26.1	0.144	64.4	0.364	-0.146	0.047
	IV	23.3	-	0.318	-	23.2	0.148	105.9	0.661	-0.295	-
T6	I	23.6	24.6	0.253	0.278	-	-	26.6	0.114	-0.025	0.006
	II	24.6	23.8	0.268	0.272	29.0	0.149	53.2	0.249	-0.074	0.028
	III	24.1	23.4	0.273	0.289	54.8	0.284	79.3	0.409	-0.148	0.070
	IV	23.5	-	0.284	-	75.6	0.392	108.6	0.605	-0.246	-
T6N	I	23.6	24.7	0.288	0.282	-	-	25.2	0.106	-0.305	0.002
	II	24.0	24.2	0.286	0.288	32.1	0.136	52.1	0.231	-0.069	0.012
	III	23.6	23.1	0.279	0.290	50.2	0.224	78.5	0.381	-0.121	0.039
	IV	23.0	-	0.287	-	78.7	0.381	108.8	0.585	-0.191	-

three types of specimens were higher than ultimate results of the corresponding monotonic specimen. The increased failure strain and the reduction in modulus with successive cycles indicates that cyclic loading damages the material.

The tension-tension behavior of the F condition specimen (Figure 36) was similar to that of the F condition unidirectional specimen. The specimen yielded on the first cycle at 10.7 ksi and unloaded linearly. A fairly constant yield stress and linear range of 21.4 - 26.1 ksi were exhibited during the second, third, and final cycle. This type of strain hardening behavior, where a constant elastic range is maintained, is called kinematic hardening [25].

The cyclic tension stress-strain behavior of the T6 condition $[0/\pm45/0]_s$ specimen (Figure 38) is similar to the T6 condition [0] specimen. The specimen did not yield in the first cycle and during the second cycle the yield stress was 29.0 ksi; unloading was linear for both cycles. On the third and fourth cycles the yield stress was the same as the previous highest stress and the unloading portion of the third cycle was linear.

The yield behavior of the T6N condition specimen (Figure 40) is very similar to the T6 condition $[0/\pm45/0]_s$ specimen. The specimen initially yielded during the second cycle at 32.1 ksi; the yield stresses for the third and fourth cycles were approximately the same as the maximum stress of the previous cycle. In all cases the unloading portion of the cycle was linear with the maximum linear range being 78.7 ksi.

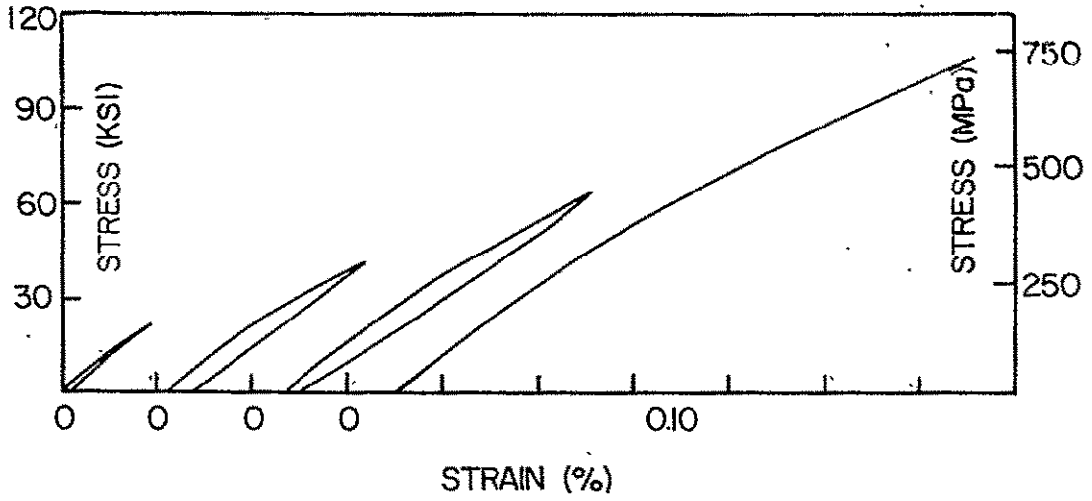

FIGURE 36. CYCLIC TENSION STRESS–STRAIN DIAGRAM FOR $[0/\pm45/0]_s$ B/Al LAMINATE, F CONDITION.

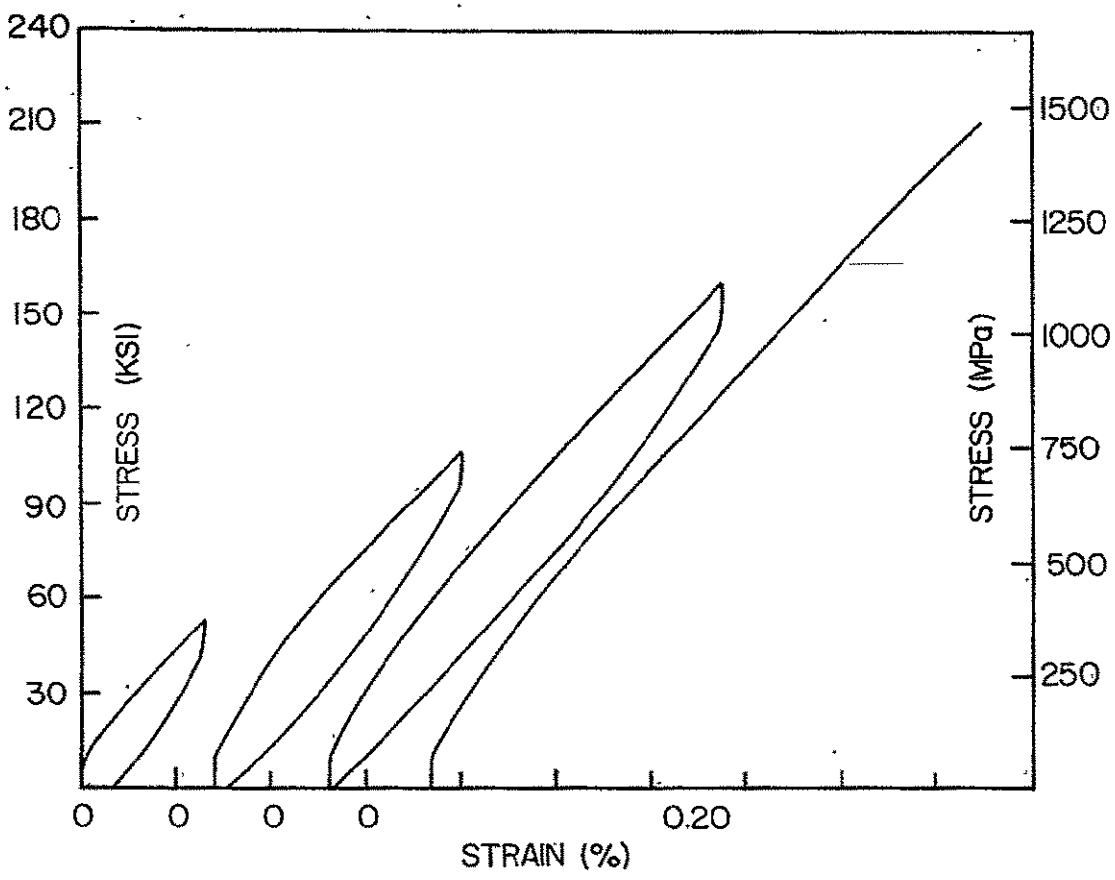

FIGURE 37. CYCLIC COMPRESSION STRESS–STRAIN DIAGRAM FOR $[0/\pm45/0]_s$ B/Al LAMINATE, F CONDITION.

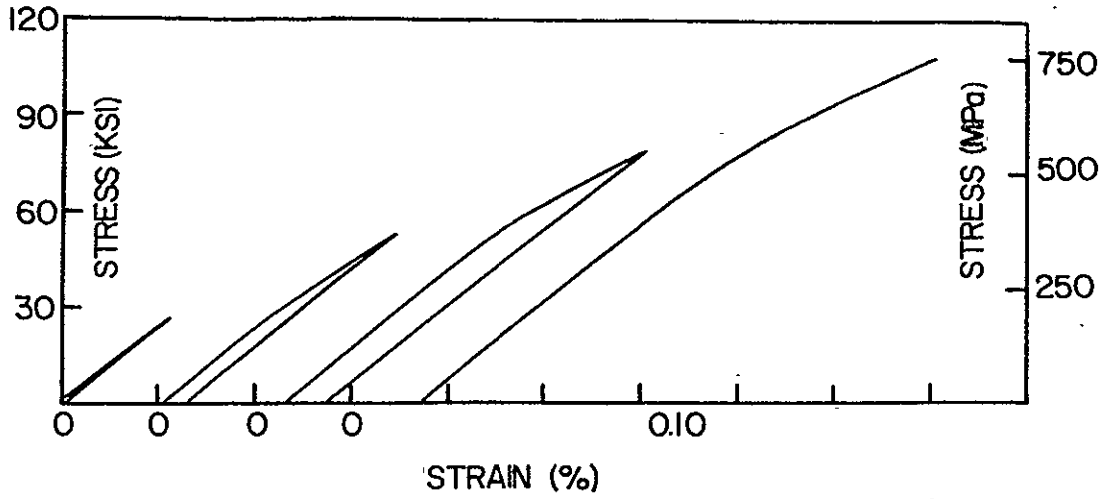

FIGURE 38. CYCLIC TENSION STRESS-STRAIN DIAGRAM FOR $[0/\pm45/0]_s$ B/Al LAMINATE, T6 CONDITION.

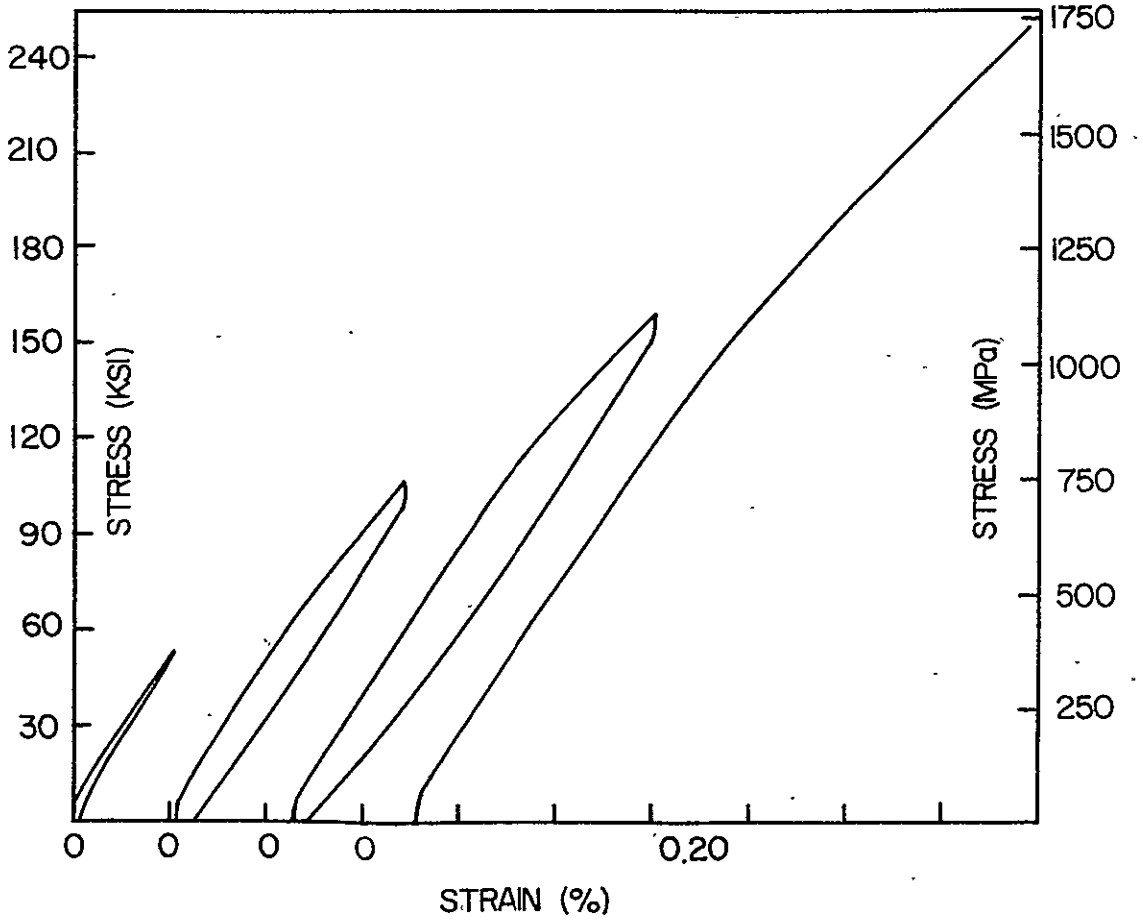

FIGURE 39. CYCLIC COMPRESSION STRESS-STRAIN DIAGRAM FOR $[0/\pm45/0]$ B/Al LAMINATE, T6 CONDITION.

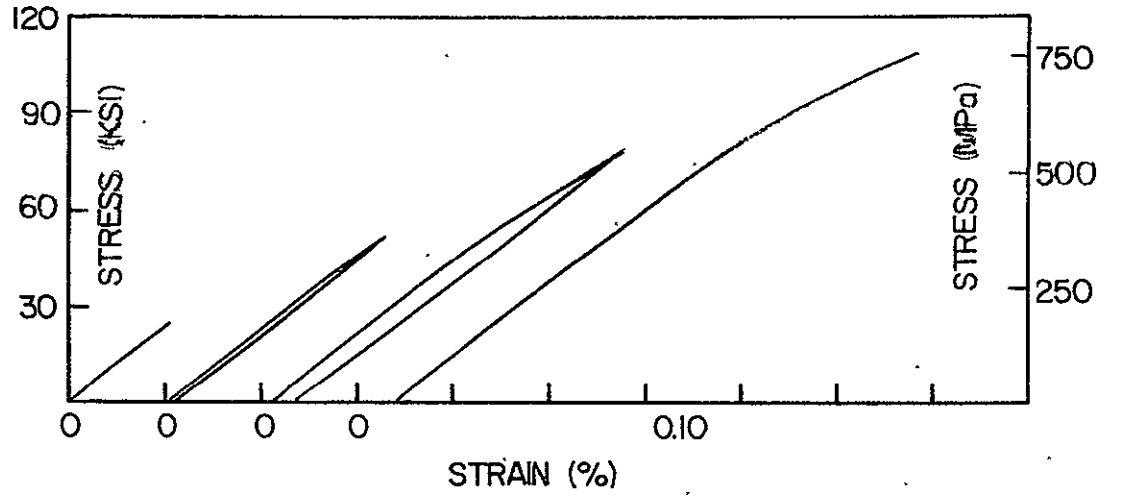

FIGURE 40. CYCLIC TENSION STRESS–STRAIN DIAGRAM FOR $[0/\pm45/0]_s$ B/Al LAMINATE, MODIFIED T6 CONDITION.

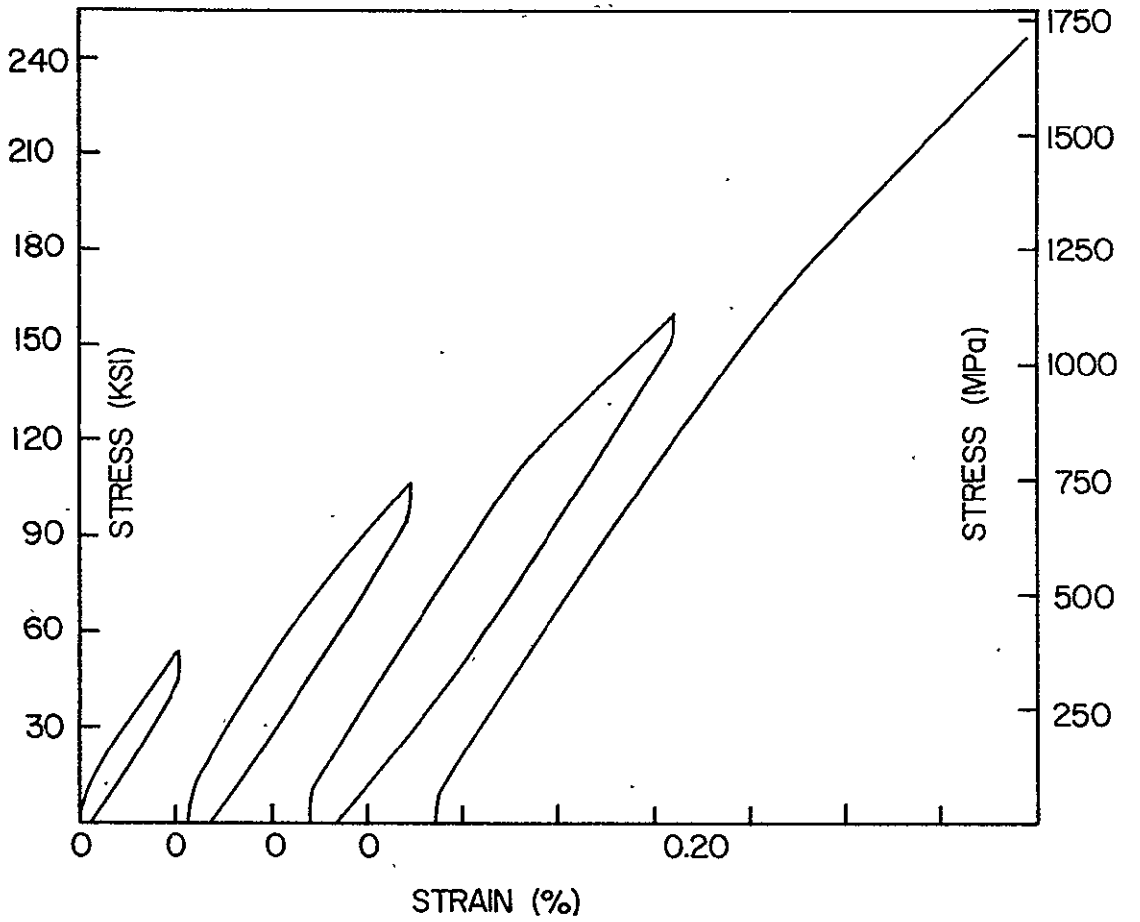

FIGURE 41. CYCLIC COMPRESSION STRESS–STRAIN DIAGRAM $[0/\pm45/0]_s$ B/Al LAMINATE, MODIFIED T6 CONDITION.

As expected, the stress-strain behavior of all three types of $[0/\pm45/0]_s$ specimens is a function of the stress-strain behavior of the laminae. For example, the F condition specimen developed a maximum linear range during cyclic loading and this linear range was maintained for the remainder of the test; this is precisely the behavior of the F condition unidirectional specimen. Also, the heat treated specimens yielded at the highest previous stress and always unloaded linearly just as the T6 and T6N condition [0] and $[\pm45]_s$ specimens did.

5.5.2.2 Compression

The cyclic compression curves for the $[0/\pm45/0]_s$ laminate, as with compression tests on all other laminates, were influenced by the fixture. The initial 8 - 10 ksi at the beginning of each cycle and at the beginning of the unloading portion of each cycle are the portions of the curve affected by the fixture loading. The F, T6, and T6N cyclic compression specimens (Table 19) exhibited a similar type of modulus reduction as the cyclic tension specimens. The decrease of modulus is not as large as that of the tensile specimens and the modulus does not consistently decrease with each cycle, but for all three types of specimens the decrease from the first cycle to the last cycle is approximately 9 percent.

The F condition compression-compression specimen (Figure 37) behaves in a manner similar to the F condition tension-tension specimen. The initial modulus of the first cycle is 26.5 Msi and the modulus of the final cycle is 24.2 Msi. The yield stress and the linear range

TABLE 19

INFLUENCE OF TEMPER CONDITION ON THE CYCLIC COMPRESSION STRESS-STRAIN BEHAVIOR OF $[0/\pm45/0]_S$ BORON-ALUMINUM

TEMPER CONDITION	CYCLE	E_x^L (Msi)	E_x^{UL} (Msi)	ν_{xy}^L	ν_{xy}^{UL}	$\sigma_x^{y\,*}$ (ksi)	ε_x^y (%)	$\sigma_x^{m\,*}$ (ksi)	ε_x^m (%)	ε_y^m (%)	ε_x^R (%)
F	I	26.5	23.5	0.367	0.331	-15.3	-0.040	-53.6	-0.261	0.170	-0.078
	II	25.2	25.8	0.315	0.303	-39.7	-0.198	-106.9	-0.604	0.458	-0.117
	III	23.6	24.4	0.315	0.327	-45.7	-0.273	-159.7	-0.949	0.791	-0.131
	IV	24.2	-	0.312	-	-40.2	-0.266	-210.9	-1.288	1.117	-
T6	I	22.7	24.2	0.309	0.295	-	-	-53.4	-0.214	0.064	0.000
	II	24.0	24.0	0.290	0.306	-59.8	-0.245	-107.1	-0.487	0.188	-0.058
	III	23.4	23.5	0.313	0.307	-104.3	-0.479	-160.1	-0.808	0.388	-0.107
	IV	22.5	-	0.315	-	-119.0	-0.613	-250.6	-1.375	0.790	-
T6N	I	23.1	24.0	0.313	0.302	-37.8	-0.133	-53.8	-0.208	0.072	-0.027
	II	24.5	24.6	0.303	0.310	-50.6	-0.196	-107.2	-0.494	0.214	-0.078
	III	23.6	24.2	0.320	0.320	-104.3	-0.487	-160.7	-0.826	0.425	-0.144
	IV	22.7	-	0.325	-	-97.0	-0.571	-246.1	-1.381	0.826	-

* Fixture influence

increased on successive cycles (Table 19) through the third cycle where both the loading and unloading portions of the curve had a linear range of 46 ksi. The yield stress was reduced, however, to -40 ksi during the fourth cycle. The reduction in yield stress coupled with the decrease in modulus on each cycle indicates that the specimen has been damaged by the cyclic loading.

The linear range of the T6 condition compression-compression specimen appears to be dependent upon the load direction during the cycle (Figure 39). The specimen did not yield during the first cycle and unloaded linearly. The yield stress for the second cycle was -60 ksi; unloading was nonlinear with a linear range of 91 ksi. On the third cycle the specimen yielded at -104 ksi, approximately the highest previous stress, but the linear range upon unloading was still 90 ksi. However, on the fourth cycle the yield stress was increased to -119 ksi, a larger linear range than on the unloading portion of the third cycle. This load path dependent behavior was not exhibited by the cyclic tension specimens or the F condition cyclic compression specimen.

The T6N condition specimen (Figure 41) exhibited behavior similar to the T6 condition cyclic compression specimen. The specimen yielded on the first cycle at -38 ksi and unloaded linearly. The yield stress for the second cycle was increased to the maximum previous stress, -51 ksi, and upon unloading the response was nonlinear with a linear range of 65 ksi. During the third cycle the yield stress was -104 ksi, and upon unloading the linear range was 78 ksi. However, on the fourth cycle of loading the yield stress was increased to -97 ksi. As with the

T6 condition cyclic compression specimen, the yield stress and linear range during unloading increased with each cycle, but the linear range on the unloading portion was smaller than the linear range of the loading portion of the cycle.

5.5.2.3 Tension-Compression

The desired load path for some tension-compression specimens was not completed because of tab debonding as mentioned in Section 5.1. Thus, only the first two cycles of a T6N condition specimen are presented and no results for the T6 condition specimens are reported.

The results of a typical tension-compression test on F condition $[0/\pm45/0]_s$ material are shown in Table 20 and Figure 42. The yield behavior of the specimen resembled a Baushinger effect (i.e. loading into the tensile nonlinear region and increasing the linear range upon unloading into compression but the magnitude of the yield stress is not equal to the maximum previous stress). The linear range was increased on each successive cycle from 34 ksi for the first cycle to 54 ksi for the third cycle. It is important to note that the low modulus values for loading into tension from compression or compression from tension are a result of the fact that the specimen is stressed beyond the linear range, and they are not a result of damage to the laminate.

Two cycles of the tension-compression tests on the T6N condition $[0/\pm45/0]_s$ specimen were completed before failure occurred during the tensile portion of the third cycle (Figure 43). The specimen was loaded in tension on the fourth cycle but again tab failure occurred.

TABLE 20

INFLUENCE OF TEMPER CONDITION ON THE TENSION-COMPRESSION STRESS-STRAIN BEHAVIOR OF $[0/\pm45/0]_s$ BORON-ALUMINUM

TEMPER CONDITION	CYCLE	E_x^L (Msi)	E_x^{UL} (Msi)	σ_x^{m*} (ksi)	ε_x^m (%)	ε_y^m (%)	ε_x^R (%)
F	I-T	22.8	23.3	28.4	0.127	-0.039	0.033
	I-C	22.8	24.1	-52.7	-0.265	0.176	-0.004
	II-T	18.2	22.2	55.0	0.279	-0.034	0.045
	II-C	17.5	24.4	-104.5	-0.600	0.462	-0.096
	III-T	16.0	22.2	82.5	0.456	0.012	0.048
	III-C	16.0	23.6	-156.2	-0.930	0.751	-0.112
	IV-T	15.4	-	110.9	0.655	0.072	-
T6N	I-T	24.9	23.5	26.7	0.091	-0.027	0.028
	I-C	23.5	23.5	-52.8	-0.217	0.069	-0.033
	II-T	24.1	22.7	51.7	0.207	-0.062	0.029
	II-C	22.4	24.7	-106.0	-0.498	0.199	-0.083
	III-T	20.9	-	72.5	0.339	-0.086	-
	IV-T	21.5	-	68.2	0.315	-0.083	-

* Fixture influence

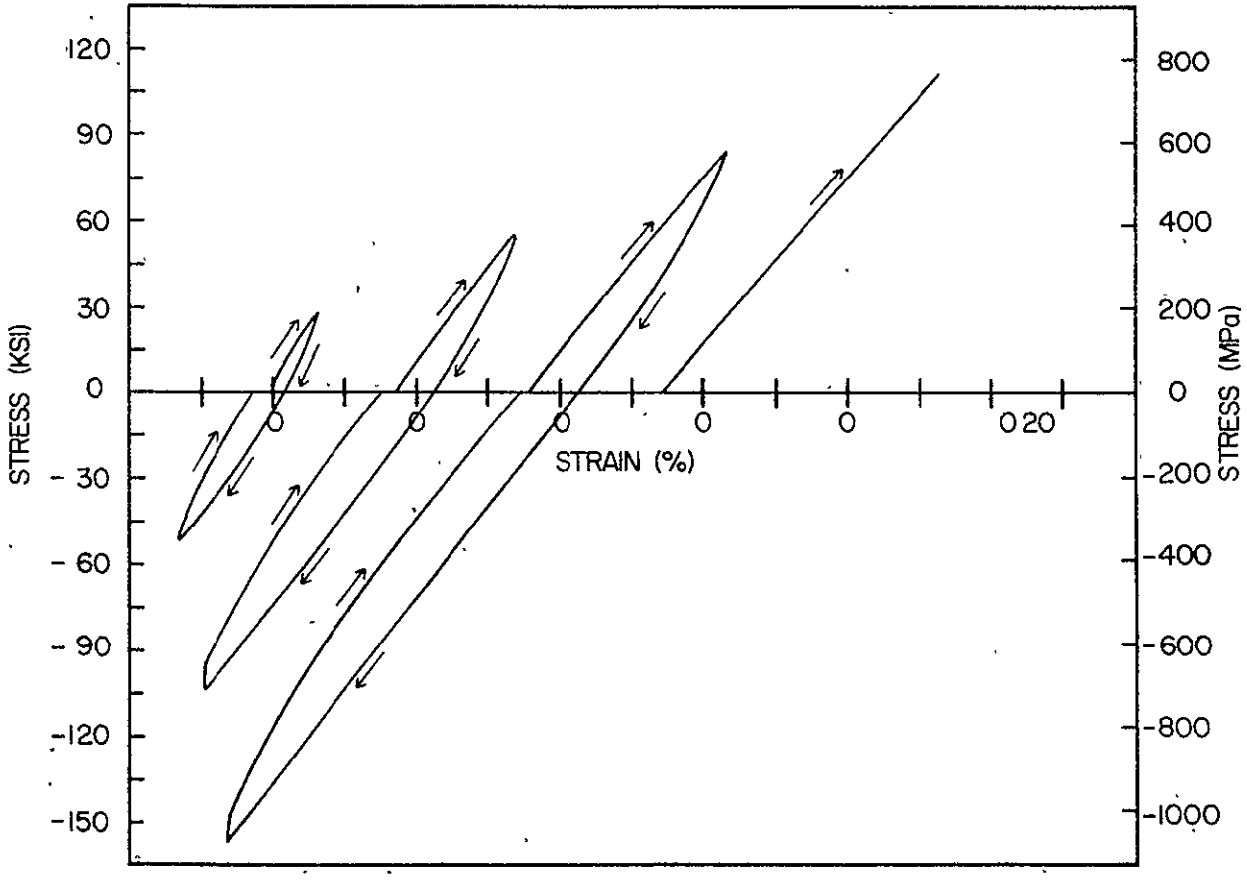

FIGURE 42. CYCLIC TENSION-COMPRESSION STRESS-STRAIN DIAGRAM FOR $[0/\pm 45/0]_s$ B/Al LAMINATE, F CONDITION.

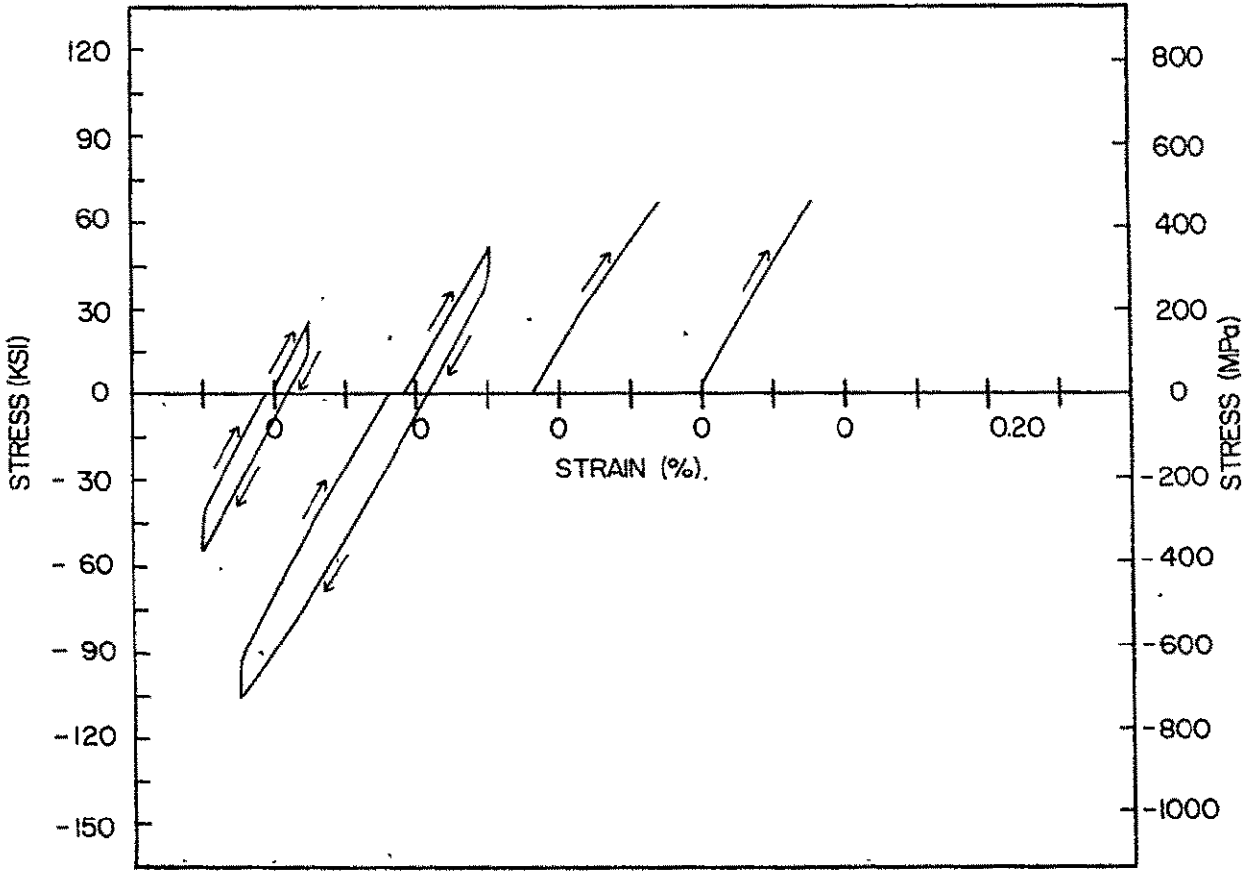

FIGURE 43. CYCLIC TENSION COMPRESSION STRESS--STRAIN DIAGRAM FOR $[0/\pm45/0]_S$ B/Al LAMINATE, MODIFIED T6 CONDITION.

The T6N condition specimen exhibited Baushinger behavior as the F condition specimen did under tension-compression loading. The loading during the first cycle was linear throughout the tensile portion of the curve and yielded in compression at -34 ksi, a linear range of 61 ksi. The specimen yielded in tension during the second cycle at 16 ksi, increasing the linear range to 60 ksi. The compressive yield stress for the second cycle was -31 ksi increasing the linear range to 83 ksi. The linear range was decreased to 40 ksi when unloading from the maximum compressive stress of the second cycle, thus the entire portion of the third cycle was in the nonlinear range. The tabs debonded on the third cycle at a stress level of 72.5 ksi. New tabs were bonded on the specimen and they debonded on the fourth cycle.

5.5.3 Conclusions

The temper condition of the specimen influenced the yield behavior of the $[0/\pm45/0]_s$ laminate. The monotonic tests showed that the yield stress was increased in both tension and compression by heat treating the F condition material to a T6 condition. The liquid nitrogen exposure increased the tensile yield stress and strength, but it reduced the compressive yield stress.

The cyclic tension tests showed that the strain hardening behavior was dependent upon the temper condition. Cyclic loading of the F condition specimen developed a maximum linear range which was exhibited for each of the remaining cycles. The T6 and T6N condition specimen's strain hardened differently than the F condition material. The specimen

yielded at the previous highest stress and unloaded linearly on each cycle.

The F condition cyclic compression specimen behaved similar to the F condition cyclic tension specimen. A linear range of approximately 40 ksi was developed by cycling the specimen, and that range was maintained for the entire test. The T6 and T6N condition specimens exhibited loading direction dependent yield phenomenon. The yield stress on the loading portion and the linear range on the unloading portion increased with each successive cycle. However, the yield stress of a cycle was always larger than the linear range upon unloading.

In addition, the cyclic tension and cyclic compression tests on specimens having all three temper conditions showed the elastic stiffness to decrease as the maximum load of the cycles was increased. This modulus decrease indicates that the cyclic loading is damaging the specimen.

The results from the tension-compression tests do not provide enough information to compare the yield phenomenon for the three temper conditions under axial loading. The F condition tension-compression specimen exhibited a Baushinger effect, contrary to the results from the F condition cyclic tension and cyclic compression tests. No data was reported from the tension-compression tests on T6 condition material because the tabs debonded before the desired load path was completed. The T6N condition specimens behaved for the most part in a Baushinger manner. No additional cycles were completed so the yield behavior is not satisfactorily defined.

It is clear from the monotonic tension and compression and cyclic tension tests that the stress strain behavior of $[0/\pm45/0]_s$ boron-aluminum shows characteristics of the [0] and $[\pm45]_s$ laminates. The effect of temper condition on the yield stress and strength is analogous to the [0] material. The nonlinear unloading of the F condition material and linear unloading of the T6 and T6N condition material are also characteristic of the unidirectional material under cyclic tension loading.

It is also obvious that some of the stress-strain characteristics of the $[0/\pm45/0]_s$ laminates are not typical of the laminae. The nonlinear unloading in compression of the $[0/\pm45/0]_s$ material was not exhibited by either the unidirectional or $[\pm45]_s$ material. Also the loading direction dependent linear range was not characteristic of the laminae. This atypical behavior of the $[0/\pm45/0]_s$ laminates suggests the possibility of interlaminar influence of anisotropic composite materials.

5.6 The $[0/\pm45]_s$ Laminate

5.6.1 Monotonic Tension and Compression Tests

Comparision of the tensile and compressive stress-strain behavior of $[0/\pm45]_s$ boron-aluminum having different temper conditions is shown in Figure 44 and Tables 21 and 22. The initial modulus does not exhibit any significant difference between the results from the tension tests and the compression tests. The variation in modulus values was 18.6 Msi to 23.0 Msi with an average value of 20.8 Msi; laminate analysis pre-

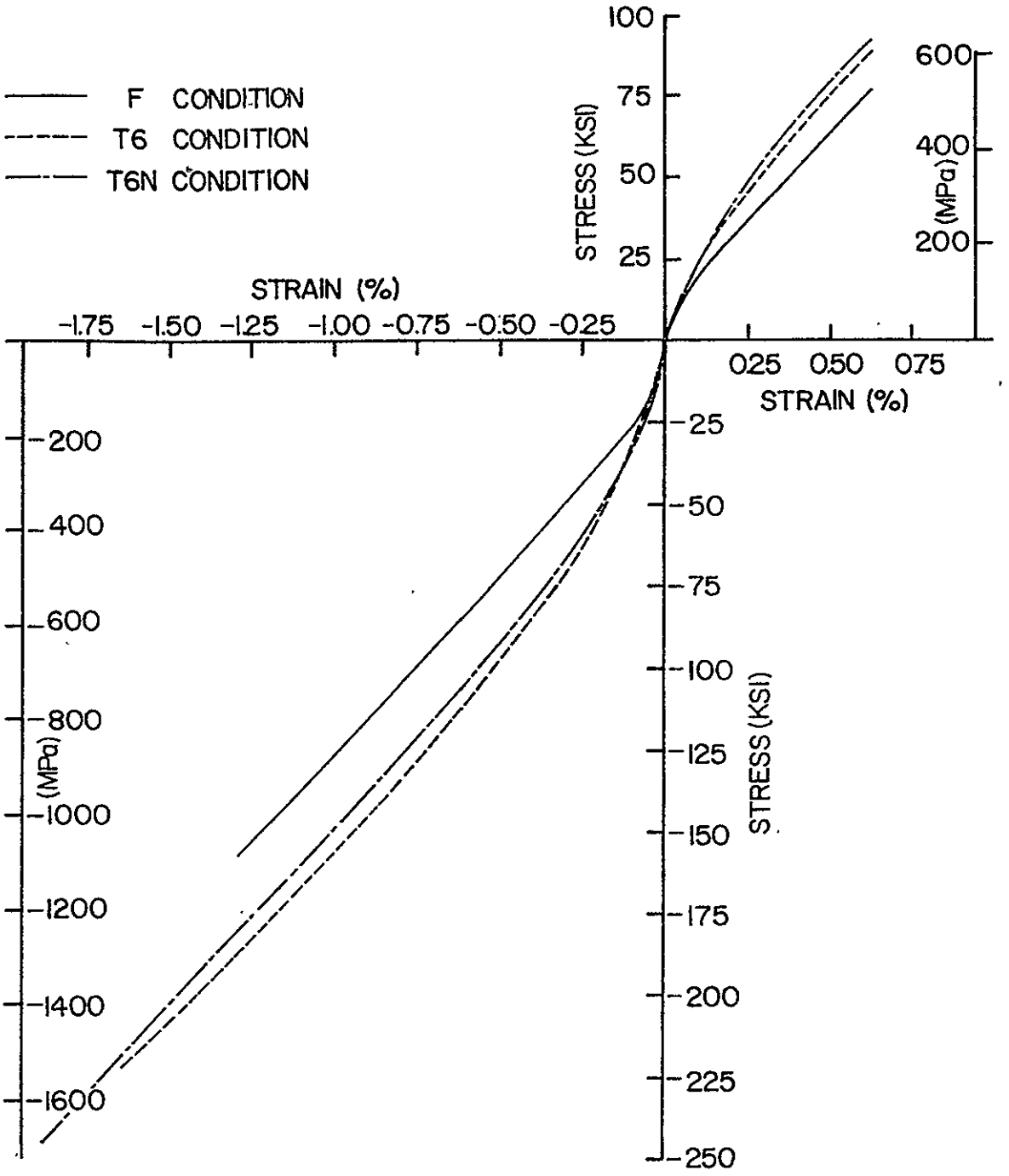

FIGURE 44. COMPARISON OF $[0/\pm45]_s$ B/Al LAMINATE WITH DIFFERENT TEMPER CONDITIONS IN TENSION AND COMPRESSION.

TABLE 21

INFLUENCE OF TEMPER CONDITION ON THE TENSILE STRESS-STRAIN OF $[0/\pm45]_s$ BORON-ALUMINUM

TEMPER CONDITION	E_x (Msi)	ν_{xy}	σ_x^y (ksi)	ε_x^y (%)	σ_x^u (ksi)	ε_x^u (%)	ε_y^u (%)
F	23.0	0.289	8.58	0.038	71.7	0.600	-0.314
T6	19.6	0.296	13.83	0.066	87.5	0.629	-0.255
T6N	20.8	0.297	18.07	0.086	90.5	0.620	-0.266

TABLE 22

INFLUENCE OF TEMPER CONDITION ON THE COMPRESSIVE STRESS-STRAIN $[0/\pm45]_s$ BORON-ALUMINUM

TEMPER CONDITION	E_x (Msi)	ν_{xy}	σ_x^y * (ksi)	ε_x^y (%)	σ_x^u * (ksi)	ε_x^u (%)	ε_y^u (%)
F	18.6	0.384	-19.75	-0.065	-153.2	-1.262	1.264
T6	22.4	0.329	-47.52	-0.171	-228.2	-1.582	1.270
T6N	20.4	0.342	-42.75	-0.164	-252.3	-1.991	1.572

* Fixture influence

dicts a modulus of 24.9 Msi, a difference of 20 percent. As with the $[0/\pm45/0]_s$ laminate, the experimental moduli are lower than the laminate analysis prediction indicating that the residual stress and the matrix are sufficiently large to cause nonlinear response of these components in the 45° degree laminae.

The major Poisson's ratio from the tension tests was consistently lower than the compression results, but the temper condition of the laminate did not effect Poisson's ratio. The average Poisson's ratio for all three classes of tension specimens was 0.294 as compared to 0.352 for the compression tests.

Heat treating the $[0/\pm45]_s$ laminate increased the yield stress for both the tension and compression tests. The tensile yield stress of the F, T6, and T6N condition specimens was 8.58 ksi, 13.83 ksi, and 18.07 ksi, respectively. The F condition compressive yield stress was -19.75 ksi as compared to -47.45 ksi and -42.75 ksi for the T6 and T6N compression specimens. The liquid nitrogen exposure altered the stress-strain behavior in tension and compression by shifting the tension and compression curves in the positive load direction (Figure 44). Consequently, the tensile yield stress of the T6N condition specimen was increased relative to the T6 condition specimen but the compressive yield stress of the T6N condition specimen was reduced as compared to the T6 condition specimen.

The tensile strength of the laminate was increased by heat treating the materal. The strengths of the F, T6, and T6N condition specimens were 71.7 ksi, 85.5 ksi, and 90.5 ksi, respectively, which also shows

the influence of the liquid nitrogen exposure on the strength as compared to the T6 condition material. The compressive failure stresses and failure strains of the heat treated specimens were significantly higher than the F condition failure stress and strain. The F, T6, and T6N compressive failure stresses were -153.2 ksi, -228.2 ksi, and -252.3 ksi, respectively. However, influence of the fixture on the failure of the specimen implies that the failure stresses of the specimen do not correspond to the material strength.

5.6.2 Cyclic Tests

5.6.2.1 Tension

Results of the tension-tension tests were consistent with the monotonic tension results. The initial stiffness of the first cycle for all three types (i.e. F, T6, T6N) of specimens ranged from 22.6 Msi to 20.6 Msi (Table 23). All specimens exhibited decreasing modulus with each successive cycle. The modulus of the F condition specimen varied from 22.6 Msi for the first cycle to 18.5 Msi on the unloading portion of the third cycle. The modulus of the T6 condition specimens decreased from 22.7 Msi on the first cycle to 19.6 Msi during the fourth cycle. The T6N condition specimen followed a similar pattern with a reduction in modulus from 22.7 Msi to 18.8 Msi.

The F condition tension-tension specimen (Figure 45) exhibited the most nonlinearity of the F, T6, and T6N condition specimens, just as was the case for the $[0/\pm45/0]_s$ laminate. The specimen yielded on the first cycle at 8.9 ksi and the unloading portion of the curve was linear. The

TABLE 23

INFLUENCE OF TEMPER CONDITION ON THE CYCLIC TENSION STRESS-STRAIN BEHAVIOR OF $[0/\pm45]_s$ BORON-ALUMINUM

TEMPER CONDITION	CYCLE	E_x^L (Msi)	E_x^{UL} (Msi)	ν_{xy}^L	ν_{xy}^{UL}	σ_x^y (ksi)	ε_x^y (%)	σ_x^m (ksi)	ε_x^m (%)	ε_y^m (%)	ε_x^R (%)
F	I	22.6	19.2	0.308	0.308	8.9	0.041	19.3	0.109	-0.036	0.018
	II	20.9	19.8	0.314	0.328	19.3	0.113	38.3	0.269	-0.118	0.055
	III	19.7	18.5	0.323	0.331	21.0	0.164	57.1	0.446	-0.227	0.075
	IV	19.0	-	0.337	-	22.1	0.186	84.6	0.726	-0.412	-
T6	I	20.9	22.7	0.270	0.289	-	-	19.6	0.091	-0.029	0.005
	II	22.3	21.9	0.282	0.305	20.6	0.097	38.8	0.202	-0.065	0.021
	III	21.4	20.4	0.299	0.305	36.8	0.195	57.9	0.348	-0.120	0.066
	IV	20.5	19.6	0.302	0.296	37.5	0.245	77.2	0.522	-0.194	0.122
	V	20.6	-	0.292	-	29.9	0.267	90.5	0.653	-0.252	-
T6N	I	20.6	22.7	0.246	0.260	16.5	0.084	19.7	0.097	-0.021	0.004
	II	20.9	20.5	0.272	0.299	20.4	0.102	38.7	0.204	-0.055	0.014
	III	20.2	19.3	0.298	0.313	36.7	0.197	57.8	0.343	-0.108	0.043
	IV	19.5	18.8	0.299	0.295	36.5	0.229	77.0	0.515	-0.180	0.090
	V	19.4	-	0.295	-	30.4	0.247	83.5	0.583	-0.205	-

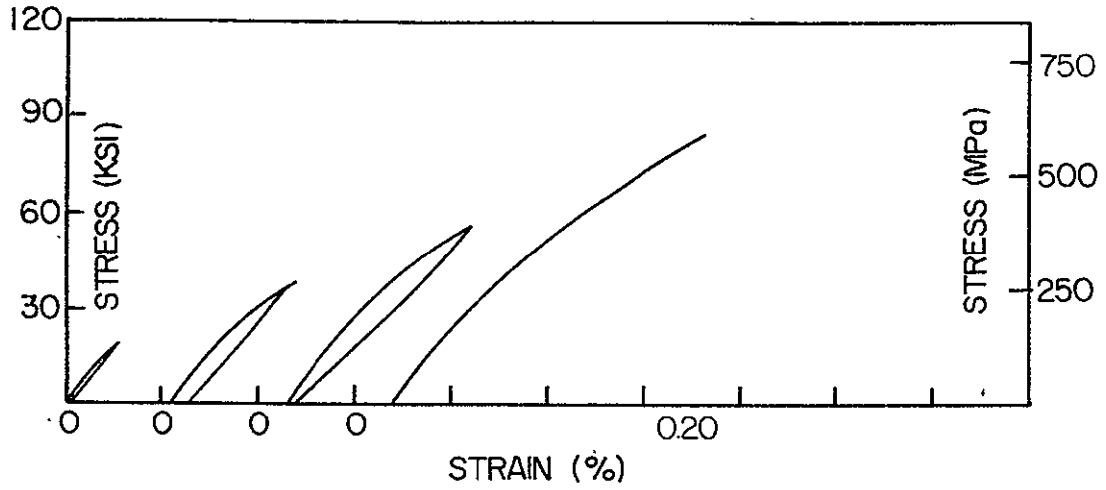

FIGURE 45. CYCLIC TENSION STRESS-STRAIN DIAGRAM FOR $[0/\pm45]_s$ B/Al LAMINATE, F CONDITION.

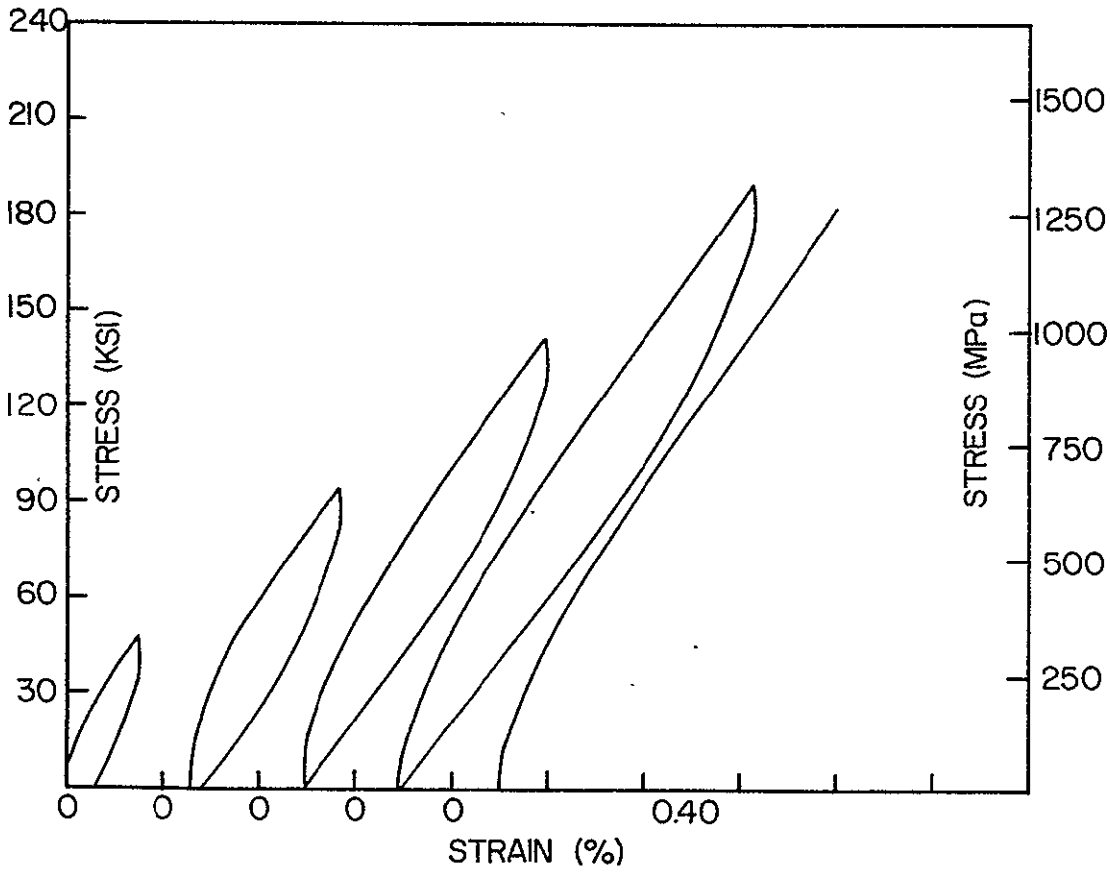

FIGURE 46. CYCLIC COMPRESSION STRESS-STRAIN DIAGRAM FOR $[0/\pm45]_s$ B/Al LAMINATE, F CONDITION.

linear range of the second, third, and fourth cycles was basically constant with a small variation between 19.3 ksi and 22.1 ksi, and the yield phenomenon can best be characterized as kinematic hardening.

The T6 condition tension-tension (Figure 47) specimen does not exhibit kinematic hardening as did the F condition specimen. The specimen initially yielded on the second cycle at 20.6 ksi, unloading from the maximum stress was linear. The yield stress of the third cycle was 36.8 ksi, approximately the highest previous stress; again unloading was linear from the maximum stress (Table 23). The yield stress of the fourth cycle was increase to 37.5 ksi and the linear range on the unloading portion of the cycle was 47.3 ksi. The yield stress on the final cycle was reduced to 29.9 ksi.

The T6N condition specimen (Figure 49) exhibited yield behavior very similar to the T6 condition tension-tension specimen. The initial yield stress (16.5 ksi) was lower for the T6N condition specimen than the specimen having a T6 temper condition. For the second and third cycles the yield stress was approximately equal to the maximum previous stress and unloading was linear from the maximum stress. The yield stress did not change significantly on the fourth cycle and on the fifth cycle it was reduced to 30.4 ksi. The linear range upon unloading on the fourth cycle was 51.2 ksi.

The nonlinear behavior of the T6 and T6N condition specimens suggests that the linear range is dependent upon the loading direction, because the linear range of the unloading portion of the curve is significantly larger than the yield stress values for the third, fourth,

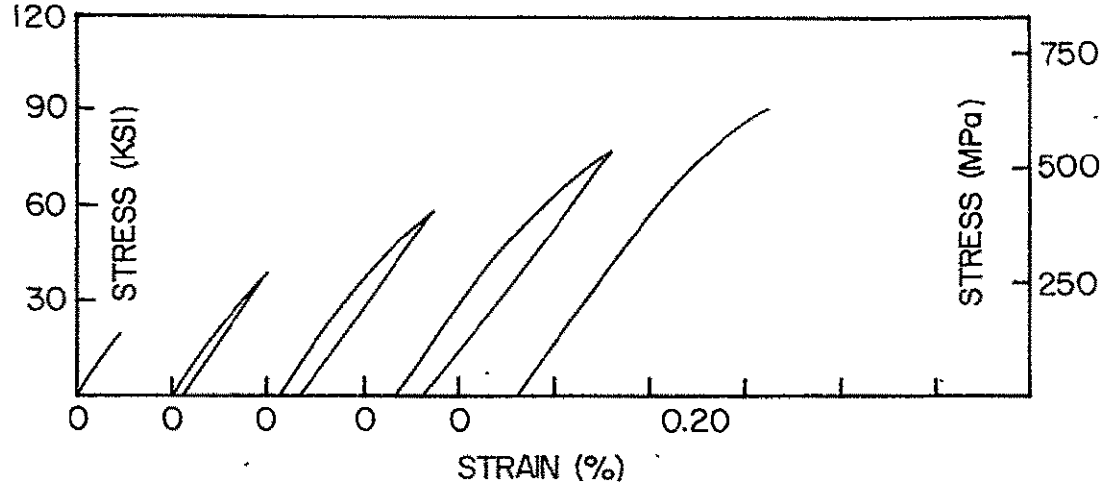

FIGURE 47. CYCLIC TENSION STRESS-STRAIN DIAGRAM FOR $[0/+45]_s$ B/Al LAMINATE, T6 CONDITION.

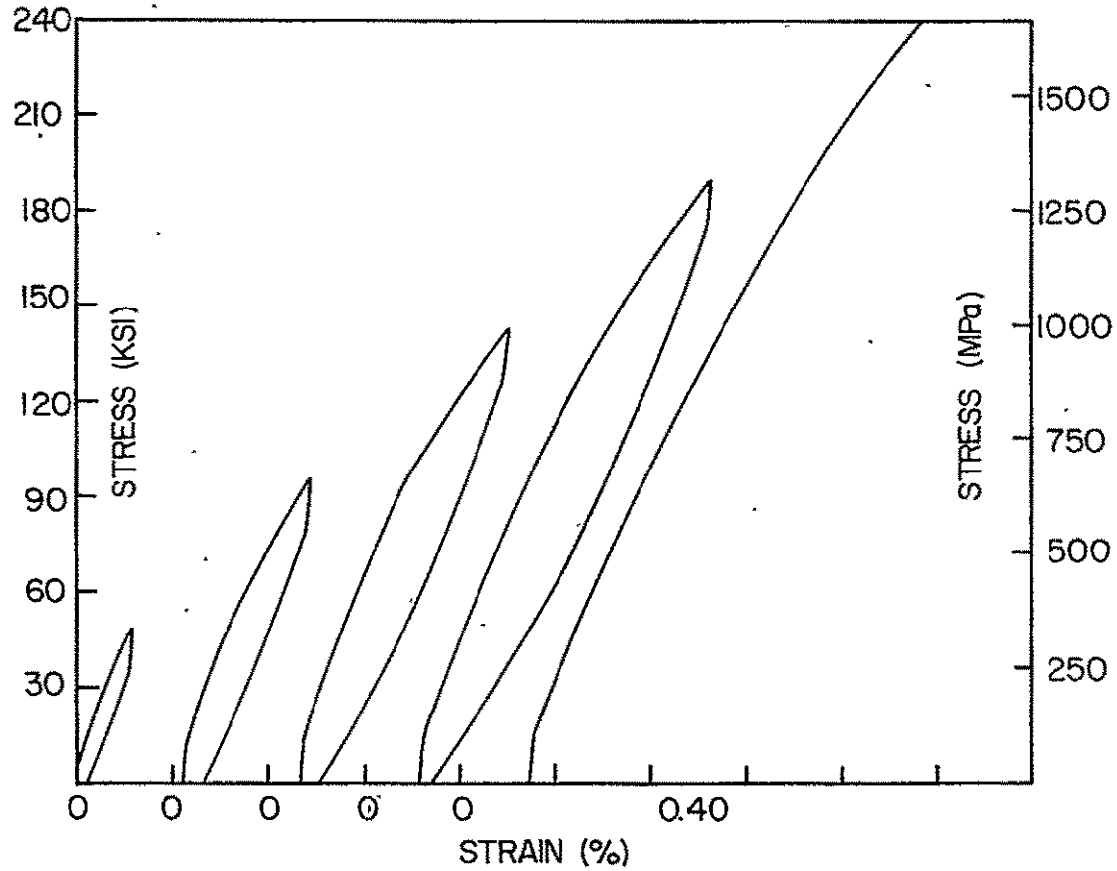

FIGURE 48. CYCLIC COMPRESSION STRESS-STRAIN DIAGRAM FOR $[0/\pm45]_s$ B/Al LAMINATE, T6 CONDITION.

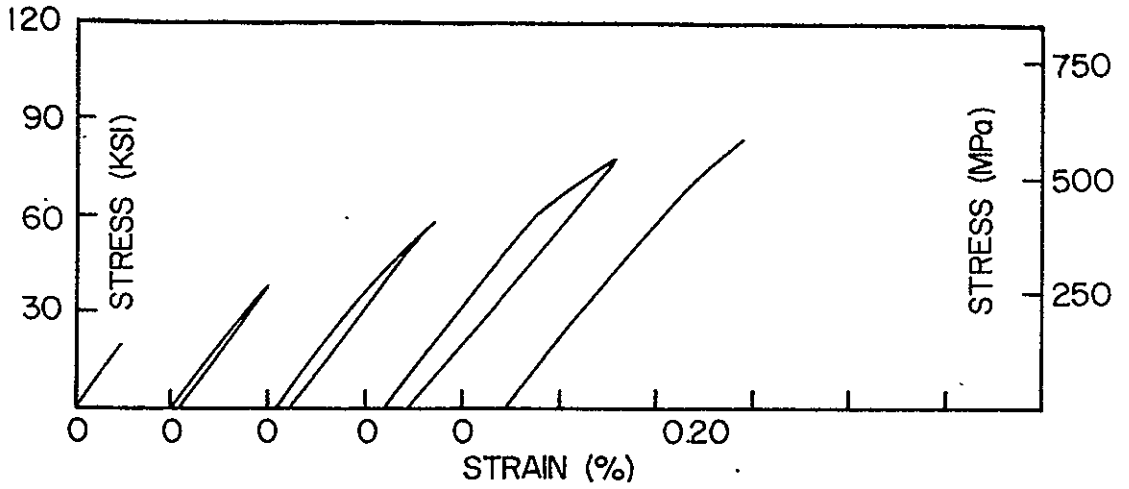

FIGURE 49. CYCLIC TENSION STRESS-STRAIN DIAGRAM FOR $[0/\pm45]_s$ B/Al LAMINATE, MODIFIED T6 CONDITION.

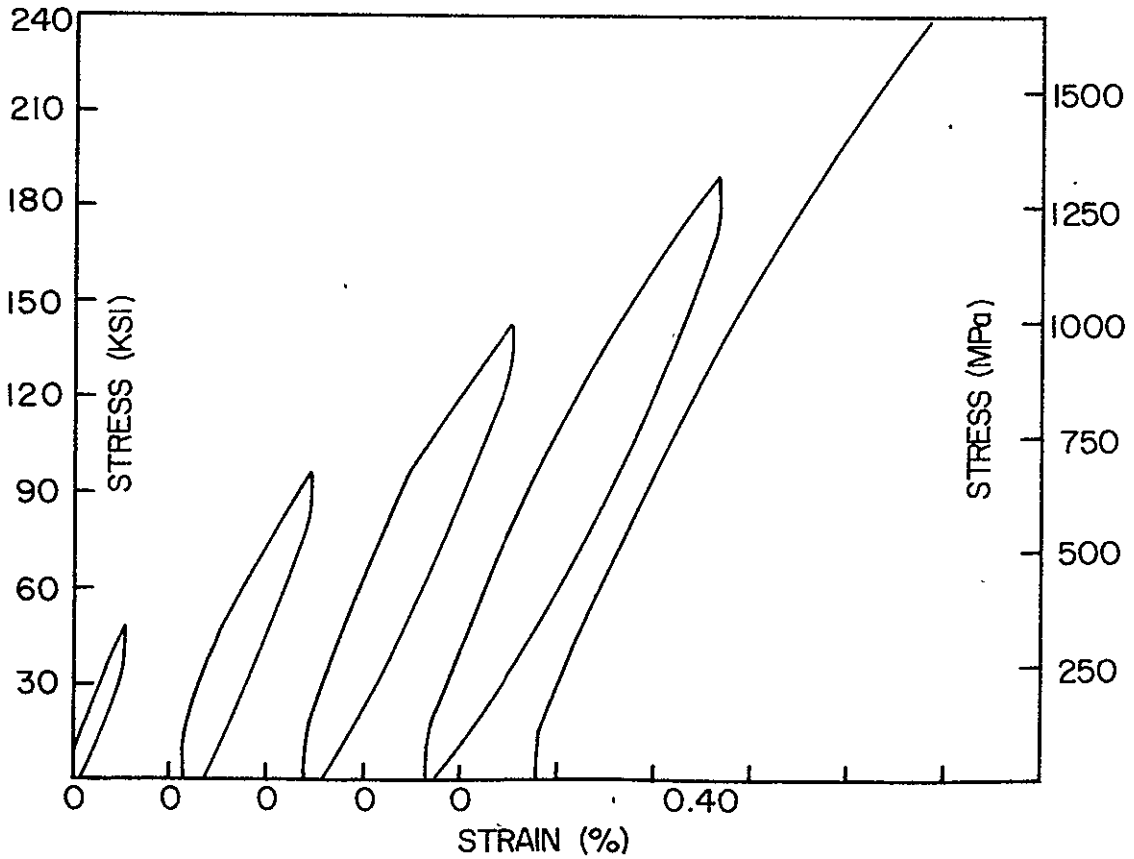

FIGURE 50. CYCLIC COMPRESSION STRESS-STRAIN DIAGRAM FOR $[0/\pm45]_s$ B/Al LAMINATE, MODIFIED T6 CONDITION.

and fifth cycles. Also, the reduction in yield stress of the fifth cycle and the decrease in modulus with successive cycles indicates the composite has been damaged.

5.6.2.2 Compression

In general, the nonlinear stress-strain behavior of the $[0/\pm45]_s$ boron aluminum is similar to that of the tension-tension tests. Difficulty was encountered when determining the linear range of many of the cycles of a test because of the influence of the fixture. Consequently, the yield stress and, especially, the modulus values (Table 24) vary significantly. It is not clear from the modulus results if the modulus of the $[0/\pm45]_s$ material was reduced by cyclic loading of the specimen. In all cases the final modulus was lower than the initial modulus of the test; however, no consistent reduction in modulus was exhibited by the intermediate cycles.

The F condition cyclic compresssion specimen (Figure 46) exhibited the most nonlinearity and the smallest elastic range for the three types of $[0/\pm45]_s$ specimens. The yield stress on the first cycle was approximately -17 ksi; the unloading portion of the cycle was nonlinear with a linear range of 37 ksi. The yield stress on the second cycle was increased to -46.7 ksi, approximately the maximum stress of the previous cycle. The unloading portion of the second cycle was also nonlinear with a linear range of 45 ksi. The third, fourth, and fifth cycles had yield stresses of -40.3 ksi, -38.2 ksi, and 41.2 ksi, respectively. The linear range on the third and fourth cycles was 42 ksi and 44 ksi.

TABLE 24

INFLUENCE OF TEMPER CONDITION ON THE CYCLIC COMPRESSION STRESS-STRAIN BEHAVIOR OF $[0/\pm45]_S$ BORON-ALUMINUM

TEMPER CONDITION	CYCLE	E_x^L (Msi)	E_x^{UL} (Msi)	ν_{xy}^L	ν_{xy}^{UL}	$\sigma_x^{y\,*}$ (ksi)	ε_x^y (%)	$\sigma_x^{m\,*}$ (ksi)	ε_x^m (%)	ε_y^m (%)	ε_x^R (%)
F	I	18.3	20.6	0.351	0.329	-16.8	-0.046	-47.7	-0.299	0.209	-0.118
	II	20.7	20.5	0.403	0.341	-46.7	-0.295	-94.7	-0.744	0.669	-0.172
	III	20.1	20.7	0.309	0.347	-40.3	-0.328	-142.8	-1.201	1.175	-0.183
	IV	18.7	21.0	0.291	0.369	-38.2	-0.335	-189.9	-1.668	1.690	-0.197
	V	17.7	-	0.308	-	-41.2	-0.370	-182.9	-1.610	1.650	-
T6	I	20.0	20.1	0.352	0.354	-34.0	-0.132	-48.1	-0.215	0.082	-0.039
	II	20.9	20.0	0.354	0.371	-49.7	-0.222	-95.5	-0.565	0.313	-0.126
	III	19.6	21.0	0.368	0.366	-55.6	-0.354	-142.8	-0.997	0.672	-0.223
	IV	19.3	21.8	0.351	0.391	-56.7	-0.466	-190.1	-1.443	1.319	-0.279
	V	18.1	-	0.377	-	-54.6	-0.525	-238.6	-1.942	1.844	-
T6N	I	18.4	19.8	0.360	0.325	-37.7	-0.153	-48.2	-0.218	0.079	-0.046
	II	20.3	19.5	0.329	0.362	-50.4	-0.231	-95.1	-0.586	0.315	-0.151
	III	18.9	18.4	0.367	0.379	-65.9	-0.424	-143.0	-1.020	0.671	-0.246
	IV	17.9	20.5	0.352	0.355	-79.2	-0.620	-189.7	-1.473	1.072	-0.299
	V	17.2	-	0.317	-	-56.9	-0.558	-238.0	-1.942	1.556	-

* Fixture influence

After the first cycle, which had a yield stress of -16.8 ksi, the F condition $[0/\pm45]_s$ specimen maintained a relatively constant linear range of 38 ksi to 42 ksi. This type of yield behavior is analogous to the kinematic hardening behavior of the F condition tension-tension specimen.

The T6 condition cycle compression specimen (Figure 48) exhibited a much larger linear range than the F condition $[0/\pm45]_s$ specimen; however, the yield phenomenon was much the same. The yield stress of the first cycle was -34 ksi and the unloading portion for the cycle was linear. The yield stress of the second cycle was -50 ksi and the linear range of the unloading portion of the cycle was 59 ksi. The linear range of the third, fourth, and fifth cycles was 54 ksi to 62 ksi. Again, a rather constant linear range was established and maintained for the remainder of the test, indicating that the laminate hardens kinematically.

The T6N condition cyclic compression specimen (Figure 50) exhibited different yield behavior than the T6 condition specimen. The cyclic loading did not develop a constant linear range for the specimen, instead the yield stress and linear range were increased on each successive (Table 24) cycle from the yield stress of -34 ksi on the first cycle to 85 ksi on the unloading portion of the third cycle. The linear range was then reduced for the fourth and fifth cycles with the yield stress on the fifth cycle being -56.9 ksi. The type of yield behavior of the T6N cyclic compression specimen does not resemble kinematic hardening as the F and T6 condition specimens and the reduced yield

stress of the fifth cycle seems to indicate damage to the composite.

5.6.2.3 Tension-Compression

The tension-compression curves for the F, T6, and T6N condition specimens exhibit small linear elastic ranges and large inelastic ranges. The modulus values presented in Table 25 vary between 10.5 Msi and 25.1 Msi; the very low modulus values are taken from the nonlinear portion of the curve, as the specimen has already yielded before initial loading into tension or compression. The influence of the fixture on the stress-strain curve along with the primarily nonlinear behavior of the composite caused extreme difficulty in determining the linear range of the cycle and thus an accurate modulus in the linear range.

The F condition tension-compression specimen (Figure 51) developed a linear range of approximately the same magnitude as the linear range established by compression-compression cycling of an F condition $[0/\pm45]_s$ specimen. The tensile yield stress of the first cycle was not determined because of the fixture influence. The linear range upon unloading from tension was 40 ksi and upon unloading from the maximum compressive stress the linear range was 46 ksi. For the next two cycles the linear range varied from 38-47 ksi, the entire fourth cycle was loading in the nonlinear region of the stress-strain curve and failure occurred at 83.7 ksi. As with the F condition cyclic compression specimen, the yield behavior of the F condition tension-compression specimen could best be characterized as kinematic hardening.

The T6 condition tension-compression specimen (Figure 52) exhibited

TABLE 25

INFLUENCE OF TEMPER CONDITION ON THE TENSION-COMPRESSION STRESS-STRAIN BEHAVIOR OF $[0/\pm45]_S$ BORON-ALUMINUM

TEMPER CONDITION	CYCLE	E_x^L (Msi)	E_x^{UL} (Msi)	σ_x^{m*} (ksi)	ε_x^m (%)	ε_y^m (%)	ε_x^R (%)
F	I-T	-	24.9	23.0	0.076	0.023	0.043
	I-C	22.0	22.0	-46.4	-0.263	0.171	-0.125
	II-T	17.5	22.4	46.0	0.243	-0.051	0.085
	II-C	16.4	23.8	-94.1	-0.682	0.557	-0.194
	III-T	11.3	18.9	69.4	0.455	-0.053	0.117
	III-C	12.1	22.3	-142.0	-1.106	0.917	-0.213
	IV-T	10.5	-	83.7	0.516	0.047	-
T6	I-T	23.3	23.3	23.0	0.074	-0.018	0.034
	I-C	23.3	21.6	-45.8	-0.175	0.058	-0.030
	II-T	22.2	21.3	45.6	0.209	-0.062	0.022
	II-C	21.3	23.7	-95.1	-0.488	0.235	0.010
	III-T	17.6	19.5	68.8	0.385	-0.096	0.051
	III-C	18.2	24.3	-71.9	-0.337	0.174	-0.050
	IV-C	22.8	20.5	-142.2	-0.895	0.582	-0.217
	IV-T	13.5	-	83.9	0.498	-0.037	-
T6N	I-T	25.1	25.1	23.3	0.081	-0.018	0.058
	I-C	25.1	25.1	-48.1	-0.158	0.060	-0.036
	II-T	22.7	21.3	46.8	0.217	-0.056	0.072
	II-C	20.3	22.7	-95.2	-0.491	0.273	-0.116
	III-T	16.7	19.4	70.0	0.378	-0.076	0.103
	III-C	18.0	24.3	-140.5	-0.886	0.603	-0.244
	IV-T	12.4	-	97.9	0.622	-0.068	-

* Fixture influence

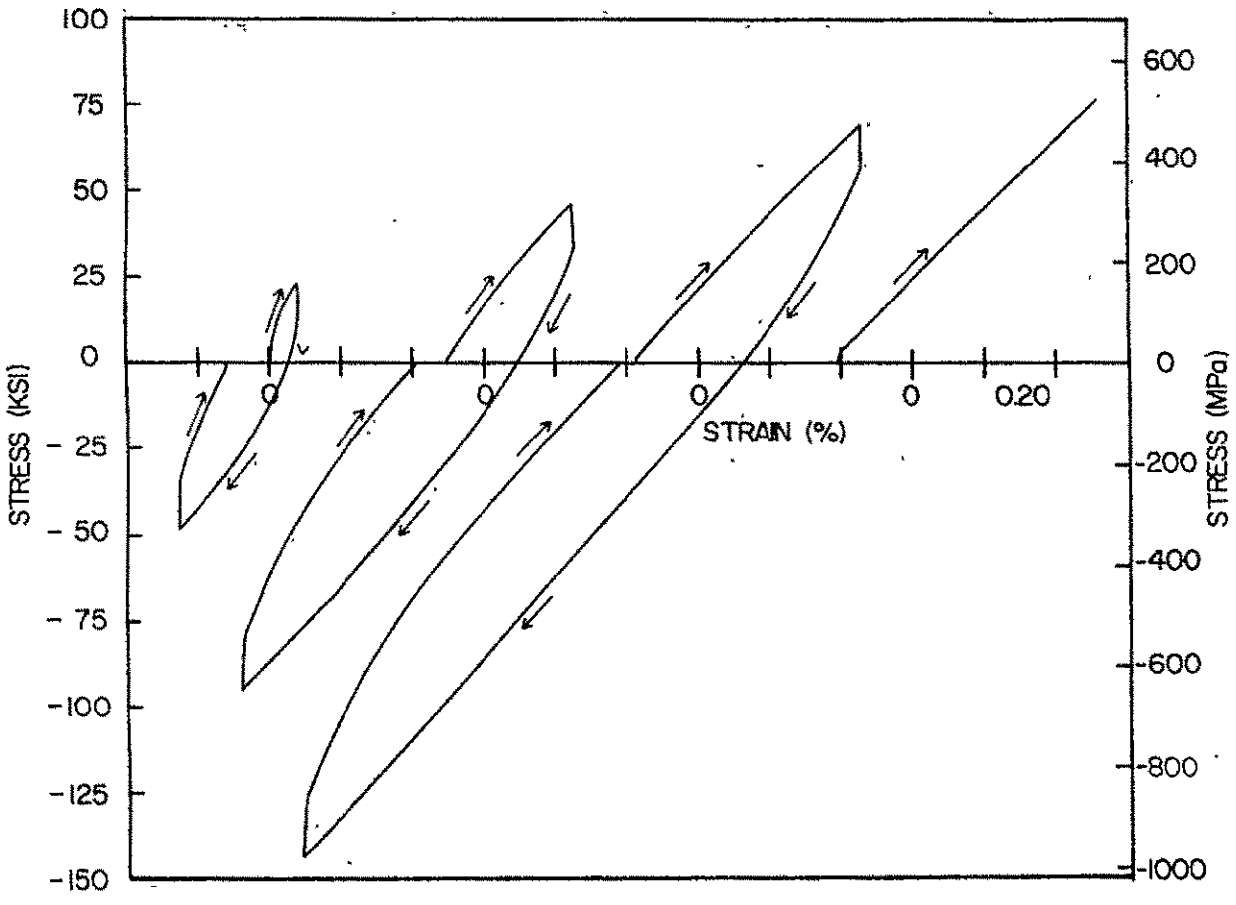

FIGURE 51. CYCLIC TENSION-COMPRESSION STRESS-STRAIN DIAGRAM FOR $[0/\pm45]_s$ B/Al LAMINATE, F CONDITION.

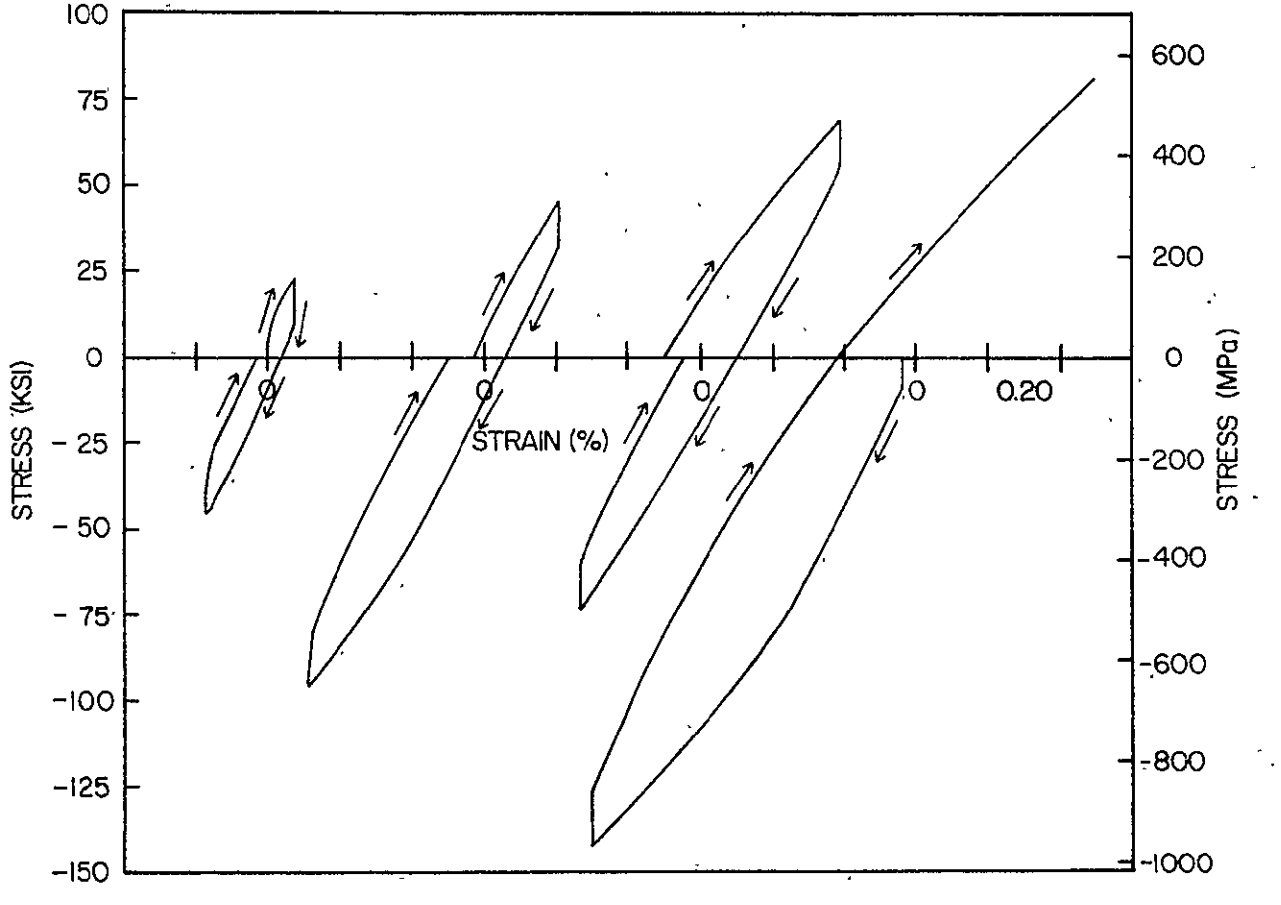

FIGURE 52 CYCLIC TENSION – COMPRESSION STRESS–STRAIN DIAGRAM FOR $[0/\pm45]_s$ B/Al LAMINATE, T6 CONDITION.

linear ranges between 45 ksi and 84 ksi. The linear range of the first cycle upon unloading from the maximum tensile stress was 45 ksi, and upon unloading from the maximum compressive stress was 75 ksi. The linear range was increased on the second cycle to 84 ksi when unloading from the maximum tensile stress, but the linear range was reduced to 67 ksi when unloading from the maximum compressive stress of the second cycle. This linear range was maintained through the third cycle. The wrong maximum load was set on the MTS machine and the maximum compressive stress was only -71.9 ksi. Thus, the compression portion of the third cycle was rerun with the correct maximum compressive stress, -142 ksi. For the fourth cycle the linear range was increased to 81-83 ksi, suggesting path dependent stress-strain behavior of the laminate.

The T6N condition tension-compression specimen (Figure 53) behaved similarly to the F condition specimen. Due to influence of the fixture on the stress-strain curve, no yield stress was determined for the tensile portion of the first cycle and the specimen did not yield until the second cycle. The linear range varied between 68 ksi and 73 ksi during the second and third cycles; no yield stress was recorded for the fourth cycle as the linear range was expended when unloading from the maximum compressive stress of the third cycle. The constant linear range for the cycles again indicates that kinematic hardening characterizes the yield behavior.

5.6.3 Conclusions

As with all other laminates discussed previously, heat treating the

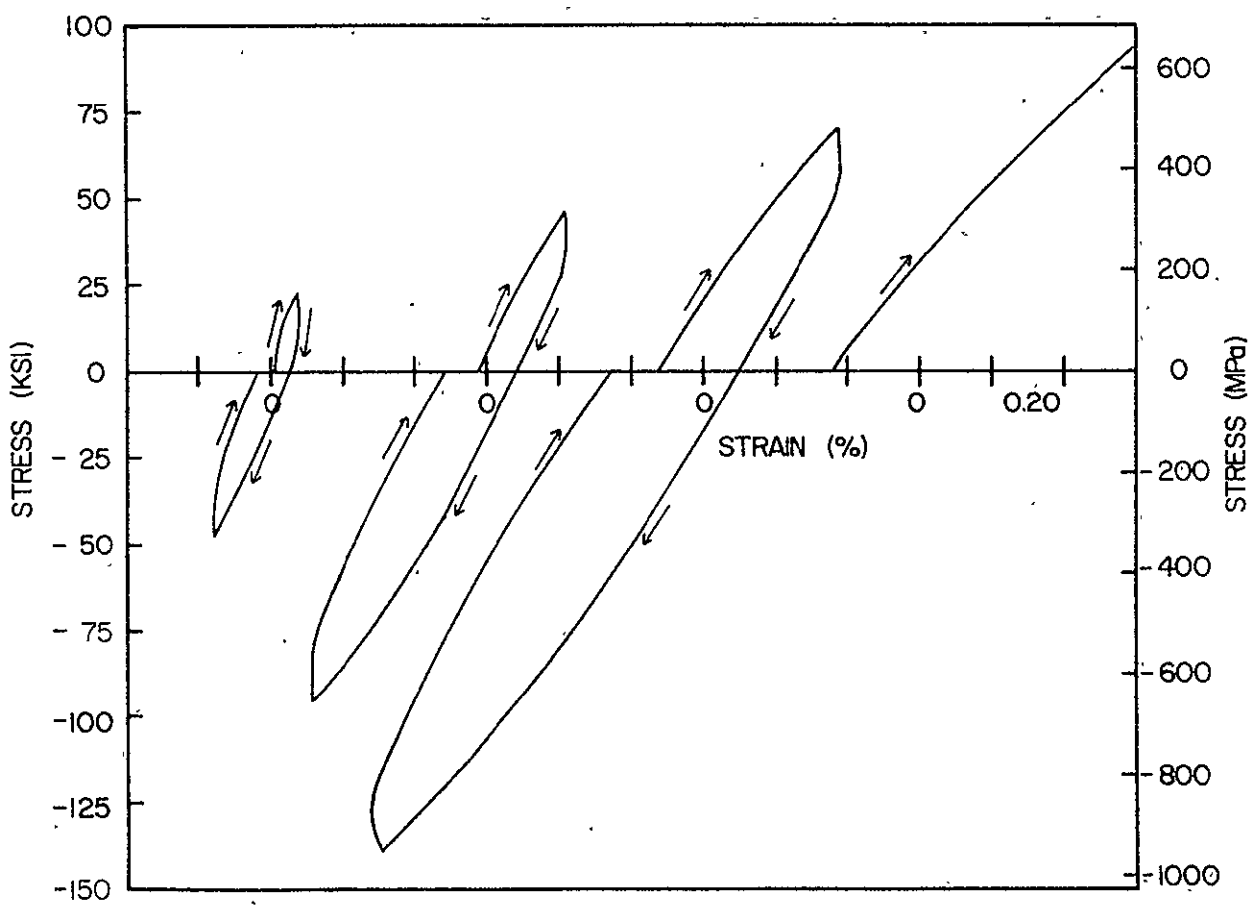

FIGURE 53. CYCLIC TENSION–COMPRESSION STRESS–STRAIN DIAGRAM FOR $[0/\pm45]_s$ B/Al LAMINATE, MODIFIED T6 CONDITION.

$[0/\pm45]_s$ laminate increased the initial yield stress relative to the F condition material; there was also an associated increase in strength. The liquid nitrogen exposure did not have the profound effect on the yield stress and strength that the T6 conditioning produced, but it did increase the tensile yield stress and strength and reduce the compressive yield stress relative to the T6 condition boron-aluminum.

The yield phenomenon, for the most part, resembled kinematic hardening. Typically the yield stress increased for the first one or two cycles after which a constant linear range was maintained. This type of behavior was basically independent of temper condition or the type of test. Several exceptions to this type of yield behavior must be noted. The T6 and T6N condition tension-tension specimens and the T6 condition tension-compression specimens indicate the possibility of a loading direction dependent linear range. Also several of the cyclic specimens exhibited decreasing yield values for the concluding cycles of a test; however, the decreasing yield values along with the decreasing modulus indicate that the cyclic loading damages the laminate.

It must be noted that the characterization of the yield phenomenon was difficult for this laminate because of the small linear ranges and influence of the fixture on the stress-strain curve.

The tension-tension tests on all three types of $[0/\pm45]_s$ specimens exhibited decreasing modulus with increasing maximum loads in successive cycles. The cyclic compression and tension-compression results did not exhibit this behavior; however, the influence of the fixture on the stress-strain curve may have affected the results.

It is obvious from the results of the $[0/\pm45]_s$ laminate that the material characteristics of the laminate do not always resemble the properties of the individual lamina. For example, the fact that the yield behavior of the [0] and $[\pm45]_s$ has either resembled a Baushinger effect or isotropic hardening but the $[0/\pm45]_s$ does not exhibit the same type of behavior shows that the characteristic behavior of the laminae is not necessarily typical of the laminate.

5.7 The $[\pm45/0]_s$ Laminate

5.7.1 Monotonic Tension and Compression Tests

The typical monotonic tension and compression stress-strain behavior of $[\pm45/0]_s$ boron-aluminum having F, T6, and T6N temper conditions is shown in Figure 54; numerical results are listed in Tables 26 and 27. The average elastic modulus of the tension and compression specimens varied between 20.4 Msi and 23.7 Msi, a 16 percent variation. The type of test (i.e. tensile or compressive) did not influence the initial modulus results. The laminate analysis program predicted a modulus of 24.9 Msi. As with the $[0/\pm45]_s$ laminate, the experimental moduli from the $[\pm45/0]_s$ laminate were lower than the laminate analysis prediction for reasons discussed in Section 5.4.1. Poisson's ratio was again higher for the compression tests than the tension tests. The average Poisson's ratio for the compression specimens including all three temper condition groups was 0.354; the average results from the tension tests was 0.249.

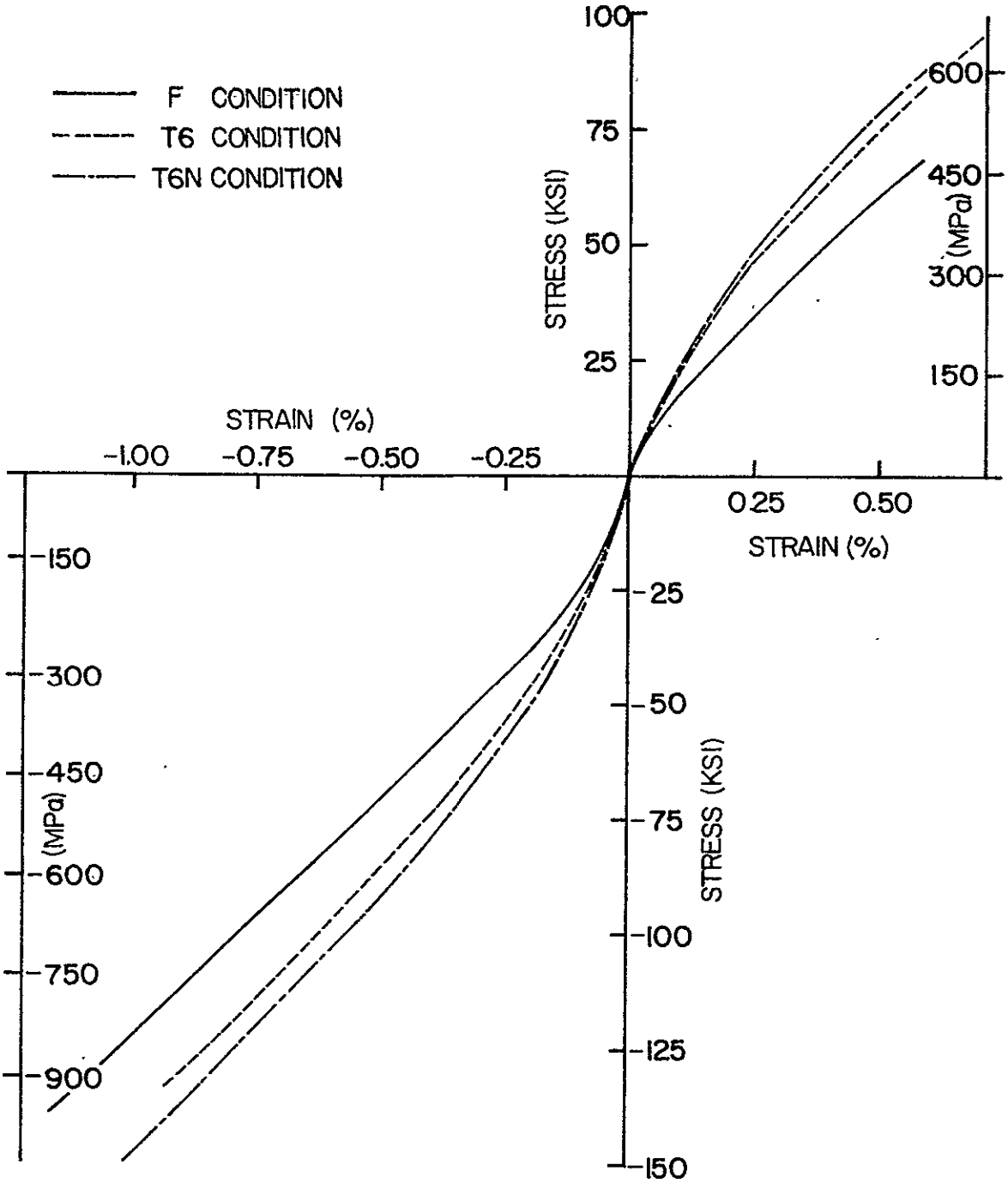

FIGURE 54. COMPARISON OF $[\pm 45/0]_s$ B/A1 LAMINATE WITH DIFFERENT TEMPER CONDITIONS IN TENSION AND COMPRESSION.

TABLE 26

INFLUENCE OF TEMPER CONDITION ON THE TENSILE STRESS-STRAIN BEHAVIOR OF $[\pm 45/0]_s$ BORON-ALUMINUM

TEMPER CONDITION	E_x (Msi)	ν_{xy}	σ_x^y (ksi)	ε_x^y (%)	σ_x^u (ksi)	ε_x^u (%)	ε_y^u (%)
F	23.7	0.194	8.71	0.039	73.8	0.615	-0.237
T6	21.4	0.248	20.80	0.093	98.9	0.718	-0.287
T6N	22.1	0.306	17.65	0.080	90.1	0.610	-0.244

TABLE 27

INFLUENCE OF TEMPER CONDITION ON THE COMPRESSIVE STRESS-STRAIN BEHAVIOR OF $[\pm 45/0]_s$ BORON-ALUMINUM

TEMPER CONDITION	E_x (Msi)	ν_{xy}	σ_x^y * (ksi)	ε_x^y (%)	σ_x^u * (ksi)	ε_x^u (%)	ε_y^u (%)
F	20.4	0.393	-22.77	-0.067	-119.5	-0.896	0.726
T6	20.6	0.307	-37.35	-0.150	-124.6	-0.827	0.498
T6N	22.7	0.361	-40.42	-0.146	-149.2	-0.989	0.638

* Fixture influence

Heat treating the laminate increased the yield stress in both tension and compression, as compared to the F condition material. The increase was approximately two-fold (Tables 26 and 27) for both the tension and compression tests. The liquid nitrogen exposure affected the tensile and compressive stress-strain behavior; the tensile yield stress for the T6N condition specimens was reduced by 15 percent as compared to the T6 condition specimens and the compressive yield stress was increased by 8 percent. Examination of the curves in Figure 54 shows that the tensile T6N condition curve is shifted above the T6 condition stress-strain curve and the same is true for the compressive curves. The fact that the T6N curve is shifted above the T6 curve but the tensile yield stress is decreased and the compressive yield stress is increased is not a consistent set of results. However, it appears that the load in fixture is higher for the T6N than T6 condition specimen which could reverse the trends in the compression mode.

Heat treating the F condition material also increased the tensile strength of the laminate. The tensile strengths of the F, T6, T6N condition specimens were 73.8 ksi, 98.9 ksi, and 90.1 ksi. The failure strain of the T6 condition material was also increased relative to the F condition specimens. Exposing the T6 condition specimens to liquid nitrogen decreased the strength and failure strain.

5.7.2 Cyclic Tests

5.7.2.1 Tension

The F condition cyclic tension specimen (Figure 55, Table 28)

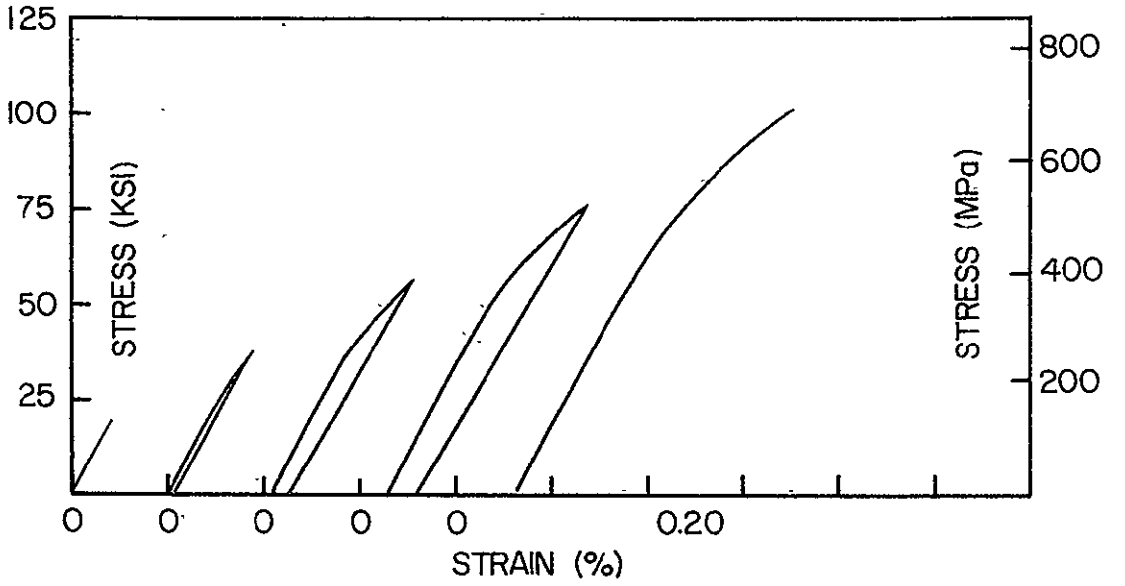

FIGURE 55. CYCLIC TENSION STRESS-STRAIN DIAGRAM FOR $[\pm 45/0]_s$ B/Al LAMINATE, T6 CONDITION.

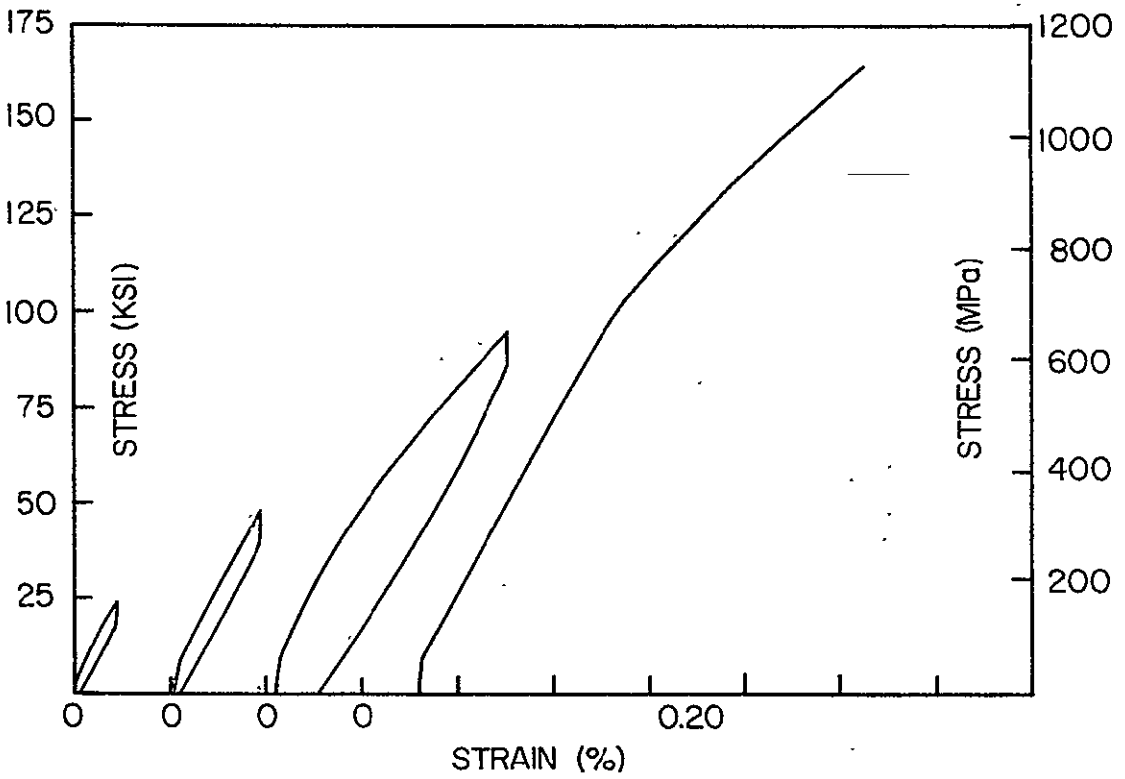

FIGURE 56. CYCLIC COMPRESSION STRESS-STRAIN DIAGRAM $[\pm 45/0]_s$ B/Al LAMINATE, T6 CONDITION.

TABLE 28

INFLUENCE OF TEMPER CONDITION ON THE CYCLIC TENSION STRESS-STRAIN BEHAVIOR OF $[\pm 45/0]_s$ BORON-ALUMINUM

TEMPER CONDITION	CYCLE	E_x^L (Msi)	E_x^{UL} (Msi)	ν_{xy}^L	ν_{xy}^{UL}	σ_x^y (ksi)	ε_x^y (%)	σ_x^m (ksi)	ε_x^m (%)	ε_y^m (%)	ε_x^R (%)
F	I	24.1	22.7	0.214	0.287	8.0	0.047	19.1	0.108	0.214	0.023
	II	22.4	21.0	0.286	0.278	18.9	0.127	38.5	0.274	0.286	0.069
	III	22.0	20.0	0.300	0.298	20.3	0.185	57.6	0.450	0.300	0.094
	IV	21.4	-	0.307	-	23.2	0.227	88.0	0.753	0.307	-
T6	I	23.8	24.5	0.294	0.302	-	-	19.4	0.081	0.294	0.001
	II	23.7	23.1	0.296	0.296	22.0	0.094	38.2	0.181	0.296	0.015
	III	23.0	22.3	0.293	0.304	39.2	0.187	57.3	0.316	0.293	0.059
	IV	22.6	21.6	0.291	0.309	49.2	0.280	76.3	0.480	0.291	0.122
	V	22.0	-	0.306	-	43.8	0.320	101.7	0.713	0.306	-
T6N	I	22.2	22.0	0.271	0.285	-	-	19.5	0.082	0.271	0.000
	II	22.3	21.7	0.289	0.267	20.8	0.090	38.7	0.183	0.289	0.009
	III	22.0	21.6	0.288	0.241	40.3	0.194	57.7	0.314	0.288	0.045
	IV	21.7	21.4	0.274	0.228	51.2	0.284	76.6	0.475	0.274	0.100
	V	21.6	-	0.260	-	41.4	0.296	96.1	0.662	0.260	-

exhibited nonlinear behavior similar to the F condition $[0/\pm45]_s$ cyclic tension specimen. The specimen yielded on the first cycle at 8.0 ksi, and unloading was linear. On the second cycle the yield stress was increased to 18.9 ksi, but unloading was nonlinear with a linear range of 25.1 ksi. The loading and unloading linear ranges for the third cycle were 20.3 ksi and 27.5 ksi, respectively. The yield stress of the fourth cycle was 23.2 ksi, and the specimen failed at 88.0 ksi. The yield behavior of the F condition cyclic tension specimen closely resembles kinematic hardening, a linear range of 20.3 ksi to 27.5 ksi is established and maintained for the last three cycles of the test.

The T6 condition (Figure 57) and T6N condition (Figure 59) specimens exhibit the same type of behavior under tension-tension loading. Both specimens behaved linearly on the first cycle and yielded on the second cycle at approximately 21 ksi. The unloading portion of the second cycle was linear, and the yield stress of the third cycle was increased to approximately 40 ksi; unloading was again linear. The yield stress for the specimen was increased to approximately 50 ksi on the fourth cycle and the linear range upon unloading was 53 ksi. The yield stress of the fifth cycle, however, was reduced to approximately 42 ksi.

The lower modulus values for each cycle of the tension-tension tests indicates that the laminate is damaged with each successive cycle. The F condition specimen had a modulus reduction from 24.1 Msi to 21.4 Msi; the T6 condition specimen a reduction from 24.5 Msi to 21.6 Msi, and the T6N condition specimen's modulus reduced from 22.2 Msi to 21.4

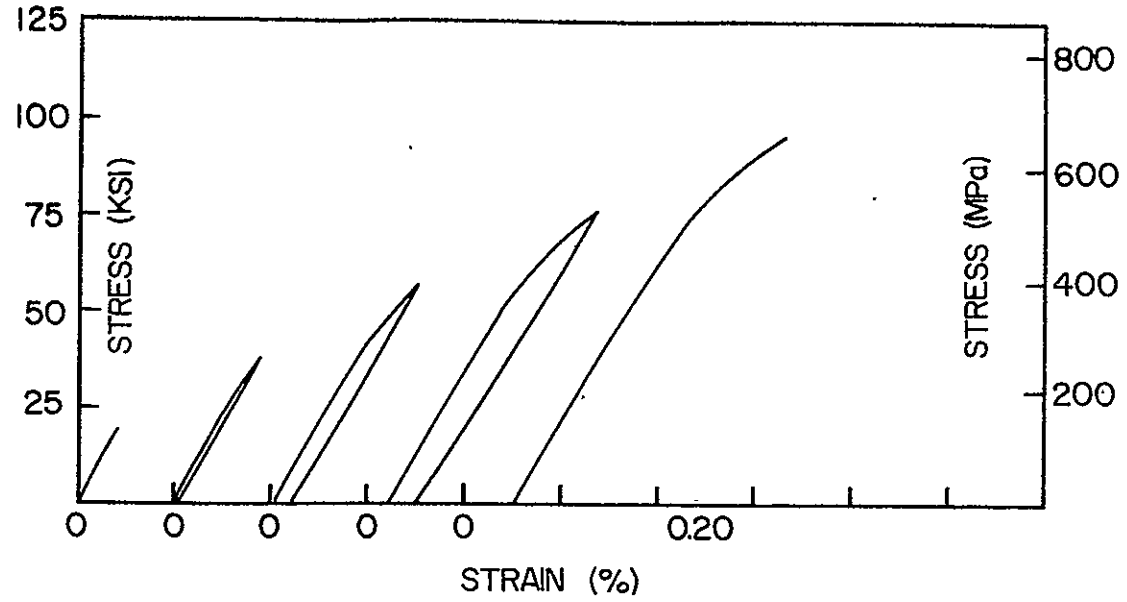

FIGURE 57. CYCLIC TENSION STRESS-STRAIN DIAGRAM FOR $[\pm 45/0]_s$ B/Al LAMINATE, MODIFIED T6 CONDITION.

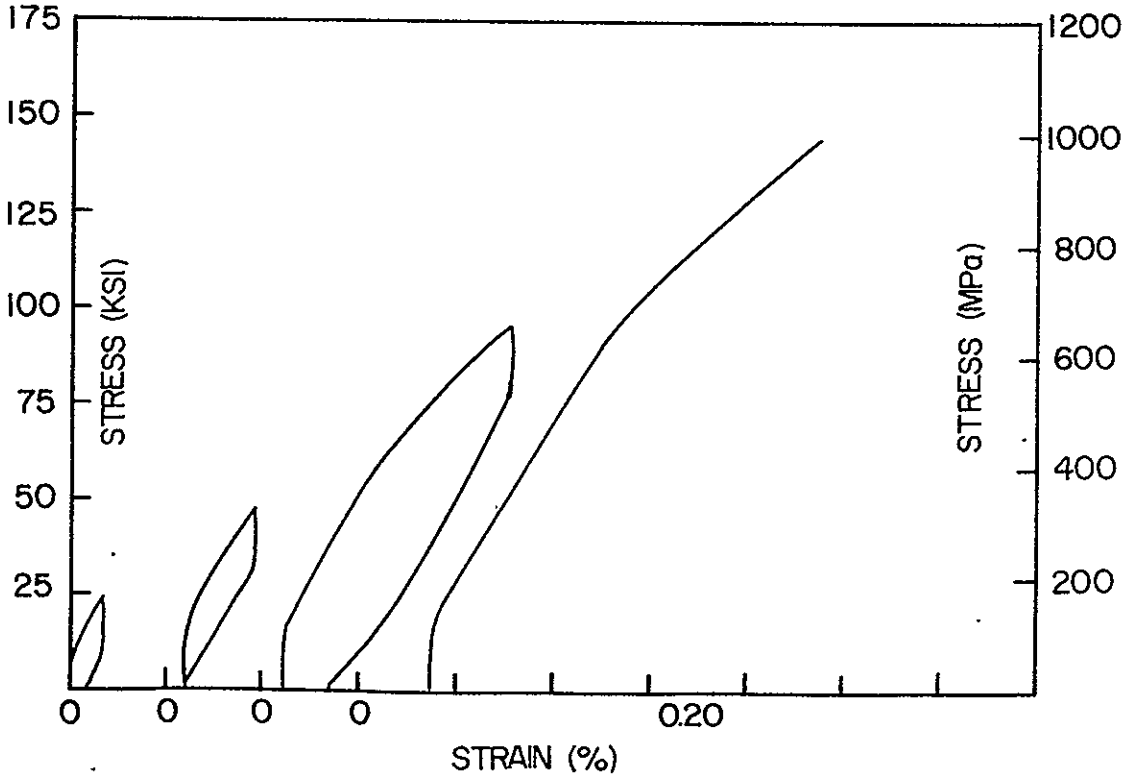

FIGURE 58. CYCLIC COMPRESSION STRESS-STRAIN DIAGRAM FOR $[\pm 45/0]_s$ B/Al LAMINATE, MODIFIED T6 CONDITION.

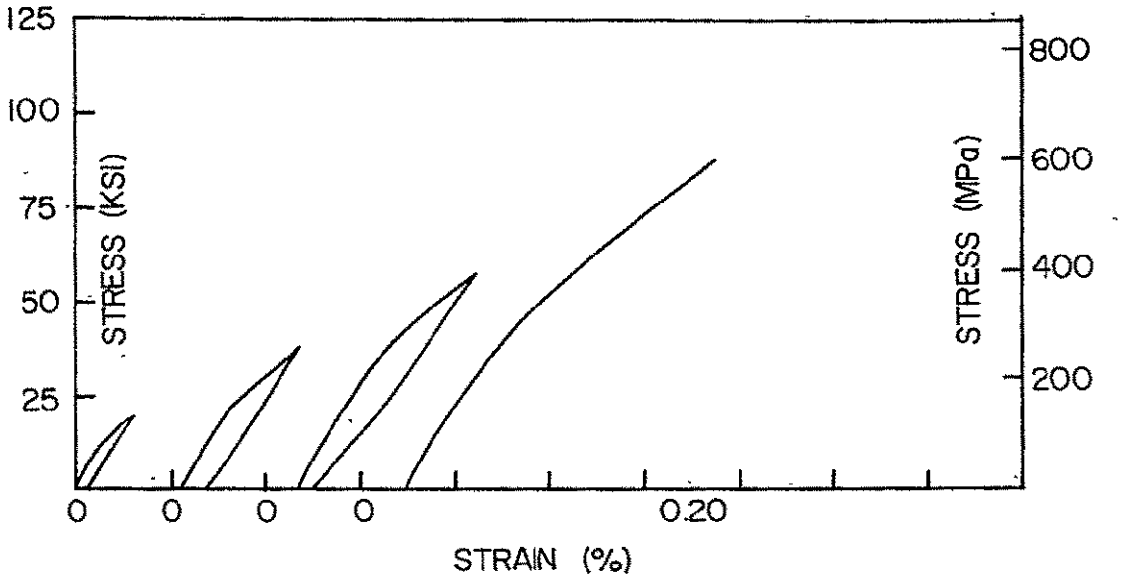

FIGURE 59. CYCLIC TENSION STRESS–STRAIN DIAGRAM FOR $[\pm 45/0]_s$ B/Al LAMINATE F CONDITION.

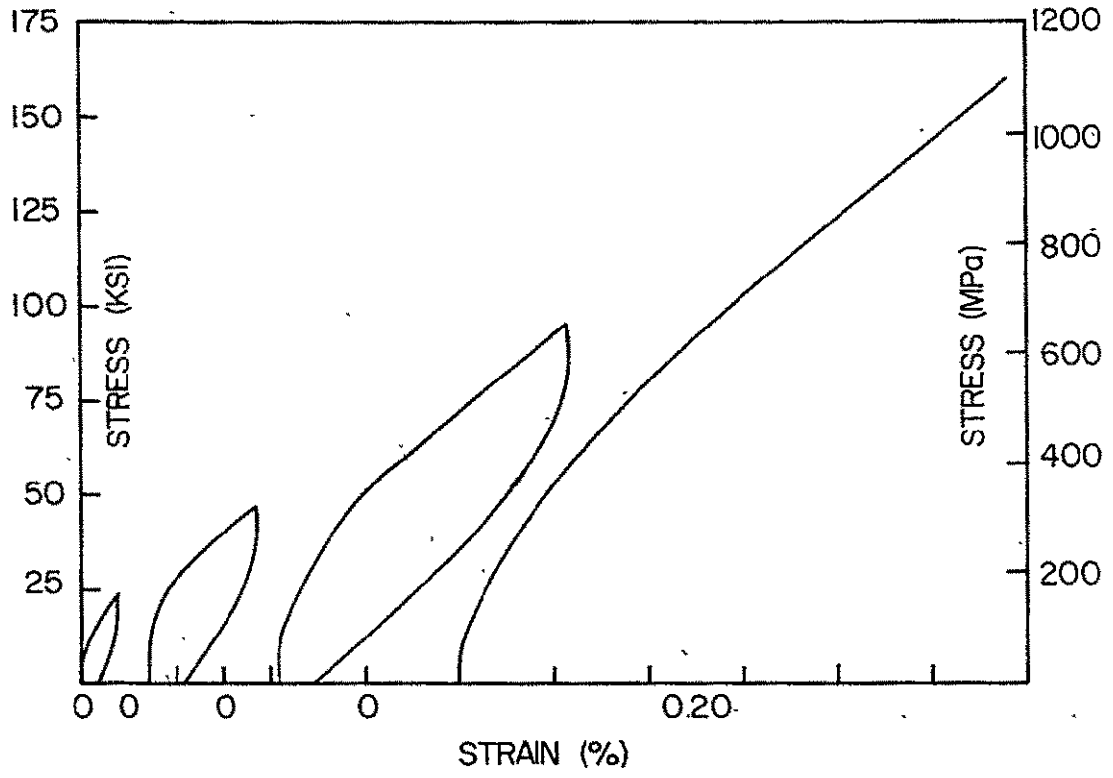

FIGURE 60. CYCLIC COMPRESSION STRESS–STRAIN DIAGRAM FOR $[\pm 45/0]_s$ B/Al LAMINATE, F CONDITION.

Msi. The fact that the composite is damaged by cyclic loading also explains the reduced yield stress of the T6 and T6N condition specimens on the final cycle.

5.7.2.2 Compression

The compression-compression tests on $[\pm 45/0]_s$ boron-aluminum (Table 29) do not exhibit a reduction in stiffness with each successive cycle. For the T6 and T6N condition specimens the modulus of the last cycle is lower than the initial modulus of the first cycle, but the values for the intermediate cycles do not consistently reduce. It is likely that the specimens do exhibit a decreasing modulus, but the influence of the fixture has resulted in inaccurate modulus values for some of the cycles.

The F condition specimens did not exhibit a linear elastic range for any of the cycles (Figure 56) and for most of the cycles fixture influence on the stress-strain curves made it impossible to define the point on the curve where the fixture stopped loading and specimen started loading. Thus, no yield stress values are presented for the F condition compression specimen nor are modulus values presented for the first two cycles.

Few conclusions concerning the yield behavior and elastic properties of the F condition cyclic compression (Figure 56) can be made for reasons discussed in the previous paragraph. For the second, third and fourth cycles, the stress-strain curve was nonlinear to approximately the maximum previous stress, after which the curve was linear; the

TABLE 29

INFLUENCE OF TEMPER CONDITION ON THE CYCLIC COMPRESSION STRESS-STRAIN BEHAVIOR OF $[\pm 45/0]_s$ BORON-ALUMINUM

TEMPER CONDITION	CYCLE	E_x^L (Msi)	E_x^{UL} (Msi)	ν_{xy}^L	ν_{xy}^{UL}	σ_x^{y} * (ksi)	ε_x^y (%)	σ_x^m * (ksi)	ε_x^m (%)	ε_y^m (%)	ε_x^R (%)
F	I	-	-	-	-	-	-	-24.2	-0.078	0.034	-0.038
	II	-	-	-	-	-	-	-47.6	-0.272	0.188	-0.116
	III	22.2	19.9	-	-	-	-	-95.0	-0.731	0.581	-0.195
	IV	21.7	-	-	-	-	-	-159.5	-1.363	1.195	-
T6	I	22.8	22.9	0.394	0.301	-	-	-24.0	-0.088	0.033	-0.012
	II	23.5	23.5	0.336	0.275	-36.0	-0.137	-47.9	-0.196	0.072	-0.021
	III	23.7	23.8	0.292	0.346	-44.7	-0.182	-95.3	-0.511	0.290	-0.112
	IV	21.7	-	0.277	-	-85.8	-0.466	-164.0	-1.057	0.804	-
T6N	I	22.4	21.8	0.329	0.326	-	-	-24.5	-0.070	0.022	-0.031
	II	21.1	22.4	0.349	0.319	-25.3	-0.073	-48.4	-0.188	0.065	-0.042
	III	23.9	23.5	0.319	0.348	-50.5	-0.196	-95.5	-0.514	0.277	-0.137
	IV	21.3	-	0.334	-	-72.7	-0.414	-144.2	-0.947	0.638	-

* Fixture influence

unloading portion of the cycle exhibited reversed nonlinearity.

Unlike the F condition specimen, the T6 condition specimen exhibited an increasing yield stress with each successive cycle. The specimen yielded first (Figure 58) on the second cycle at -36.0 ksi and unloading was linear. The yield stress increased to -44.7 ksi on the third cycle and the linear range upon unloading was approximately the same magnitude as the yield stress. However, for the fourth cycle the yield stress increased to -85.8 ksi. The fact, that the linear range upon unloading on the third cycle was not increased as compared to the magnitude of the yield stress but the yield stress on the fourth cycle was increased, suggests a path dependent yield behavior.

The T6N condition compression-compression specimen exhibited the same type of path dependent yield behavior as the T6 condition specimen. The yield stress was increased to -50.5 ksi over the first three cycles (Figure 60), and the unloading portion of the third cycle was linear for a range of 49.1 ksi. As with the T6 condition specimen, the yield stress was increased to -72.7 ksi on the fourth cycle, an increase of 23.6 ksi over the linear range upon unloading on the third cycle.

5.7.2.3 Tension-Compression

Tension-compression tests for the $[\pm 45/0]_s$ laminate were not conducted as the specimens were not available.

5.7.3 Conclusions

The results from the monotonic tests showed that the tensile and

compressive yield stresses were increased by heat treating F condition material to a T6 condition. The liquid nitrogen exposure decreased the tensile yield and ultimate stress and increased the compressive yield stress. Heat treating also increased the strength of the laminate relative to the F condition specimens.

The yield phenomenon was not consistent for the F condition specimens as compared to the T6 or T6N condition specimens nor was it the same in tension and compression. The F condition tension-tension specimen exhibited behavior resembling kinematic hardening. The T6 and T6N condition tension-tension specimens had an increasing yield stress through four cycles of loading; however, on the fifth cycle the yield stress was reduced.

The F condition cyclic compression specimens did not exhibit a linear elastic range, and thus the yield behavior is not discussed. The T6 and T6N condition specimens exhibited increasing yield stress with each successive cycle; however, the fact that the linear range upon unloading did not increase and the yield stress on the final cycle did increase suggests path dependent yield behavior.

The cyclic tension specimens exhibited decreasing moduli on each successive cycle. Also tensile cyclic loading increased the ultimate stress and strain as compared to the monotonic tension tests. The decreasing modulus and the increased failure strain indicate that the composite is damaged by the cyclic loading.

6. SUMMARY AND CONCLUSIONS

The discussion in Chapter 5 has been concerned with the stress-strain behavior of six laminates of boron-aluminum having a F, T6, or T6N temper condition. The results show that the modulus, yield stress, strength, and material nonlinearity are a function of the laminate configuration.

The significant conclusions resulting from this investigation are listed below.

1. The modulus and tensile strength are primarily a function of the laminate configuration. The temper condition has an insignificant effect on the modulus, and the strength of only the unidirectional material is significantly affected by the T6 heat treatment; the strength of all other laminates studied was affected to a lesser extent.
2. Lamination theory predicts higher modulus than was experimentally determined for the [0,±45] class of laminates. The lower experimental moduli are believed to be the result of residual curing stresses which have stressed the matrix and ±45° laminae into their nonlinear regions.
3. The T6 heat treatment significantly increased the tensile and compressive yield stress of all six laminates.
4. In general, liquid nitrogen exposure of the laminates with 0° plies increased the tensile yield stress and reduced the compressive yield stress; however, the $[\pm 45/0]_s$ laminate

exhibited the opposite effect.

5. The $[0/\pm45]_s$ and $[\pm45/0]_s$ laminates exhibited larger tensile failure strains in a T6 condition, but the tensile failure strain of all other laminates was reduced by heat treating.
6. The influence of cryogenic exposure on the tensile strength was inconclusive with some laminates exhibiting small increases and other exhibiting small decreases.
7. The laminates containing ±45° plies exhibited modulus reduction on successive loading cycles indicating material degradation.
8. All laminates, independent of temper condition, exhibited an increasing linear range during cyclic loading which, after several cycles, reached a maximum value. The yield behavior resembled kinematic hardening, Baushinger effect, or isotropic hardening depending upon the laminate configuration and temper condition.
9. The T6 heat treatment increased the maximum linear range during cyclic loading for all six laminates studied.
10. In general, a maximum linear range was developed during cyclic loading of the [0], [90], $[\pm45]_s$, and F condition [0,±45] family and was maintained for the remaining cycles. The T6 and T6N [0,±45] family either exhibited the same type of behavior or the linear range decreased due to material degradation.

11. The F condition $[\pm 45]_s$ specimen exhibited fiber rotation of up to 10° and failure strains of approximately 23%. The fiber rotation was insignificant for heat treated $[\pm 45]_s$ laminates and the $[0,\pm 45]$ family.

12. The compression specimen chosen for this work was not satisfactory in that load was transferred into the fixture, thereby influencing the compressive stress-strain diagrams; in addition, compressive failure strengths were influenced by the specimen design.

REFERENCES

1. Thomas T. Bales, H. Ross Wiant and Dick M. Royster, "Brazed Borsic - Aluminum Structural Panels", NASA TMX-3432, 1977.

2. J. Mangiapane, et al, Paper No. 68-1037, presented at 5th AIAA Annual Meeting, October, 1968.

3. R. A. Garrett, et al, "Design, Process Development, Manufacture, Test and Evaluation of Boron-Aluminum for Space Shuttle Components", McDonnell Douglas Astronautics Company - East, MDC E0825, July, 1973.

4. H. P. Cheskis and R. W. Heckel, "In Situ Measurements of Deformation Behavior of Individual Phases in Composites by X-Ray Diffraction", Metal Matrix Composites, ASTM STP 438, American Society for Testing and Materials, 1968, pp. 76-91.

5. A. A. Baker and D. Cratchley, "Stress-Strain Behavior and Toughness of a Fibre-Reinforced Metal", Applied Materials Research, April, 1966, pp. 92-103.

6. K. Kreider and M. Marciano, "Mechanical Properties of BORSIC Aluminum Composites", Transactions of the Metallurgical Society of AIME, Vol. 245, 1969, pp. 1279-1286.

7. James R. Long, "The Evaluation of the Mechanical Behavior of Metal Matrix Composites Reinforced with SiC-Coated, Boron Fibers," AFML-TR-69-291, Vol. I, November, 1969.

8. Carl T. Herakovich, John G. Davis, Jr. and Chittur N. Viswanathan, "Tensile and Compressive Behavior of Borsic/Aluminum", Composite Materials: Testing and Design (Fourth Conference), ASTM STP 617, American Society for Testing and Materials, 1977.

9. A. C. Knoell, "Evaluation of Boron/Aluminum Tubes in Compression", AIAA/ASME/SAE 16th Structures, Structural Dynamics and Materials Conference, Denver, Colorado, AIAA Paper 75-789, May, 1975.

10. N. R. Adsit and J. P. Forest, "Compression Testing of Aluminum-Boron Composites", Composite Materials Testing and Design, ASTM 460, American Society for Testing and Materials, 1969, pp. 108-121.

11. J. F. Dolowy and R. J. Taylor, "Thermal/Mechanical Strengthening of 6061 Al-B Composites", (1969) Proceedings of SAMPE Meeting 1969, pp. 369-377.

12. K. M. Prewo and K. G. Kreider, "The Transverse Tensile Properties of Boron Fiber Reinforced Aluminum Matrix Composites", Metallurgical Transactions, Vol. 3, August, 1972, pp. 2201-2211.

13. G. D. Swanson and J. R. Hancock, "Off-Axis and Transverse Tensile Properties of Boron Reinforced Aluminum Alloys, "Composite Materials: Testing and Design (Second Conference), ASTM STP 497, American Society for Testing and Materials, 1972, pp. 469-482.

14. K. M. Prewo and K. G. Kreider, "High Strength Boron and Borsic Fiber Reinforced Aluminum Composites", J. Composite Materials, Vol. 6, July, 1972, pp. 338-357.

15. B. D. Cullity, Elements of X-ray Diffraction, Addison and Wesley, 1956.

16. R. E. Allfred, W. R. Hoover and J. A. Horak, "Elastic-Plastic Poisson's Ratio of Borsic-Aluminum", J. Composite Materials, Vol. 8, January, 1974, pp. 15-28.

17. C. C. Chamis and T. L. Sullivan, "A Computational Procedure to Analyze Metal Matrix Laminates with Lamination Residual Strains", Composite Reliability, ASTM STP 580, American Society for Testing and Materials, 1975, pp. 327-339.

18. J. E. Ramsey, J. P. Waszczak and F. L. Klouman, "An Investigation of the Nonlinear Response of Metal-Matrix Composite Laminates," AIAA/ASME/SAE 16th Structures, Structural Dynamics, and Materials Conference, Denver, Colorado, AIAA Paper 75-787, May, 1975.

19. Gary D. Renieri and Carl T. Herakovich, "Nonlinear Analysis of Laminated Fibrous Composites", VPI & SU Report VPI-E-76-10, June, 1976.

20. Robert M. Jones, Mechanics of Composite Materials, Scripta Book Company, 1975, pp. 31-236.

21. "Tensile Properties of Oriented Fiber Composites", 1973 Annual Book of ASTM Standards, Part 25, November, 1973, pp. 608-613.

22. G. C. Grimes, P. H. Francis, G. E. Commerford, G. K. Wolfe, "An Experimental Investigation of the Stress Levels at Which Significant Damage Occurs in Graphite Fiber Plastic Composites", AFML-TR-72-40, May, 1972.

23. B. Walter Rosen, "A Simple Procedure for Experimental Determination of the Longitudinal Shear Modulus of Unidirectional Composites", J. Composite Materials, Vol. 6, October, 1972, pp. 552-554.

24. C. W. Richards, Engineering Materials Science, Brooks/Cole Publishing Company, 1961, pp. 152-156.

25. J. N. Goodier and P. G. Hodge, Elasticity and Plasticity, John Wiley & Sons, Inc., New York, 1956.

DISTRIBUTION LIST

Dr. Wolf Elber
Mail Stop 188E
NASA-Langley Research Center
Hampton, VA. 23665

Dr. Nicholas J. Pagano
WPAFB/MBM
Wright Patterson Air Force Base
OH 45433

Dr. R. Byron Pipes
Dept. of Mechanical & Aerospace Engr.
107 Evans Hall
University of Delaware
Newark, DE 19711

Dr. Edmund F. Rybicki
Battelle
Columbus Laboratories
505 King Avenue
Columbus, OH 43201

Dr. George P. Sendeckyj
Structures Division
Air Force Flight Dynamics Lab.
Wright-Patterson Air Force Base
OH 45433

Dr. Carl H. Zweben
Textile Fibers Dept.
E. I. DuPont de Nemours & Co. Inc.
Experimental Station/B262
Wilmington, DE 19898

Dr. B. W. Rosen
Materials Science Corporation
Blue Bell Office Campus
Blue Bell, PA 19422

Dr. S. V. Kulkarni
Materials Sciences Corporation
Blue Bell Office Campus
Blue Bell, PA 19422

Dr. S. W. Tsai
Nonmetallic Materials Division
Air Force Materials Laboratory
Wright-Patterson Air Force Base
OH 45433

Dr. J. M. Whitney
Nonmetallic Materials Division
Air Force Materials Laboratory
Wright-Patterson Air Force Base
OH 45433

Dr. John G. Davis, Jr.
Mail Code No. 188A
Langley Research Center
Hampton, VA 23665

Dr. I. M. Daniel, Manager
IIT Research Institute
10 West 35 Street
Chicago, IL 60616

NASA Scientific and Technical
Information Facility
P.O. Box 8757
Baltimore/Washington International
Airport
Baltimore, MD 21240

Dr. Larry Roderick
Langley Research Center
Mail Stop 188E
Hampton, VA 23665

Mr. M. E. Waddoups
General Dynamic Corp.
Fort Worth, TX 76101

Dr. J. C. Halpin
Flight Dynamics Lab.
Wright-Patterson Air Force Base
OH 45433

Dr. Longin B. Greszczuk
McDonnell Douglass Astronuatics Co.
5301 Bolsa Avenue
Huntington Beach, CA 92647

Professor R. E. Rowlands
Dept. of Engineering Mechanics
University of Wisconsin
Madison, WI 53706

Dr. R. L. Foye
U. S. Army Mobility Res. & Dev. Lab.
Langley Research Center, Mail Stop 188A
Hampton, VA 22065

Dr. John R. Davidson
Mail Code 188E
MD-Structural Integrity Branch
Langley Research Center
Hampton, VA 23665

Dr. Darrel R. Tenney
Mail Code 188M
MD-Materials Research Branch
Langley Research Center
Hampton, VA 22065

Mr. John M. Kennedy
Mail Stop 188E
NASA-Langley Research Center
Hampton, VA. 23665

Professor Donald F. Adams
Dept. of Mechanical Engineering
University of Wyoming
Larmie, WY 82070

Professor Phil Hodge
107 Aeronautical Engr. Bldg.
University of Minnesota
Minneapolis, MN 55455

Mr. Glen C. Grimes, Engr. Specialist
Structures R & T, Dept. 3780/62
Northrop Corp., Aircraft Div.
3901 W. Broadway
Hawthorne, CA 90250

Dr. Martin M. Mikulas
Mail Stop 190
NASA-Langley
Hampton, VA 23665

Dr. Paul A. Cooper
Mail Stop 208
NASA-Langley
Hampton, VA 23665

Mr. Edward L. Hoffman
Mail Stop 188A
NASA-Langley Research Center
Hampton, VA 23665

Dr. N. J. Johnson
Mail Stop 226
NASA-Langley Research Center
Hampton, VA 23665

Dr. Michael F. Card
Mail Stop 190
NASA-Langley Research Center
Hampton, VA 23665

Mr. Vic Mazzio
Boeing Vertol Company
MS P38-21
P.O. Box 16858
Philadelphia, PA 19142

Dr. H. T. Hahn
Nonmetallic Materials Div.
Air Force Materials Laboratory
Wright-Patterson Air Force Base
Ohio 45433

Dr. Donald W. Oplinger
Army Materials & Mechanics Research Center
Department of the Army
Watertown, Mass. 02172

Dr. Keith T. Kedword
Kedward, Kawa & Associates LTD
400 Kelvin Blvd.
Winnipeg, Manitoba
Canada R3P 0J2

Dr. Michael P. Renieri
McDonald Aircraft Co.
Bldg. 34, Post 350
St. Louis, MO 63166

Dr. Gary D. Renieri
McDonald Douglas Astronautics Co-East
P.O. Box 516
Bldg. 106, Level 4, Post C-5
St. Louis, MO 63166

Dr. Nicholas Perrone, Director
Structural Mechanics Program
Department of the Navy
Office of Naval Research
Arlington, VA 22217

Dr. Clifford J. Astill
Solid Mechanics Program
National Science Foundation
Washington, D. C. 20550

Mr. Larry R. Markham
Lockheed-California
Dept. 7572, Bldg. 63 Plant A1
P.O. Box 551
Burbank, CA 91520

Mr. Jerry W. Deaton
Mail Stop 188A
NASA-Langley Research Center
Hampton, VA 23665

Dr. Peter W. Hsu
2195 Rockdell Dr., Apt. #6
Fairborn, OH 45324

Dr. James H. Starnes, Jr.
Mail Stop 190
NASA-Langley Research Center
Hampton, VA. 23665

Dr. E. G. Henneke
ESM Dept.
VPI & SU
Blacksburg, VA. 24061

Dr. W. W. Stinchcomb
ESM Dept.
VPI & SU
Blacksburg, VA. 24061

Dr. K. L. Reifsnider
ESM Dept.
VPI & SU
Blacksburg, VA. 24061

Dr. H. F. Brinson
ESM Dept.
VPI & SU
Blacksburg, VA. 24061

Dr. R. A. Heller
ESM Dept.
VPI & SU
Blacksburg, VA. 24061

Dr. D. Frederick
ESM Dept.
VPI & SU
Blacksburg, VA. 24061

Dr. M. P. Kamat
ESM Dept.
VPI & SU
Blacksburg, VA. 24061

Dr. T. A. Weisshaar
Aero & Ocean Engr. Dept.
VPI & SU
Blacksburg, VA. 24061

Dr. Charles W. Bert, Director
School of Aerospace, Mechanical
& Nuclear Engineering
The University of Oklahoma
Norman, Oklahoma 73069

Dr. N. R. Adsit
General Dynamics Convair
P.O. Box 80837
San Diego, CA. 92138

Dr. Frank Crossman
Lockheed Research Lab
Org. 52-41, Bldg. 204
3251 Hanover Street
Palo Alto, CA. 94034

SECURITY CLASSIFICATION OF THIS PAGE (When Data Entered)

REPORT DOCUMENTATION PAGE		READ INSTRUCTIONS BEFORE COMPLETING FORM
1. REPORT NUMBER VPI-E-77-18	2. GOVT ACCESSION NO.	3. RECIPIENT'S CATALOG NUMBER
4. TITLE (and Subtitle) INFLUENCE OF TEMPER CONDITION ON THE NONLINEAR STRESS-STRAIN BEHAVIOR OF BORON-ALUMINUM		5. TYPE OF REPORT & PERIOD COVERED 6. PERFORMING ORG. REPORT NUMBER VPI-E-77-18
7. AUTHOR(s) John M. Kennedy, Carl T. Herakovich, and Darrel R. Tenney		8. CONTRACT OR GRANT NUMBER(s) NASA NGR-47-004-129
9. PERFORMING ORGANIZATION NAME AND ADDRESS Virginia Polytechnic Institute & State Univ. Engineering Science & Mechanics Blacksburg, Virginia 24061		10. PROGRAM ELEMENT, PROJECT, TASK AREA & WORK UNIT NUMBERS
11. CONTROLLING OFFICE NAME AND ADDRESS National Aeronautics & Space Administration Langley Research Center Hampton, Virginia 23665		12. REPORT DATE June, 1977 13. NUMBER OF PAGES
14. MONITORING AGENCY NAME & ADDRESS(if different from Controlling Office) Virginia Polytechnic Institute & State Univ. Engineering Science & Mechanics Blacksburg, Virginia 24061		15. SECURITY CLASS. (of this report) Unclassified 15a. DECLASSIFICATION/DOWNGRADING SCHEDULE

16. DISTRIBUTION STATEMENT (of this Report)

Approved for public release; distribution unlimited.

17. DISTRIBUTION STATEMENT (of the abstract entered in Block 20, if different from Report)

Approved for public release; distribution unlimited.

18. SUPPLEMENTARY NOTES

19. KEY WORDS (Continue on reverse side if necessary and identify by block number)

Boron-Aluminum, Composites, Tension, Compression, Nonlinear Behavior, Cyclic Loading, Heat Treatment, Cryogenic Exposure

20. ABSTRACT (Continue on reverse side if necessary and identify by block number)

see page ii

DD FORM 1 JAN 73 1473 EDITION OF 1 NOV 65 IS OBSOLETE

SECURITY CLASSIFICATION OF THIS PAGE (When Data Entered)